High thioredoxin-1 levels in rheumatoid arthritis patients diminish binding and signalling of the monoclonal antibody Tregalizumab

Dissertation
zur Erlangung des Doktorgrades
der Naturwissenschaften

vorgelegt beim Fachbereich 14
Biochemie, Chemie und Pharmazie
der Johann Wolfgang Goethe - Universität
in Frankfurt am Main

von
Dipl. Pharm. Katharina Julia Heim
aus Freiburg im Breisgau

Frankfurt 2016
D30

vom Fachbereich 14 der
Johann Wolfgang Goethe – Universität Frankfurt am Main
als Dissertation angenommen.

Dekan: Prof. Dr. Michael Karas

Gutachter: Prof. Dr. Theodor Dingermann und PD Dr. Karin Schirrmacher

Datum der Disputation:_____

Doch Forschung strebt und ringt, ermüdend nie,

Nach dem Gesetz, dem Grund, Warum und Wie.

Johann Wolfgang von Goethe

Summary / Zusammenfassung

Zum Schutz des Organismus vor schädlichen Einflüssen aus der Umwelt spielt das Immunsystem die wichtigste Rolle. Um gefährlichen Infektionserreger wie Viren, Bakterien oder Parasiten entgegen zu wirken, hat sich im Laufe der Evolution ein komplexes System von verschieden Verteidigungsmechanismen entwickelt[1,2]. Zur Aufrechterhaltung der immunologischen Balance und zur Verhinderung einer überschießenden Immunreaktion, stellen regulatorische T-Zellen eine wichtige Subpopulation von CD4+ T-Zellen dar[3]. Durch Suppression von T-Effektorzellen leisten sie einen wichtigen Beitrag zur Prävention von Allergien, Graft-versus-Host-Reaktionen und Transplantant-abstoßungen[4,5]. Autoimmunerkrankungen können unter anderem durch funktionale Defizite oder durch einen Mangel an regulatorischen T-Zellen bedingt sein[6]. Als Bespiel von Autoimmunerkrankungen ist Rheumatoide Arthritis (RA) zu nennen, welche mit einer Prävalenz von 1 % die häufigste chronisch-entzündliche Gelenkserkrankung darstellt[7,8]. Als Ursachen und Risikofaktoren für die Entstehung von Rheumatoider Arthritis werden verschiedene genetische Prädispostionen und Umwelteinflüsse gesehen, die zu Bildung von Antikörpern gegen citrullinierte Proteine führen[9,10]. Weitere Studien beschreiben eine signifikante Verbindung zwischen Rheumatoider Arthritis und oxidativem Stress, welcher durch reaktive Sauerstoffspezies hervorgerufen wird[11–13]. Eine Möglichkeit des Organismus, oxidativen Stress zu verhindern oder zu reduzieren, stellt die Oxidoreduktase Thioredoxin (Trx1) dar. Thioredoxin, das zusammen mit seinem Enzym Thioredoxin Reduktase (TrxR) agiert[14], ist ein 12 kilo Dalton (kDa) großes Protein, und spielt in der Redoxhomöostasis eine sehr wichtige Rolle[14]. Verschiedene Studien zeigten erhöhte Konzentrationen von Trx1 in Serum, Plasma und Synovialflüssigkeit von RA-Patienten[15–19]. Überdies wurde eine Korrelation zwischen Krankheitsaktivität und erhöhten Trx1-Plasmaspiegeln, respektive Trx1-Aktivität, nachgewiesen[17,18]. Diese erhöhten Konzentrationen konnten mittels einem anti-Thioredoxin ELISA und Plasma von RA-Patienten in eigenen Versuchen dieser Arbeit verifiziert werden (s. Kapitel 4.22).

Als eine neue Option in der Therapie von Autoimmunerkrankungen und Rheumatoider Arthritis wird die Aktivierung von CD4+ CD25+ regulatorischen

T-Zellen untersucht, welche das immunologische Gleichgewicht des Organismus wieder herstellen soll. Dafür wurden einige anti-CD4 Antikörper untersucht, die die supprimierende Funktion von CD25+ regulatorischen T-Zellen aktivieren können, was die Rolle von CD4 als interessantes Targetprotein in den Mittelpunkt rückt[20,21].

Tregalizumab (BT-061) stellt einen nicht depletierenden, monoklonalen IgG1 Antikörper dar, welcher an ein einzigartiges Epitop auf dem CD4-Molekül bindet[22,23]. Er repräsentiert den ersten humanisierten monoklonalen Antikörper, welcher *in vitro* regulatorische T-Zellen gezielt aktivieren kann[22,23]. Tregalizumab bindet als Agonist an ein nicht lineares Epitop auf der Domäne 2 (D2) des CD4 Moleküls wobei er eine Signalkaskade aktiviert, die die Protein Tyrosinkinase $p56^{Lck}$ involviert[22]. Für diese $p56^{Lck}$ vermittelte Aktivierung ist eine Kreuzvernetzung des Fc-Teils des Antikörpers mit dem Fc-gamma Rezeptor 1 (CD64, FcγRI) auf den Monozyten notwendig. Durch die Aktivierung des CD4 Signalwegs wird dieser Rezeptor konzentrationsabhängig herunter reguliert und steigt erst nach einigen Tagen, je nach Konzentration, wieder an. Zusätzlich wird der Tregalizumab/CD4-Komplex internalisiert. Dieser pharmakodynamische Effekt kann *in vitro* und *in vivo* gemessen werden und dient als Marker zur Bestimmung der Aktivität des Antikörpers[23,24].

Um die Dosis-Wirkungszusammenhänge von Tregalizumab besser zu verstehen, wurde ein pharmakokinetisch-pharmakodynamisches Modell (PK-PD-Modell) etabliert, dass die Modulation von CD4 Molekülen auf der Oberfläche von T-Zellen aus mehreren klinischen Studien zugrunde legt[24]. Das auf Daten aus klinischen Studien von RA-Patienten und gesunden Probenbanden basierende Modell, zeigte überraschenderweise einen höheren pharmakodynamischen Effekt von Tregalizumab in den gesunden Probanden im Vergleich zu RA-Patienten. Überdies wurde in der letzten klinischen Studie 2b (TREAT 2b, T-cell Regulating Arthritis Trial 2b, ClinicalTrials.gov Identifier: NCT01999192 und EudraCT No. 2013-000114-38) der primäre Endpunkt nicht erreicht.

Im Rahmen der Dissertation wurde eine Reihe an Experimenten durchgeführt, die Aufschluss über den Zusammenhang zwischen der höheren CD4

Herunterregulation in gesunden Probanden im Vergleich zu RA-Patienten geben sollen. Um für diese Beobachtung eine Erklärung zu finden, wurde die Interaktion zwischen Tregalizumab und CD4 nochmals genauer analysiert.

Tregalizumab bindet an ein spezielles Epitop auf der Domäne 2, welches nahe einer intramolekularen Disulfidbrücke zwischen Cystein(155) und Cystein(184), lokalisiert ist[22,23]. Der Abstand zwischen dem zu Tregalizumab gehörenden Tyrosin(105) und der Disulfidbrücke in der Domäne D2 von CD4, wurde auf 7,0 bis 11,0 Å errechnet. Da Tregalizumab in geringer Entfernung zu dieser Disulfidbrücke bindet, ist ein Einfluss durch eine potentielle Konformationsänderung auf die Bindung von Tregalizumab an CD4 vorstellbar. Da Matthias *et al.* beschreiben, dass Trx1 diese Disulfidbrücke in der Domäne 2 des CD4 Moleküls selektiv reduzieren kann[25], wurden im Rahmen dieser Arbeit der Einfluss von Trx1 auf die Interaktion von Tregalizumab und CD4 evaluiert.

Versuche dieser Arbeit bestätigen die Resultate von Matthias *et al.* und zeigten, dass Trx1 rekombinantes humanes lösliches CD4 (rh sCD4) sowohl alleine als auch in Kombination mit seinen physiologischen Reaktionspartnern Thioredoxin-Reduktase und NADPH reduzieren kann (s. Kapitel 5.8).

Mittels eines auf Elektrochemolumineszens basierten ELISA konnte weiterhin gezeigt werden, dass die Bindung von Tregalizumab an rh sCD4 durch Trx1-Behandlung reduziert wird (s. Kapitel 5.10). Im Unterschied zu der nicht behandelten Kontrolle, reduzierte Trx1 die Bindung von Tregalizumab konzentrationsabhängig. Zusätzlich wurde der Einfluss von Trx1 au304 unterschiedliche anti-CD4 Antikörper untersucht, welche an verschiedene Domänen des CD4 Moleküls binden. Da die Reduktion der Disulfidbrücke der Domaine D2 durch Trx1 und eine damit potentiell assoziierte Konformationsänderung des gesamten CD4-Moleküls das Bindungsverhalten von unterschiedlichen Antikörpern beeinflussen kann, wurden kommerziell erhältliche monoklonale Antikörper untersucht. MT441, welcher - wie Tregalizumab - an die Domäne 2 von CD4 bindet, OKT-4, der Domäne 3 erkennt und die beiden an Domäne 1 bindenden Antikörper SK3 und RPA-T4 wurden eingesetzt. Es zeigte sich, dass die an Domäne 2 bindenden Antikörper am stärksten in ihrer Bindung von Thioredoxin beeinflusst werden. OKT-4,

welcher an eine Domäne ohne Disulfidbrücke bindet, wies nur einen geringen Unterschied zur unbehandelten Kontrolle auf. Die Bindung von SK3 und RPA-T4 an rh sCD4 wurden durch Trx1 ebenfalls beeinflusst, jedoch nicht so ausgeprägt wie bei Tregalizumab und MT441.

Um den beobachteten Effekt von Trx1 auf rh sCD4 auch auf Zellen zu untersuchen, wurden CD4+ HPB-ALL Zellen zusammen mit Trx1 vorinkubiert und danach die Bindung von Tregalizumab mittels Durchflusszytometrie untersucht (s. Kapitel 5.12). Im Vergleich zu den unbehandelten Zellen verringerte auch eine Vorbehandlung der CD4+ Zellen mit Trx1 die Bindung von Tregalizumab signifikant. Ein noch größerer Effekt wurde durch Vorinkubation mit dem physiologischen Trx1/TrxR/NADPH System erzielt. Als Kontrolle wurde die inaktive Mutante Trx1-SS eingesetzt, bei welcher die beiden aktiven Cysteine (Cys 32 und Cys 35) durch Serin substituiert wurden und wodurch das Protein kein Reduktionsvermögen aufweist. Die Kontrolle zeigte keine Einwirkung auf die Bindung von Tregalizumab an CD4+ HPB-ALL Zellen. Die Ergebnisse konnten mit isolierten mononukleären Zellen des peripheren Blutes (*Peripheral Blood Mononuclear Cell,* PBMC) verifiziert werden (s. Kapitel 5.12.3), sodass ein Einfluss durch Trx1 auf die Bindung von Tregalizumab an CD4+ Zellen des peripheren Blutes erwartet werden kann.

Reduziertes Glutathion (GSH) diente zur Prüfung, ob auch andere physiologisch relevante Proteine die Bindung von Tregalizumab an CD4 beeinflussen (s. Kapitel 5.13). Im Vergleich zu Trx1 zeigte eine Vorinkubation der Zellen mit GSH - mit physiologischer Konzentration von 10 mM[26,27] - jedoch keinen signifikanten Einfluss auf Bindung von Tregalizumab an CD4 auf PBMC.

Für eine Signaltransduktion und CD4 Herunterregulation in T-Zellen ist, neben einer CD4 Stimulation durch Tregalizumab, eine Kreuzvernetzung des Antikörpers mit CD64 auf Monozyten essentiell[28]. Daher wurde auch der Einfluss von Trx1 und GSH auf die Bindung eines monoklonalen anti-CD64 Antikörper an Monozyten analysiert (s. Kapitel 5.14). Durchflusszytometrische Untersuchungen zeigten jedoch weder einen Effekt von Trx1, noch von GSH, auf die Bindung des anti-CD64 Antikörpers an CD64, sodass eine Einwirkung von Trx1 auf CD64 nicht anzunehmen ist.

Des Weiteren konnte gezeigt werden, dass die Disulfidbrücke in Domäne 2 des CD4-Moleküls per se einen wichtigen Einfluss auf das Bindungsverhalten von Tregalizumab aufweist (s. Kapitel 5.15). Die Bindung von Tregalizumab an eine CD4-Mutante, welche keine Cysteine (Cys(155) und Cys(184)) in Domäne 2 mehr enthält, war signifikant niedriger im Vergleich zu dem monoklonalen Antikörper OKT-4, welcher an Domäne 3 bindet. Hierfür wurden CD4 negative U266B1 Zellen mittels CD4 und mutierter CD4-DNA und nicht mutierter CD4-DNA transfiziert und die Bindung der beiden Antikörper mit Hilfe von Durchflusszytometrie gemessen.

Da aufgrund des Einfluss von Trx1 auf den Detektionsantikörpers der CD4 Herunterregulation diese nicht bestimmt werden konnte, wurde als Substitut der erste Schritt der Signaltransduktion analysiert. Helling *et al.* zeigten, dass Tregalizumab eine Phosphorylierung von $p56^{Lck}$, ZAP-70 und anderen Signalmolekülen induziert, welche mit dem Phosphorylierungsmuster von OKT-3 verglichen wurde[22]. Um den Einfluss von Trx1 und seinem physiologischen Partnern auf die ersten Moleküle der Tregalizumab Signalkaskade ($p56^{Lck}$ und ZAP-70) zu prüfen, wurden PBMC mit der Trx1/TrxR/NADPH vorinkubiert und die Phosphorylierung der beiden Signalmoleküle mittels Durchflusszytometrie nach Stimulation mit Tregalizumab oder OKT3 untersucht (s. Kapitel 5.16). Trx1-Vorinkubation resultierte in einer signifikanten Reduktion der Aktivierung von $p56^{Lck}$, wobei kein Einfluss auf OKT3 erkennbar war. Betrachtet man ZAP-70, so hatte Trx1 hier keinen signifikanten Einfluss.

Aufgrund der Ergebnisse dieser Arbeit kann gefolgert werden, dass Trx1 in Kombination mit seinen physiologischen Partnern TrxR und NADPH sowohl einen Einfluss auf die Bindung, als auch auf die CD4 vermittelte Signaltransduktion von Tregalizumab ausübt.

Um zu verifizieren, ob der *in vitro* beobachtete Effekt von Trx1 auf die Bindung von Tregalizumab an CD4 auch *in vivo* zu beobachten ist, wurden retrospektive Daten hinsichtlich der Bindung von Tregalizumab an CD4 aus der Biotest Studie 979 und Biotest Studie 985 ausgewertet (s. Kapitel 5.17). Es konnte gezeigt werden, dass im Vergleich zu gesunden Probanden, die relative Bindung von Tregalizumab (Verhältnis der mittleren Fluoreszenzintensität

zwischen Tregalizumab und dem nicht-kompetierenden anti-CD4 Antikörper SK3) in RA-Patienten signifikant niedriger ist.

Zusammenfassend kann festgehalten werden, dass Trx1 einen negativen Einfluss auf die Bindung und die Signaltransduktion von Tregalizumab an CD4 *in vitro* und *in vivo* zeigt. Daher liegt die Hypothese nahe, dass ein erhöhter Trx1-Spiegel im Plasma von RA-Patienten eine mögliche Ursache für die im PK-PD Modell beobachtete niedrige Heruntermodulation von CD4 nach Tregalizumab-Applikation im Vergleich zu gesunden Probanden darstellen. Möglicherweise liefern diese Ergebnisse auch eine Erklärung für die in der letzten klinischen Studie beobachteten negativen Resultate. Diese Thesis verdeutlicht ferner, dass die Bindung von Tregalizumab an CD4 in besonderer Weise in RA Patienten beeinflusst wird. Bei einer potentiellen Suche nach neuen Indikationen für Tregalizumab sollte daher der Einfluss von oxidativem Stress und hohen Trx1- Level in besonderer Weise berücksichtigt werden.

Contents

List of figures

List of tables

List of abbreviations

°C	degree celsius
µg	microgram
µL	microliter
µM	micromolar
5-ASA	5-aminosalicylic acid
Å	Ångström
Ab	antibody
ACPA	anti–citrullinated protein antibodies
ACR	american College of Rheumatology
ad	to
ADCC	antibody-dependent cell-mediated cytotoxicity
ahIgG	anti-human IgG
Akt	protein kinase B
Ala	Alanine
amIgG	anti-mouse IgG
AMP	adenosine monophosphate
AP-1	activator protein 1
APC	allophycocyanin
APC	antigen presenting cells
APRIL	proliferation-inducing ligand
ASK1	apoptosis signal-regulating kinase 1
Asn	asparagine
ATP	adenosine triphosphate
B cells	B lymphocytes
BAFF	B cell activating factor of the TNF family
BCA	bicinchoninic acid
BCR	B cell receptor
BD	becton Dickinson
Bis-Tris	bisamino-trismethan
BLys	B lymphocyte stimulator
BSA	Bovine serum albumin
C	constant
C	constant; carboxyl-terminus
Ca	calcium
cAMP	cyclic AMP
CCP	cyclic citrullinated peptides
CD	cluster of differentiation
CDC	complement dependent cytotoxicity
CDR	complementary determining regions
cf	carrier free
CI	confidence interval
CO_2	carbon dioxide
COX	cyclooxygenase
CTL	cytotoxic T lymphocyte
CTLA-4	cytotoxic T-lymphocyte antigen 4
Cys_2	cystine
D	domain
DAMPs	damage-associated molecular patterns
DC	dendritic cell
dest.	destillata
DKFZ	German Cancer Researh Center
DMARD	disease-modifying antirheumatic drugs
DMSO	dimethyl sulfooxide
DNA	deoxyribonucleic acid
D-PBS	Dulbecco's Phosphate-Buffered Saline
DTNB	5,5'-dithiobis-(2-nitrobenzoic acid)
DTT	dithiothreitol
DW	distilled water
e.g.	exempli gratia
E2	bimolecular elimination
ECEF	eosinophil cxtotoxicity-enhancing factor
EDTA	ethylenediaminetetracetic acid
ELISA	enzyme-linked immunosorbent assay
ENTPD1	ectonucleoside triphosphate diphosphohydrolase 1
ERK	extracellular signal-regulated kinases
et al.	et alii
etc.	et cetera
Fab	fragment antigen-binding
FACS	fluorescence-activated cell sorting
FAD	flavin adenine dinucleotide
Fc	fragment crystallizable
FcR	Fc receptor
FCS	fetal calf serum
FcγRI	Fc gamma receptor I
FITC	fluorescein isothiocyanate
FoxP3	forkhead box P3
FSC	forward scatter channel
g	gramm
g	gravity
GARP	glycoprotein A repetitions predominant
GCP	good clinical practice
GM-CSF	granulocyte-macrophage colony-stimulating factor
GSH	reduced glutathione
GSSG	oxidized glutathione
h	hour
H^+	proton

H_2O_2	hydrogen peroxide
hCD4	human CD4
Hif-1	hypoxia-inducible factor 1
HIV	human immunodeficiency virus
HLA	Human leukocyte antigen
HLA-DRB_1	HLA class II histocompatibility antigen, DRB1 beta chain
HSA	human serum albumin
ICER	Inducible cAMP early repressor
ICH	International Council on Harmonisation of Technical Requirements for Registration of Pharmaceuticals for Human Use
IDO	indoleamine-2,3-dioxygenade
IFN-γ	interferon-γ
Ig	immunoglobulin
IKK	inhibitor of kB kinase
IL	interleukin
IL-2	interleukin 2
IPEX	immune dysregulation, polyendocrinopathy, enterophathy, X-linked
IPTG	isopropyl β-D-1-thiogalactopyranoside
ITAM	Immunoreceptor tyrosine-based activation motif
Itk	interleukin-2-inducible T-cell kinase, ERK
iTreg	inducible Tregs
IκB α	nuclear factor of kappa light polypeptide gene enhancer in B-cells inhibitor, alpha
JNK	c-Jun N-terminal kinase
K	kilo
K_D	dissociation constant
kDa	kilodalton
kJ	kilojoule
L	Liter
LAG-3	lymphocyte-activation gene 3
LAP	latency-associated peptide
LAT	linker for activation of T-cells
LB	lysogeny broth
LDS	lithium dodecyl sulfate
LPS	lipopolysaccharide
mAb	monoclonal antibody
MAPK	mitogen-activated protein kinase
MEK	mitogen-activated protein kinase kinase
MFI	mean fluorescence intensity
mg	milligram
MHC	major histocompatibility complex
min	minute
mL	milliliter
MLR	mixed lymphocyte reaction
mM	millimolar
$MM(PEG)_{24}$	Methyl-PEG_{24}-Maleimide
MMP	matrix metalloproteinase
MSD	Meso Scale Discovery
mTOR	mechanistic Target of Rapamycin
MTX	methotrexate
mut	mutated
MWCO	molecular weight cut off
n	Number
N	amino-terminus
N	normal
na	not applicable
Na_2HPO_4	sodium hydrogen phosphate
NADPH	nicotinamide adenine dinucleotide phosphate
NEM	N-Ethylmaleimide
NFAT	nuclear factor of activated T-cells
NFATc1	nuclear factor of activated T-cell c1
NF-κB	nuclear factor kappa-light-chain-enhancer of activated B cells
NK cell	natural killer cell
NKT cell	natural killer T-cell
NLR	nucleotide-binding domain and leucine-rich repeat containing
NLR	nucleotide-binding oligomerization domain like receptors
nM	nanomolar
NR	non reducing
ns	not significant
NSAID	non-steroidal anti-inflammatory drug
nTregs	naturally occurring Tregs
OD	optical density
$p56^{lck}$	lymphocyte-specific protein tyrosine kinase
$p59^{fyn}$	tyrosine-protein kinase Fyn
PAMPs	pathogen-associated molecular patterns
PBMC	peripheral blood mononuclear cell
PBS	phosphate-Buffered Saline
PCR	polymerase chain reaction
PE buffer	potassium phosphate – EDTA buffer

PE	phycoerythrin
PEG	polyethylenglycol
PerCP	peridinin-chlorophyll-protein complex
PI(3)K	phosphatidylinositol-3-OH kinase
PIM1	3-cyano-4-phenyl-6-(3-bromo-6-hydroxy)phenyl-2(1H)-pyridone
pKa	acid dissociation constant
PKC	protein kinase C
PK-PD	pharmacokinetic-pharmacodynamic
PLC-γ	pphospholipase C gamma
pmaxGFP	green fluorescent protein from the copepod Pontellina p
pMHC	peptide Major histocompatibility complex
pMHC	peptide-major histocompatibility complex
PP1	4-amino-5-(4-methylphenyl)-7-(t-butyl)pyrazolo[3,4-d]-pyrimidine
PP1	protein phosphatase 1
Prx	peroxiredoxins
PTEN	phosphatase and tensin homolog
PVDF	polyvinylidene difluoride
PVDF	polyvinylidene fluoride
R	reducing
RA	rheumatoid arthritis
RANKL	receptor activator of nuclear factor kappa-B ligand
ref-1	redox factor-1
rh sCD4	recombinant human soluble CD4
RNS	reactive nitrogen species
R-OH	alcohol
R-OOH	hydroxyperoxide derivate
ROS	teactive oxygen species
rpm	tevolutions per minute
RPMI	Roswell Park Memorial Institute medium
R-SOH	sulfenic acid derivate
RT	room temperature
SBP	streptavidin-binding peptide
s.	see / siehe
sc	subcutaneous
sCD4	soluble CD4
SD	standard deviation
SDS-PAGE	sodium dodecyl sulfat polyacrylamid gelelectrophorese
SecCys	selenocysteine
Ser	serine
SF	synovial fluid
SH	thiol
SLP-76	SH2 domain containing leukocyte protein of 76kDa
S_N2	bimolecular nucleophilic substitution
SS	disulfide Bridge
SSC	side scatter channel
STAT	signal Transducers and Activators of Transcription
STS	Sulfo-tag labelled streptavidin
System x_c^-	cystine – L-glutamate antiporter
TAM	Trx80 activated monocytes
TBP-2	Thioredoxin binding protein-2
TBS	Tris-buffered saline
TCR	T-cell receptor
TE buffer	Tris – EDTA buffer
Teff	effector T-cells
TGF-β	transforming Growth Factor beta
TGR	thioredoxin glutathione reductase
Th	T-helper cell
TIGIT	T-cell immunoreceptor with Ig and ITIM domains
TLR	toll-like receptor
TMB	3,3′,5,5′-Tetramethylbenzidine
$TMM(PEG)_{12}$	(Methyl-PEG_{12})$_3$-PEG_4-Maleimide
TNF-α	tumor necrosis factor alpha
Tregs	regulatory T cells
Tris	tris(hydroxymethyl) aminomethane
TRP	transient receptor potential
Trx1	thioredoxin-1
Trx80	truncated thioredoxin
TrxR	thioredoxin reductase
TXNIP	thioredoxin interacting protein
UV	ultraviolet
V	variable
V	Volt
VDUP1	vitamin D3 unregulated protein 1
vs	versus
w/v	weight per volume
w/w	weight per weight
ZAP-70	zeta-chain-associated protein kinase 70
κ	kappa

Amino acids

Ala	A	Alanine
Arg	R	Arginine
Asn	N	Asparagine
Asp	D	Aspratic acid
Cys	C	Cysteine
Glu	E	Glutamic acid
Gln	Q	Glutamine
Gly	G	Glycine
His	H	Histidine
Ile	I	Isoleucine
Leu	L	Leucine
Lys	K	Lysine
Met	M	Methionine
Phe	F	Phenylalanin
Pro	P	Proline
Ser	S	Serine
Thr	T	Threonine
Trp	W	Tryptophan
Tyr	Y	Tyrosine
Val	V	Valine

1 Abstract

The humanized non-depleting anti-CD4 monoclonal antibody Tregalizumab (BT-061) is able to selectively activate the suppressive function of regulatory T-cells and has been investigated up to phase 2b in clinical trials in patients suffering from rheumatoid arthritis (RA).

A pharmacokinetic-pharmacodynamic model, which is based on clinical data from RA and healthy subjects, used the cell surface CD4-down-modulation as marker of the antibodies' activity. This model surprisingly revealed a stronger effect of Tregalizumab in healthy subjects compared to RA patients. This thesis presents a series of experiments performed to understand this phenomenon.

To counteract oxidative stress, which is strongly associated with RA pathophysiology, the organism employs the small oxidoreductase thioredoxin-1 (Trx1). Therefore, augmented expression and secretion of Trx1 was seen in many studies the synovial fluid and plasma of RA patients. Moreover, the binding site of Tregalizumab is in close proximity to a disulfide bond in domain 2 (D2) of CD4, which is a known target for a reduction by Trx1. So, this thesis also evaluated the influence of Trx1 on binding of Tregalizumab to its target CD4.

With the experiments reported herein, it was possible to demonstrate that specific reduction of the D2 disulfide bond of CD4 by Trx1 led to diminished binding of Tregalizumab to recombinant human soluble CD4 (rh sCD4) and membrane-bound CD4 on T-cells from a human leukemia cell line and peripheral blood mononuclear cells (PBMC). Moreover, the experiments revealed that this caused changes in the Tregalizumab-induced CD4 signalling pathway via the lymphocyte-specific protein tyrosine kinase $p56^{Lck}$.

In summary, this thesis provides evidence that high Trx1-levels in RA patients compared to healthy subjects are a potential valid reason for diminished binding of Tregalizumab to CD4-positive T-cells and offers an explanation for the observed decreased CD4 down-modulation in RA patients in comparison with healthy subjects. It emphasizes that binding of Tregalizumab is impaired in a particular way in RA patients.

2 Introduction

2.1 The immune system

The immune system assures the defence against microbial attack and tumor development, thereby, keeping autoimmunity in check. To defend the organism from dangerous pathogens, a complex system of different mechanisms has been developed over the course of evolution to counteract viruses, bacteria, fungi or parasites. It can be distinguished between the innate and the adaptive immune system, at what different specialized sentinels are responsible for clearly defined functions. Besides inter alia mucus membranes and skin, which account for the physical barrier in humans, various cells are responsible for the first defence. Pathogen structures can be recognized in an unspecific way by different cells, which belong to the innate immune system. Macrophages (and monocytes as their precursors) are localized in many tissues. As one of the first defense cells, they are able to eliminate infectious agents by phagocytosis. Moreover, mast cells, granulocytes, natural killer cells and dendritic cells are parts of the innate immune system. This group has to be distinguished from cells of the adaptive immune system, which are highly specialized; however, they intervene delayed in time. T lymphocytes (T-cells) and B lymphocytes (B-cells) rank among cells with highly specific tasks and exhibit a big, round nucleolus. B cells develop in the bone marrow and express B cell receptors (BCR) on their cell surface, which represent immunoglobulins and which are anchored in the membrane. In contrast, T cells derive from the thymus and recognize pathogens by means of their T cell receptor (TCR)[1,2].

2.2 T-cells and CD4

T lymphocytes play an important role for the immune systems since they defend pathogens. Many subsets can be found within this lymphocyte population like T-helper cells, cytotoxic T-cells, memory T-cells, natural killer T-cells and regulatory T-cells[1,2].

Cytotoxic T-cells express cluster of differentiation 8 (CD8) on their surface interacting with the major histocompatibility complex (MHC) I. In contrast, cluster of differentiation 4 (CD4) is located on T helper cells and cooperates

with the MHC II[29,30]. T helper cells can distinguish between own and foreign antigens: the antigenic peptide is endocytosed and processed by antigen presenting cells (APC), like B-cells, dendritic cells (DC) and macrophages[1]. On their cell surface, these cells present antigen fragments with the help of MHC II (pMHCII) and which are recognized by T helper cells[1,30,31]. CD4-positive (CD4+) cells express the heterodimeric variable T-cell receptor (TCR) along with the invariant cluster of differentiation 3 (CD3) zeta complex[1,32]. Commonly, the TCR is formed by an alpha (TCRα) and beta (TCRβ) chain. However, few T-cells exhibit a gamma (TCRγ) and a delta (TCRδ) chain instead[1]. Signals are transduced into the cell by the CD3 complex consisting of two heterodimers (CDε/CDδ and CDγ/CDε) and a zeta chain homodimer (ςς)[1,33,34]. The intracellular parts of the CD3 chains exhibit immunoreceptor tyrosine-based activation motifs (ITAMs) facilitating signal transduction[34].

The glycoprotein CD4 acts as a co-receptor to the TCR-CD3-zeta complex by allowing and increasing the recognition of pMHC[35]. After TCR engagement and activation, CD4 recruits the lymphocyte-specific protein tyrosine kinase ($p56^{Lck}$), which belongs to the src kinase family[36]. $p56^{Lck}$ is closely linked to the cytoplasmic domain of CD4[37] resulting in signalling events in the T-cell after activation[36,38,39]. After phosphorylation of ITAMs by $p56^{Lck}$, SH2 domains of ZAP-70 are allowed to bind to the zeta-chains of the CD3 complex resulting in further signalling events[40]. Besides $p56^{Lck}$, the tyrosine-protein kinase Fyn ($p59^{Fyn}$) is essential for T-cell signalling, thereby, phosphorylating CD3 and ς immunoreceptor tyrosine-based activation motif[34,36,41–43].

The membrane bound CD4 molecule represents a 55 kDa glycoprotein and belongs to the immunoglobulin superfamily[44–46]. It is expressed by T-cells[47], dendritic cells, macrophages and monocytes[48], as well as eosinophiles[49] on the cell surface. CD4 is arranged in domains and can be divided into a C-terminal cytoplasmic domain (residues 419 - 458), a transmembran domain (residues 397 - 418) and four extracellular domains (D) located at the N-terminal side[50–52]. The extracellular part (residues 26 - 396) comprises D1 to D4 revealing a immunoglobulin-like structure[46,53,54]. The CD4 (UniProt P01730) molecule possesses a signal peptide of 25 amino acids required for import into the endoplasmatic reticulum and integration in the plasma membrane. According to

UniProtKB – P01730 ("CD4-Human"), D1 represents an Ig-like V-type, which comprises 100 amico acids (residues 26 - 125)[52]. In contrast, D2 features a length of only 78 amino acids (residues 126 - 203). Ig-like C2-type D3 includes position 204 – 317 and D4 that comprises amio acids 318 – 374[52].

Three disulfide bonds can be found in the whole CD4 molecule: D1, D2 and D4 exhibit free thiols, which can form disulfide bridges (see Figure 1)[55].

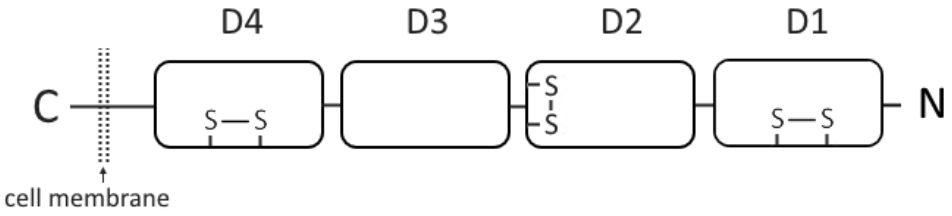

Figure 1: CD4 domain structure (schematic)

CD4 consists of 4 domains (D1 – D4) including three disulfide bonds (S-S). carboxyl-terminus (C) and amino-terminus(N). Graphic adapted from Sweet *et al.*[55] .

D1 shows a disulfide bridge between the B strand (Cys41) and the F strand (Cys109)[46,52,53,56]. As well, the disulfide bridge in D4 is arranged between the B (Cys328) and the F (Cys370) strand[52–54]. However, D2 is different from other domains. The disulfide bridge is located in the same sheet, between the C strand (Cys155) and the F (Cys184)[52] strand implying that the β barrel is cut[46,53,56]. Due to the special composition of this domain and high dihedral strain energy[57] the disulfide bond in D2 is redox active: it can be found in the reduced and oxidized form at the cell surface in equilibrium[25]. Many studies indicate that CD4 molecules operate by forming dimers or oligomers[58–61] and that the dimerization appears to play an crucial role in T-cell signalling[62]. D2 (Cys155 - Cys184) and D4 (Lys343 and Gln369) have been shown to be responsible for formation of these disulfide linked dimers [25,29,61,63]. Disulfide linked CD4 dimers of D2 are most presumably formed by conformational changes due to domain swapping and this seems to be the favoured co-receptor interacting with the pMCHII[64].

Once activated by the TCR-pMHC II and the costimulatory signal, CD4+ T-cells express the alpha unit of the IL-2 receptor (CD25) (first cloned in the 1980's[65–

[67]) and proliferate by an autocrine release of interleukin 2 (IL-2) which was first called the T-cell growth factor[1,68,69]. The activated T-cells can differentiate into various subtypes depending on the cytokine environment: differentiation of T helper cells 1 (Th1) cells is activated by interleukin-12 (IL-12) secreted by dendritic cells, monocytes and macrophages[70–72]. In contrast, Th2 cells are generated with help of interleukin-4 (IL-4)[1,72]. Moreover Th3, Th17, Th9 and Teff cells can be distinguished[73].

In infection, Th1 cells secrete IL-2, TNF-α and IFN-γ, thereby, activating again macrophages[71,74]. Th2 cells provide (besides the antigenic signal) a signal for B lymphocytes to become activated and to produce antibodies[1]. These cells release different cytokines like IL-4, IL-5, IL-6, IL-10, IL-13 and lymphotoxine-α[73,75]. T-cells are developed in the thymus from lymphoid progenitor cells by passing through positive and negative selection[76]. Cortical epithelial cells in the cortex of the thymus express self-antigens on MHC I or MHC II molecules. A positive survival signal is transmitted to thymocytes, which bind the MHC molecules in the right manner. This leads to CD4+ (interaction with MCH II) or CD8+ (interaction with MCH I) T-cells. Low or high affinity binding of MHC molecules do not induce a survival signal resulting in neglect of the thymocytes[1,2,76]. Thymic epithelial cells in the medulla are responsible for negative selection. Therefore, they transfer an apoptotic signal to cells, which show increased affinity with self-antigens, in order to destroy autoreactive T-cells[77]. Thus, autoimmunity in the periphery in prohibited. However, few self-reactive T-cells pass off from the thymus without selection. Thus, the organism needs further mechanisms preventing the induction of autoimmune diseases[1,2].

2.3 Regulatory T-cells control immune balance

One possibility for the human organism to control the immune balance is via CD4+ CD25+ FoxP3+ regulatory T-cells (Tregs), which can suppress autoreactive effector T-cells and prevent autoimmunity[78,79]. Tregs were identified in the early 1970; at that time called suppressor T-cells due to suppression of autoimmune response[80]. However, studies were paused until the IL-2 receptor α-chain (CD25) was found as a highly expressed[3], phenotypic marker by Sakaguchi in 1995[81]. Two subsets of Tregs are described: $CD25^{high}$

FoxP3+ Tregs derived from the thymus are named naturally occurring Tregs (nTregs)[82,83] representing the biggest population. Moreover, inducible Tregs (iTreg) were discovered arising from conventionally T-cells in the periphery of the body[83,84]. Helios, which belongs to the Ikaros family transcription factors, represents a new marker for nTregs and iTregs. The cells can exist as Helios+ and Helios$^-$ nTregs[85,86]. Studies revealed that Helios represents an important marker for activated regulatory T cells, which express latency- associated peptide (LAP) and Glycoprotein A repetitions predominant (GARP) and no FoxP3[87]. In the last years further surface markers of regulatory T-cells were identified. Besides CD25 (IL-2Rα), which was first discovered on CD4+ T-cells in mice[3], the transcription factor forkhead box-protein P3 (FoxP3) was found on Tregs playing a crucial role for Treg activity[88]. Mutations in the *Foxp3* gene lead to the IPEX syndrome (immune dysregulation, polyendocrinopathy, enterophathy, X-linked) resulting in disastrous immune dysregulation[89]. Thus, FoxP3 is essential for cell function and development of Tregs[90,91]. TNF-α can block expression of FoxP3. Therefore, Treg activation is suppressed via induction of protein phosphatase 1 (PP1). This results in dephosphorylation of Ser418, which is essential for FoxP3 activity[92]. However, FoxP3 expression is not restricted to Tregs. Conventional CD4+ T-cells transiently express small amounts of FoxP3 but do not exhibit any suppressive performance[93,94]. So, until now no specific and distinct Treg marker was discovered.

Before Tregs facilitate their regulatory function, they have to be activated by their TCR in combination with by IL-2[83]. The protein PTEN (Phosphatase and Tensin homolog) is essential for expression of the IL-2 receptor (CD25) and FoxP3[95,96]. IL-2 activation results in STAT5 signalling events. This is important for Treg activity due to binding of STAT5 to the *Foxp3* gene[97]. On the contrary, the phosphatidylinositol-3-OH kinase (PI(3)K) is also invoked by IL-2 which results in activation of protein kinase B (Akt) and mechanistic target of rapamycin (mTOR), and leads to an abrogated FoxP3 induction[98]. In contrast to Tregs, the lipid phosphatase PTEN is down regulated in T-cells after activation[95]. PTEN was found to catalyze the opposite reaction of PI(3)K and, therefore, blocks IL-2 receptor linked functions in Tregs[99]. So, PI(3)K is inhibited

by PTEN preventing mTor activation and retaining the suppressive function of Tregs[95,96].

The suppressive machinery of regulatory T comprises many components. Suppression of effector T-cells (Teff) can be achieved by usage of soluble factors or modulation of APC function[100]. Anti-inflammatory cytokines as TGF-β[101,102], IL-10[103] and IL-35[104] play a crucial role. Furthermore, the interacting APC can be regulated by Tregs: the coinhibitory molecule cytotoxic T-lymphocyte antigen 4 (CTLA-4, also known as CD152)[105] on Tregs can compete with CD28 on Teffs for interaction to CD80 (B7.1) and CD86 (B7.2) on APCs[106]. This is followed from a reduced T-cell activation[107]. Moreover, expression of indoleamine-2,3-dioxygenase (IDO) was shown to be increased via a recombinant soluble CTLA-4[108]. IDO usually triggers decrease of free tryptophan[109]. Degradation of tryptophan results in kynurenine and, therefore, in T-cell cycle arrest[110,111]. Glutathione (GSH) synthesis is also decreased generating a deficit of the essential amino acid cysteine, which cannot be produced by Teffs[112]. This alteration of redox environment contributes to an inhibition of proliferation of effector T-cells[112,113]. The lymphocyte-activation gene 3 (LAG-3, CD223), another coinhibitory molecule, is expressed on Tregs and binds to the MHC II molecule on dendritic cells, thereby, decreasing T-cell activation[114]. Moreover, TIGIT (T-cell immunoreceptor with Ig and ITIM domains) was found on Tregs suppressing Th1 and Th17 cells[115]. CD39, also called ectonucleoside triphosphate diphosphohydrolase 1 (ENTPD1), represents another component of the Treg suppression machinery[116]. CD39 (also CD73) acts as an ectonucleotidase and hydrolyzes ATP and AMP to ADP[117]. ADP is degradated into adenosine inducing cAMP production after binding to the adenosine A2 receptor on effector T-cells and dendritic cells. In turn, adenosine blocks ZAP-70 phosphorylation which causes inhibition of T-cell activation[118]. This cascade leads to a decreased effector T-cell signalling, a declined production of IL-2 and decreased expression of CD25[117,119]. Furthermore, immune suppression is induced[120].

Tregs were shown to up-regulate cAMP after activation[121]. cAMP is released to CD4+ effector T-cells and dendritic cells via gap junctions and blocks their proliferation and differentiation via possible inducible cAMP early repressor

(ICER) expression[122–124]. For this purpose, IL-2 expression is stopped by blockade of induction of nuclear factor of activated T-cell c1 (NFATc1/α)[125]. Moreover, release of granzyme and perforin by Tregs are described as suppression mechanism[126]. However, despite intensive research in this field, the exact molecular mechanism is not fully understood and has to be further elucidated.

Thus, Tregs play an important role in the regulation of the immune response since depletion of these cells lead to organ-specific autoimmune affliction[127,128]. In autoimmunity activity of CD4+CD25+ regulatory T-cells is impaired or decreased counts of regulatory T-cells can be found[129]. To give a reason for this, several possibilities are conceivable. For example, defective CTLA-4 performance is found in Tregs in Rheumatoid Arthritis (RA)[130], which is caused by methylation of a NFAT binding site of the *Ctla4* promotor leading to defective IDO expression[131]. Moreover, obstruction of Treg activity can be caused by cytokines, like TNF-α, due to TNF-α therapy rehabilitate their function[132]. Impaired FoxP3 activity is one explanation of decreased Treg activity after TNF-α exposure. Usually the phosphorylation site in the C-terminal FoxP3 domain (Ser418) is phosphorylated[92]. However, in RA patients TNF-α induces protein phosphatase 1 (PP1), which dephosphorylates Ser418 and accounts for impaired FoxP3 activity leading to hindered Treg function[92]. Moreover, in humans Ser422 of FoxP3 was found to be phosphorylated by PIM1 kinase that decrease suppressive function of Tregs[133].

Another reason is a link between RA and microbial infections, which play a role in this autoimmune disease[134]. These microbial compounds induce the toll like receptor pathway resulting in increased expression of coinhibitory molecules on dendritic cells and generation of IL-6[135]. This was found to decrease the suppressive mechanism of CD4+ CD25+ regulatory T-cells[135].

2.4 Rheumatoid Arthritis

Rheumatoid Arthritis (RA) represents a chronic-inflammatory autoimmune disease that shows a prevalence of 0.5 – 1 % in the world population and causes restriction of quality of life and high socioeconomic costs[7,8]. Compared

to male patients, women are afflicted three times more often[136]. Patients suffer from synovitis and structural damage of cartilage and bone[8] accompanied by systemic manifestations like vascular diseases, metabolic syndrome, cognitive dysfunction and osteoporosis[10]. Swollen joints, progressive destruction of cartilage and limited mobility represent further features of RA[10]. Moreover, auto-antibodies like rheumatoid factor and anti-citrullinated protein/peptide antibodies (ACPA) can be found in the plasma of many patients and these are fostered by environmental and genetic parameters[137]. The mortality rate of male RA patients is increased compared to healthy people[138]. One study described a mortality rate of RA patients by about 50% within 11 years, however causes of death were diverse[139].

The aetiology of this autoimmune disease is not completely understood yet. However, it is known that RA is associated with an interplay of several factors like environmental parameters[137] (cigarette smoking[140–142]), epigenetic modifications and genetic disposition[7,137,143,144]. Patients exhibiting anti-citrullinated protein antibodies (ACPAs) show a connection to human leukocyte antigen (HLA)[145]. Here, ACPAs are detectable before beginning of symptoms[146]. Some allels of the HLA-DRB_1 locus denote a difficult progression of the disease[147], at which one region (named the shared epitope) is susceptible to RA[148,149].

Besides a genetic predisposition, cytokines play a crucial role in the pathogenesis of RA. Significant high levels of several cytokines were found to be increased in RA patients[150]. TNF-α, IL-1α/β and IL-6 stimulate T-cells and other cells and contributes to the inflammation[151]. IL-6 accounts for several complaints in RA[152,153]. Furthermore, high levels of the lymphoid lineage growth factor IL-7[154], Natural Killer cell (NK) activator IL-15[155], respective IL-15 receptor alpha[156] are found in RA patients. In addition, a crosstalk between NK cells and monocytic cells also plays a pivotal role. Macrophages secrete IL-15[155], which stimulates CD69 expression in NK cells and INF-γ generation. In turn, INF-γ facilitates IL-15 production resulting in sustained TNF-α synthesis[157]. Furthermore, Th1 cells and other cells are brought into action by IL-12, IL-15 and synergistic help of IL-18 that mediates INF-γ release[158,159]. IL-32 and IL-33 were also found to contribute to the pathogenesis of RA[160,161].

Adhesion molecules, chemokines and growth factors as granulocyte-macrophage colony-stimulating factor (GM-CSF) and receptor activator of nuclear factor kappa-B ligand (RANKL) are of importance in the pathogenesis of RA[162–164]. They promote the influx and maturation of effector cells (like mast cells, natural killer cells and macrophages) into the synovium. Macrophages secrete IL-1 beta, TNF-α and other cytokines after activation by pattern-recognition receptors (PRRs) (e.g.: pathogen-associated molecular patterns (PAMPs): toll-like receptors (TLRs) and nucleotide-binding oligomerization domain like receptors (NLRs) as well as damage-associated molecular patterns (DAMPs)), due to infective agents or others activators[165–167]. This is followed from generation of matrix metalloproteinases (MMPs), which are released from synoviocytes[168]. These enzymes are responsible for the degradation of the extracellular matrix since RANKL accounts for degradation of bone due to activation of osteoclasts[162].

The TNF members B lymphocyte stimulator (BLyS) (also called B-cell activating factor (BAFF) and a proliferation-inducing ligand (APRIL) promote CD20 and CD22 expressing B-lymphocytes to become activated[169–171]. They differentiate into plasma cells producing antibodies like rheuma factor (IgG) or anti-citrullinated peptides (ACAPs) antibodies, which form immune complexes[172]. In turn, these complexes can contribute to production of cytokines by mononuclear cells, like TNF-α[173]. In addition, APRIL was found to trigger Th17 response[174].

IL-17A/F, IL-21 and IL-23 are responsible for activation and expansion of Th17 cells[175–177], which are associated with many autoimmune diseases[178]. Th17 cells represent long-living effector memory cells[179] playing a further role besides Th1 cells. Th17 cells are primarily considered to mediate the inflammation[178,180,181]. Moreover, large numbers of CD161+ Th17 lineage cells were found in the RA joints[182]. However, they appeared to be resistant to highly proliferative and functional Tregs[182]. This simply suggests that these CD161+ Th cells play a leading role in the RA disease process.

2.5 Therapy of Rheumatoid Arthritis

To break the vicious circle of RA several drugs for the therapy are available. Non-steroidal anti-inflammatory drugs (NSAIDs) and glucocorticoids are often used to decrease symptoms of RA. NSAIDs inhibit the cyclooxygenase 1 and/or 2 (COX-1/-2), thereby, blocking synthesis of prostaglandins, which are responsible for inflammation for example[183,184]. Glucocorticoids exhibit anti-inflammatory and immune-suppressive properties in many ways like inhibition of NF-κB and other cytokines (e.g.: IL-1, IL-2, IL-3, IL-4, IL-5, IL-6, IL-8, IFN-γ and GM-CSF)[185,186]. Moreover, the production of prostaglandins and leukotrienes is blocked via inhibition of COX and stimulation of annexin A1 (lipocortin-1) synthesis[184,187]. To alter the immune response for a longer term, disease-modifying anti-rheumatic drugs (DMARD) are indispensable[188]. Methotrexate (MTX) inhibits the dihydrofolate reductase and is used as first line therapy[189,190]. If side effects occur under MTX therapy, leflunomide or sulfasalazin can be applied. Teriflunomid, the active metabolite of leflunomide, inhibits dihydroorotate dehydrogenase, thereby, blocking pyrimidine synthesis[184,191]. Sulfasalazine is split into sulfapyridine and mesalazine (5-aminosalicylic acid, 5-ASA) in the colon[184]. 5-ASA acts anti-inflammatory by blocking the IL-1 stimulated NF-κB pathway[192] and TNF-α[193]. Other options represent the gold complex auranofin and the malaria agents chloroquine and hydroxychloroquine[184,188]. In the last decads, the new group of biologicals was developed that interferes with certain targets in the pathogenesis of RA. As example, adalimumab, infliximab or etanercept bind TNF – α and play an important role in the therapy of RA[194,191]. Anakinra represents an interleukin-1 receptor antagonist whereat tocilizumab binds IL-6[195]. The fusion protein abatacept (CTLA-4 with IgG1) interacts with CD80 (B7.1) and CD86 (B7.2) on APC, thereby, inhibiting the costimulatory signal CD28 in the T-cell activation process[196].

2.6 Oxidative stress in RA

Apart from environmental and genetic triggers, oxidative stress (defined as the imbalance of production of reactive nitrogen or oxygen species (RNS, ROS)) is considered to be one possible elicitor in the development and diseases activity

of rheumatoid arthritis[11,12,197,198]. In the non-stressed situation, cells sustain a reduced state in the cytoplasm, which is ensured by high levels of the intracellular redox buffer glutathione (GSH). So, GSH concentrations of 0.5 mM to 10 mM are typically found[27]. Therefore, most of the cysteines exist as thiols (-SH). In the extracellular compartments the thiols are oxidized forming disulfide bridges due to a highly oxidizing environment[199]. In the endoplasmic reticulum reduced GSH forms equilibrium with oxidized glutathione (GSSG) showing a ratio of about 1:1 outside the cell. In thy cytosol the ratio of GSH/GSSG reaches 30:1 to 100:1[200]. Consequently, GSH is important for antioxidative protection of the cell from ROS.

Usually, ROS play a pivotal role in intracellular signalling in healthy tissue[201,202]. However, in RA, generation of ROS is increased and ROS generation in synovial fluid T-cells of RA patients is fostered by the Ras signalling molecule[13,203,204]. This indicates that pathogenesis of RA is linked to an impaired function of these synovial T-cells.

Moreover, the redox balance is disturbed in RA patients and oxidative stress occurs due to a low GSH concentration and a high ROS content[205]. Oxidative stress is responsible for hyporesponsiveness of synovial T-cells, which is linked to defective synovial T-cell receptor signalling[206] and diminished levels of GSH[15]. So, low GSH levels inside the cell cause a conformal change to a cytosolic localisation of linker for activation of T–cells (LAT), which is therefore, displaced from the membrane. This results in defective T-cell signal transduction and hyporesponsiveness[205,207]. Moreover, the oxidative stress caused T-cell hyporesponsiveness was detected to be triggered by alterations of $p56^{Lck}$, LAT and the C-terminal region of the TCR zeta chain due to proteosomal degradation and protein modification[208].

Matrix components are susceptible for oxidative stress and can be altered by ROS due to apoptosis of chondrocytes, decreased synthesis of matrix molecules or direct molecule impairment[201]. So, the DNA damage, based on oxidative stress, can also be observed in RA patients[209,210].

However, there are many studies describing a protective role for ROS in connection with autoimmune diseases[211]. For example, ROS produced from

NADPH oxidase is important for Tregs' suppressive mechanism that is connected to TGF - β[212]. This indicates that the role of ROS is more complex than originally expected and has to be further elucidated.

In contrast to GSH, levels of the thiol-disulfide oxidoreductase thioredoxin-1 (Trx1) were found to be augmented in patients suffering from RA[15,16]. Moreover, expression and secretion of Trx1 by human regulatory T-cells is much higher compared to effector T-cells[213]. Beside GSH, thioredoxin is also able to protect cells from oxidative stress by defining the redox state of protein via a thiol-disulfide exchange reaction. Hence, to counteract high levels of oxidative metabolites the organism involves Trx1, which is released at the site of inflammation[214] and plays an important role in oxidative stress.

2.7 Thioredoxin system

Trx1 is a 12kDa redox protein, which is able to reduce proteins in a cysteine-disulfide exchange reaction by means of thioredoxin reductase (TrxR) and NADPH[14]. Many organisms - as bacteria, plants and mammals - exhibit a thioredoxin system revealing its general importance[14,215]. Thioredoxin was first described by Peter Reichard in 1964[216] and belongs to the thioredoxin superfamily. This family includes thioredoxin, glutaredoxin, glutathione S-transferase, glutathione peroxidase, protein disulfide isomerase and the bacterial DsbA[217,218]. All members of this family exhibit a characteristic and highly conserved -Cys-X-X-Cys- sequence called the thioredoxin-motif: they share a thioredoxin fold describing five stranded β-sheets, which are surrounded by four α-helices[219,220]. Five cysteine residues can be found in the molecule: besides the two active side cysteines (Cys32 and Cys 35), three other disulfide bonds exist in the protein (Cys(62), Cys(69) and Cys(73))[221,222]. These additional residues are prone to oxidation resulting in inactivation of the molecule due to aggregation[223]. However, dimerization can be inhibited by glutathionylation of Cys(73) in T-cells during oxidative stress[224,225]. Another modification represents the S-nitrosylation of Cys(69) which is important for anti-apoptotic effects, preserves Trx1 activity and shows an important function for the scavenging of ROS[226,227].

2.7.1 Reaction mechanism of Trx1

The two residues in the active site exert the thiol disulfide reaction[221]. Cys(32) has a low pKa value and serves as nucleophile[228]. The thiol exchange reaction is postulated as follows[228]: The target protein disulfide is attacked by the N-terminal thiolate (Cys (32)) of the thioredoxin Trx1-$(SH)_2$ molecule serving as a nucleophile. The intermediate, formed by this bimolecular nucleophilic substitution (S_N2), is then reduced with help of the C-terminal cysteine (Cys35) in the active site of Trx1. The inactive and oxidized Trx1-(SS) is subsequently reduced by TrxR with help of NADPH resulting in the active form[228–231] (Figure 2).

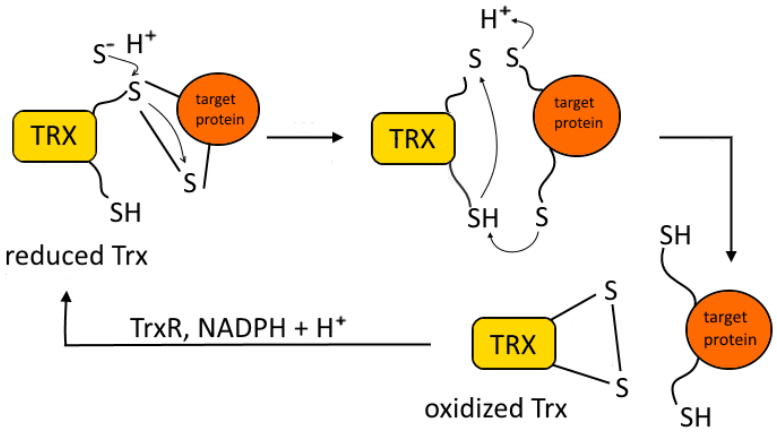

Figure 2: Reaction mechanism of thioredoxin in its physiological system

Trx1 exerts its reducing function with help of TrxR and NADPH. The active site cysteine of Trx1 attacks the target protein via the nucleophilic thiol sulfur. The arising mixed disulfide intermediate is reduced by the other active site cysteine. Consequently, the target protein presents two thiol groups and the oxidized Trx1 can be reduced by TrxR and NADPH to restart the catalytic cycle[228].

Also worth mentioning is that, different reaction mechanisms are discussed after the first occurring Michaelis-Menten S_N2 pathway. For example, a bimolecular elimination E2 competing with the S_N2 mechanism is described[232].

Two thioredoxin forms are known: Trx1 is located in the cytoplasm, on the contrary, Trx2 can be found in the mitochondria[233,234].

Trx1 is secreted by fibroblasts, airway epithelial cell, activated monocytes and lymphocytes in a non-conventional secretion pathway[235]. The mechanism is not fully understood. However, Trx1 release from T-cells (in consequence of

oxidative stress) is probably controlled by a negative feedback, which involves reactive species like H_2O_2[236].

2.7.2 Trx1 plays an important role in oxidative stress

Oxidative stress represents one field in which Trx1 plays an important role since the oxidoreductase reduces disulfides, thereby, keeping a reduced environment inside the cell.[237] Hence, besides the glutathione/glutaredoxin system, Trx1 is one responsibility for the protection of oxidative stress and a detoxify mechanism of cells[237]. Oxidative stress accounts for several diseases like malignant neoplasm, diabetes mellitus, cardiovascular diseases, inflammatory bowel diseases or autoimmune diseases[238]. Reactive species, which can be generated by endogenous or exogenous factors, cause DNA damage, lipid or protein oxidation[239,240]. This can be favoured by oxidative phosphorylation or electron transport in the mitochondrion, as well as UV radiation or ionizing radiation[237,239].

So, the thioredoxin system accounts for one protection mechanism which acts as a scavenger of ROS. One example for ROS is hydrogen peroxide[241]. To control hydroperoxide (ROOH) levels peroxiredoxins (Prxs, initially called thioredoxin peroxidase) are a ubiquitous, thiol-specific[242] enzymes with antioxidant properties since they are able to catalyze reduction of hydrogen peroxide (H_2O_2) and other organic hydroperoxides[243]. In mammalian organisms six isoenzymes of Prxs (Prx1 to Prx6) are known: they possess redox active sites with thiol groups as reducing equivalents and exhibit the thioredoxin fold[243]. Prx1, Prx2, tryparedoxin peroxidase[244] and AhpC[245] represent the typical 2-Cys peroxiredoxins. However, Prx5 is classified as atypical 2-Cys peroxiredoxin[243]. In addition, a 1-Cys peroxiredoxin (Prx6) exists[246]. The three classes differ from each other due to their recycling mechanisms and structure regarding number of redox-active cysteines[243].

For detoxification, Prxs react with H_2O_2 and get inactive after oxidation. The reduced (R-SH) cysteines in the active site (peroxidatic cysteins; C_P) of Prxs act as reducing equivalents[247]. After reduction of the peroxide, Prxs become oxidized to a disulphide bridge (R-S-S-R) via a cysteine sulfenic (R-SOH)

intermediate[243,247]. Simultaneously, hydroxyperoxide (R-OOH) is reduced to the corresponding alcohol (R-OH)[247]. The oxidized and, therefore, inactive enzyme is recycled with help of the thioredoxin system reducing the oxidized Prx back to the reduced thiol form[243,248]. However, 1-Cys Prxs use GSH for reduction to the active enzyme[249,250]. This is another example for the protection mechanisms supported by thioredoxin.

2.7.3 Other functions of Trx1

Another function of Trx1 is the regulation of apoptosis signal-regulating kinase 1 (ASK1), which belongs to the MAP kinase kinase kinase family and induces apoptosis and inflammation[251]. ASK1 is activated, amongst others, by oxidative stress (H_2O_2), lipopolysaccharide (LPS), TNF receptor and other stimuli that comprise a generation of ROS[251]. This leads to the activation of c-Jun N-terminal kinase (JNK) and the p38 MAP kinase pathway[252]. Cys(32) of reduced Trx1 binds to the N-terminal site of ASK1 forming a complex and, thereby, suppressing kinase's activity[253]. Activated by ROS, Trx1 is oxidized and dissociates from the complex[254]. Subsequently, ASK1 is activated, which leads to apoptosis of the cell[254]. In addition, ASK1 is ubiquitinated via Trx1 resulting in its degradation[255]. However, the stable disulfide-linked interaction of Trx1 and ASK1 can be inhibited by thioredoxin interacting protein (TXNIP), which is also called thioredoxin binding protein-2 (TBP-2) or vitamin D3 unregulated protein 1 (VDUP1)[256]. A mixed disulfide bond is generated between the reduced active site Cys(32) of Trx1 and the oxidized TXNIP[256]. As a result, activity and performance of Trx1 is blocked[257,258]. TXNIP and Trx1 show important function in the genesis of autoimmune disorders, malignancies and diabetes[259]. Recent studies have shown that TXNIP is able to bind to NLR protein 3 (NLRP3) after dissociation from Trx1[260]. This dissociation can be evoked by ROS[261]. The association of TXNIP and NLRP3 leads to activation of the inflammasome involving caspase-1 and release of active IL-1β[260] being an essential molecule for inflammatory events[261].

In relation to inflammatory diseases, especially RA, reduced Trx1 was found to activate transient receptor potential (TRP) channels, which are located in CD55+ fibroblast-like synoviocytes that are inflamed in this disease [262,263]. This

indicates that Trx1 is also able to activate ion channels in addition to its role as redox protein.

Some studies have revealed that Trx1 can also stimulate cell proliferation and cytokine by acting as a chemokine and co-cytokine[264–266]. Furthermore, Trx1 regulates many transcription factors for example the redox factor-1 (ref-1)[267,268], hypoxia-inducible factor 1 (Hif-1)[269] and activator protein 1 (AP-1)[270,271]. Tumor suppressor proteins p53[248] and protein phosphatase and tensin homolog (PTEN)[272,273] were also found to be controlled by Trx1.

Moreover, Trx1 is involved in the regulation of the NFκ-B signalling pathway: The p50 subunit of NF-κB encloses a cysteine (Cys(62))[274], which is sensitive to oxidation and can be reduced by Trx1[275,276]. In the cytoplasm Trx1 inhibits the dissociation of IκBα. So, the degradation of Trx1 is suppressed by the proteasome, which would lead to the translocation of NFκ-B to the nucleus. However, in the nucleus Trx1 is responsible for the linking of NF-κB to its B site resulting in NF-κB dependent gene expression[277]. Nucleoredoxin and glutaredoxin, which also belong to the redox regulation molecules, have similar functions like thioredoxin[278].

2.8 Thioredoxin-80

Besides Trx1 (*TXN* gene) and Trx2 (*TXN2* gene), a truncated form of thioredoxin (Trx80) exists that reveals totally different functions than Trx1[279]. It was first discovered in patients suffering from schistosomiasis and was initially named eosinophil cytotoxicity-enhancing factor (ECEF)[280] since it augments cytotoxic function of eosinophils[281,282]. Trx1 is cleaved into the 10 kDa protein Trx80, which includes the 80 N-terminal amino acids of thioredoxin[279,283]. Compared to Trx1, the truncated Trx80 form lacks the carboxy-terminus and therefore the typical thioredoxin fold explaining the missing reductase activity[283,284]. Moreover, Trx80 exits as a homodimer in solution[279], is mainly produced by CD14+ monocytes[282], and activates them to differentiate into Trx80-activated monocytes (TAMs)[284,285]. This process comprises the stimulation of the MAP signalling pathway p38, extracellular signal-regulated kinase (ERK) and c-Jun N-terminal kinase (JNK)[285]. A study revealed the

release of interleukin 12 (IL-12) from CD40+ monocytes in PBMC culture after Trx80 involvement and showed expression of CD14, CD40, CD54 and CD86[286]. Moreover, increased expression of CD14+ monocytes after Trx80 treatment was seen[286].

There are many functions of Trx80 of which are only a few briefly presented. Trx80 has mitogenic cytokine activity regarding resting PBMC[284]. With respect to cytokines, production of the anti-inflammatory cytokine IL-10 can be induced by Trx80 mediated TAM activation as well as release of the inflammatory cytokines TNFα, IL-1β, IL-6 and IL-8[285]. Moreover, expression of IFN-γ in T-cells in human PBMC culture were detected after incubation with IL-2 in combination with Trx80[286]. Besides, Trx80 has chemoattractant properties with regard to T-cells, neutrophils and granulocytes[279].

2.9 Thioredoxin reductase

2.9.1 Forms

Trx1 exerts its function with help of the flavoenzyme thioredoxin reductase (TrxR) catalyzing the reduction of oxidized Trx1 to reduced Trx1 by use of NADPH[287]. Besides a low molecular weight TrxR (35 kDa, found in prokarytoes, archea and low eukaryotes), a high molecular weight TrxR (55 kDa, expressed in higher eukaryotes) containing a selenocysteine residue at the carboxy-terminal elongation[288] are described[289].

Three forms of human thioredoxin reductases are known up to now. These are encoded by three genes (*TXNRD1, TXNRD2*, *TXNRD3*) resulting in the cytosolic TrxR1, mitochondrial TrxR2 and thioredoxin glutathione reductase (TGR, testis specific)[290]. For TrxR1 and TrxR2 various alternative splice forms are described[290]. As described before, the TrxR contains a selenocysteine within the conserved Gly-Cys-SecCys-Gly motif at the carboxy-terminal end, which is also observed in all mammalian TrxRs[288,291]. Moreover, a Cys(59)-Val-Asn-Val-Gly-Cys(64) sequence is found in the active site of the oxidoreductase revealing a higher homology with glutathione reductase compared to TrxR of *Escherichia coli* (Cys-Ala-Thr-Cys)[292–294]. The catalytic site of the mammalian

TrxR is located in the flavin adenine dinucleotide (FAD) domain; on the contrary the catalytic site of the *E.coli* domain is found in the NADPH domain[293].

The utilization of selenocysteine makes this system exceptional and recombinant expression of TrxR difficult. However, the reactive active site of TrxR enables the reduction of various substrates due to its high reactivity[287]. Thus, mammalian TrxR exhibit a broader substrate spectrum compared to the TrxR from *E.coli*[223,295]. Besides Trx1, this allows reduction of substrates like DTNB (Ellman's reagent)[223] or selenite[296] as example. TrxR can be found at concentrations of approximately 18 ng/mL in the plasma and is secreted by peripheral blood mononuclear cells, monocytes and some tumor cell lines[297].

2.9.2 Mechanism

As lipoamide dehydrogenase, glutathione reductase and mercuric reductase, TrxR belongs to the homodimeric flavoenzyme family[289]. This group of pyridine nucleotide disulfide oxidoreductases uses FAD as a prosthetic group to catalyze the transport of electrons from NADPH to the disulphide in the active site of the enzyme[287,289].

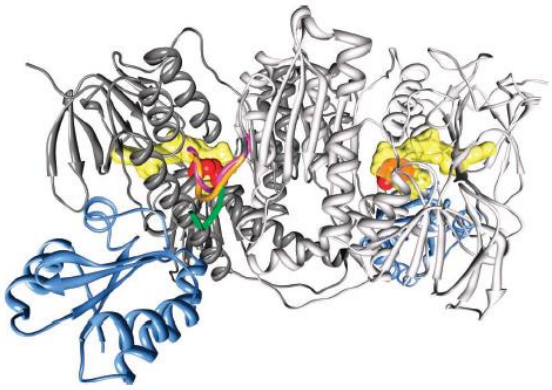

Figure 3: Trx1 is bound by TrxR

Human Trx1 (blue) is shown in complex with its partner TrxR1 (grey, shown as dimer). FAD is depicted in yellow. The N-terminal redox center is shown in red. Graphic adapted from Fritz-Wolf et al.[228].

Since the catalytic site of mammalian TrxR is located in the FAD domain, the active site cysteines are in close proximity to the isoalloxazine ring of FAD[287,298]. Consequently, electrons can be transferred from the closely bound NADPH via FAD to the reduced disulphide bridge of catalytic site of TrxR. Accordingly, the oxidized carboxy-terminal catalytic site (including the selenocysteine) is reduced after a thiol-disulfide exchange. On the other hand the Cys-Val-Asn-Val-Gly-Cys catalytic site is oxized. After this step the selenocysteine containing active site moves away and transfers electrons to the substrate (e.g. thioredoxin) resulting in reduction of the disulphide bridge[287,299].

In summary, thioredoxin catalyzes the following reaction with help of TrxR and NADPH[223]:

$$\text{Trx-(SH)}_2 + \text{protein-S}_2 \rightleftharpoons \text{Trx-S}_2 + \text{protein-(SH)}_2$$

$$\text{NADPH} + \text{H}^+ + \text{Trx-S}_2 \xrightleftharpoons{\text{TrxR}} \text{NADP}^+ + \text{Trx-(SH)}_2$$

Due to this mechanism, there are some protocols described involving dithiothreitol (DTT), Ellman's reagent (DTNB) or insulin to determine the activity of TrxR or thioredoxin photometrically[300].

2.10 Redox regulation of T-cell function

T-cell activation is accomplished in the immune synapse including TCR – MHC II engagement, cytokine release and costimulatory signals via antigen presenting cells (CD80 (B7.1) and CD86 (B7.2)) and T-cells (CD28)[1]. Depending on the predominant redox potential, apoptosis, proliferation, differentiation or growth arrest of cells occur[301]. This regulation is kineticly controlled in each zone and is not subjected to equilibrium[302].

Besides Trx1 and glutathione (GSH/GSSG), cysteine/cystine (Cys/Cys_2) control the redox potential in different compartments[303]. Naive T-cells reveal a deficit of the cystine transporter. For this purpose, they require DC to take up cysteine to supply their indispensable GSH synthesis for a proliferative response[304–306]. Cystine is included by dendritic cell's system x_c-, which is a cystine – L-glutamate antiporter[307]. Inside the cell, Cys_2 is converted into Cys via GSH, which is secreted and converted into Cys with help of γ- glutamyltranspeptidase and a dipeptidase[308,309]. Cysteine is now located in the extracellular compartment and can be taken up by T-cells. The conversion of cystine into cysteine is supposed to be conduced by Trx1[309], which is released by many cells, especially activated lymphocytes[235,310]. To stop an overshooting immune reaction, regulatory T-cells are able to control the GSH metabolism via dendritic cells to impact effector T-cells[112]. Tregs can reduce the extracellular cysteine pool *in vitro*[308]. They interact with their CTLA-4 molecule with CD80 (B7.1) and CD86 (B7.2) on DC, thereby, blocking its GSH synthesis[112,311]. Moreover, Tregs

include cysteine competing with T-cells resulting in an inhibited T-cell activation and proliferation[112].

2.11 Tregalizumab (BT-061)

2.11.1 Background, development and structure

Tregalizumab (BT-061) is a humanized monoclonal antibody, which is developed by Biotest AG, Dreieich, Germany. The antibody exerts its agonistic function by binding to a unique, non linear epitope on D2 of the human CD4 molecule and induces an intracellular signalling cascade involving the protein tyrosine kinase p56^{Lck} [22]. Tregalizumab is descended from the murine anti-CD4 antibody B-F5, which was tested in some autoimmune diseases in the 1990s[312–314]. To administer higher dosages and to avoid immunogenicity, complementary determining regions (CDR) grafting was applied to humanize the murine predecessor, then referred to hB-F5[315], which was further developed to Tregalizumab. As an IgG_1 antibody, Tregalizumab is composed of two heavy chains and two light chains, connected by disulfide bonds with a molecular weight of approximately 150 kDa[23]. A glycosylation site can be found in the Fc-part of the antibody including a glycoprotein linked to an asparagine residue. The manufacturing process of this monoclonal antibody uses SP2/O cells which are cultivated in a bioreactor.

2.11.2 Tregalizumab binds to CD4

Tregalizumab binds to a non-linear epitope on D2 of the human CD4 molecule (Figure 4)[22,23]. Amino acids 148-154, 164-168, 185, 187, 189-190 and 192 of the CD4 molecule are involved in the binding, which was evidenced by a 2.9 Å-resolution crystal structure[22,316]. The binding pocket of CD4 interacts via hydrogen bonds and polar interactions with Tyr(105) of the Tregalizumab heavy chain[22]. Moreover, Tyr(34) and Arg(104) to Asp(106) of the light chain are involved using hydrogen bonds, respectively polar interactions[22,317]. Affinity measurements revealed a dissociation constant (K_D) of Tregalizumab of approximately 2.0 nM by applying surface plasmon resonance and a sensor chips coated with soluble CD4.

Since Tregalizumab binds to the opposite side of the extracellular part of CD4 than the MHC class II molecule, sterically interference with MHC II is not given[22]. After binding of Tregalizumab to the CD4 molecule a conformal change of the CD4 molecule can be observed (Figure 5).

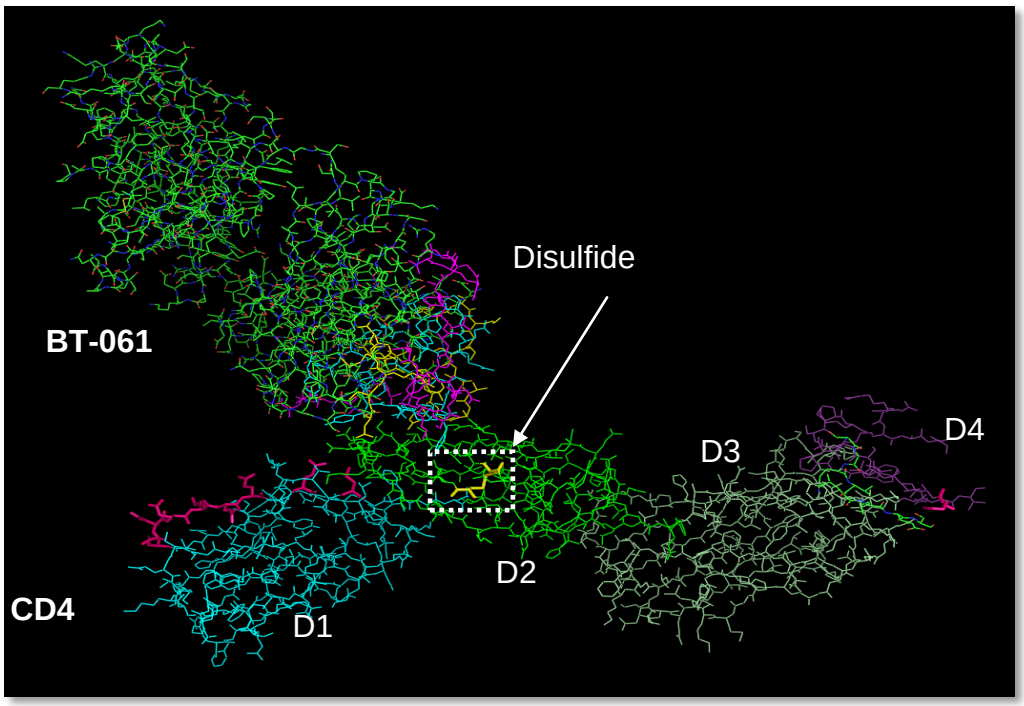

Figure 4: A disulfide bridge is located in the Tregalizumab and CD4 dimerization sites

Tregalizumab binds to a specific epitope on D2 of the CD4 molecule where a disulfide bridge is located. *Modified*: Dr. Holger Wallmeier - Scientific Computing & Consulting

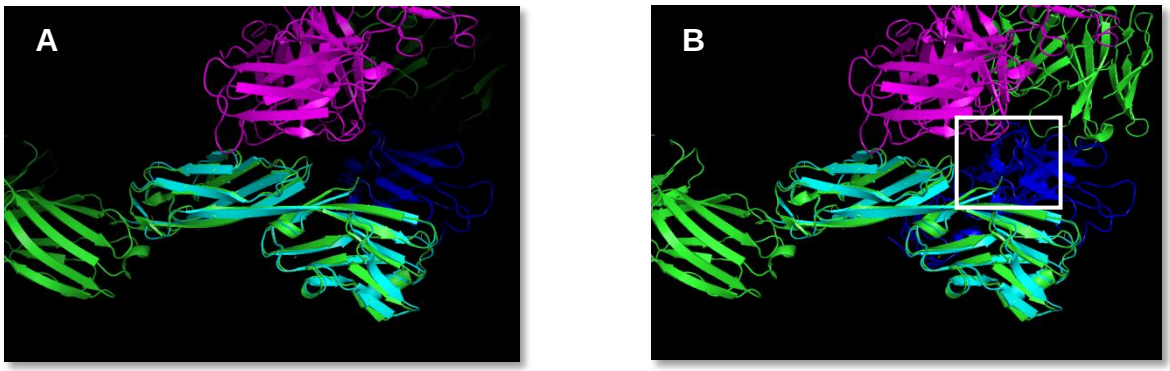

Figure 5: Binding of Tregalizumab elicits structural changes in the CD4 molecule

CD4-Tregalizumab complex vs. free CD4, 3CD4 (2.20 Å) superimposed on Proteros structure (2.9 Å) *Modified:* Dr. Holger Wallmeier - Scientific Computing & Consulting

2.11.3 CD4 down-modulation

After administration of Tregalizumab, down-modulation of CD4 expression levels on T-cells can be determined as seen for other anti-CD4 antibodies[23,318]. This CD4 down-modulation represents a marker for the activity of the antibodies[23,24]. The first step of the mode-of-action of Tregalizumab is binding to the CD4 molecule via its Fab fragment. This is followed by a cross-link with the Fcγ I receptor (CD64; which is expressed to a major extent on monocytes[319]) activating a signalling cascade[23,28]. This cross-link represents a necessary event for down-modulation of CD4[28]. After activation, the corresponding TCR-signalling pathway is activated by Tregalizumab resulting in phosphorylation of lymphocyte-specific protein tyrosine kinase ($p56^{Lck}$)[23]. Subsequently, as a down-stream result, the positive signal leads to internalization of CD4 molecules and to a decline of surface expression (Figure 7). As outcome, regulatory T-cells are activated *in vitro* and the antibody-CD4 complex on regulatory and effector T-cells, bound by Tregalizumab, is internalized[23]. This mechanism requires a functional CD4 signal pathway since CD4 down-modulation (after treatment of PBMCs with Tregalizumab) was inhibited in presence of the Src kinase inhibitor PP1[23]. However, CD4 decline is not entailed by shedding. Indeed, it was shown that Tregalizumab induces a decrease in the CD4 surface expression *in vitro* and in treated patients *in vivo*, which can be measured by flow cytometry[22–24]. CD4 down-modulation depends on the concentration of Tregalizumab (Figure 6) and recovers over time after post administration[23].

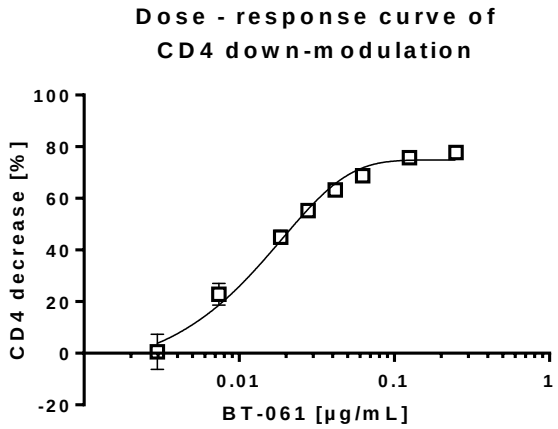

Figure 6: Dose-response curve of CD4 down-modulation

After administration of Tregalizumab down-modulation of CD4 expression levels can be determined *in vitro* and *in vivo* depending on the dosage of the antibody.

Moreover, binding of Tregalizumab to CD4 leads to an activation of LAT (linker for activation of T-cells), SLP-76 (SH2 domain containing leukocyte protein of 76kDa), PLC-γ (phospholipase C gamma), MAPK (mitogen-activated protein kinase) and MEK (mitogen-activated protein kinase kinase)[22].

However, no phosphorylation of Itk (interleukin-2-inducible T-cell kinase), ERK (extracellular signal-regulated kinases), PKC (Protein kinase C), IKK (inhibitor of kB kinase), JNK (c-Jun N-terminal kinsae), Akt and NF-kB (nuclear factor kappa-light-chain-enhancer of activated B cells) was found[22]. In addition, Tregalizumab revealed the weakest activation signal compared to other anti-CD4 antibodies as RPA-T4, MT310, QS4120 or B-A1[320].

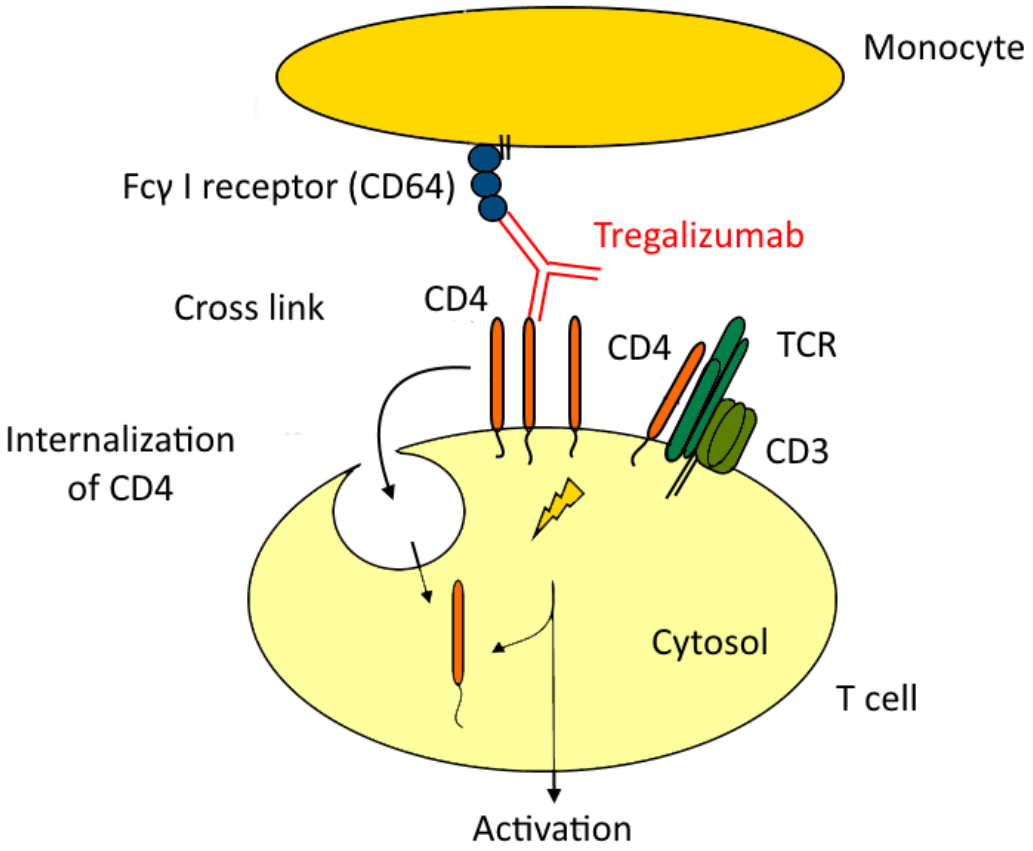

Figure 7: Tregalizumab mode-of-action and predicted CD4 modulation

Tregalizumab (BT-061) binds to CD4 of T-cells and is cross-linked via its Fc part by the Fcγ I receptor (CD64) on monocytes. This leads to a signal transduction into the cell and selective activation of regulatory Tregs. In addition, CD4 gets internalized to turn off the signalling. This CD4 down-modulation can be measured by flow cytometry *in vitro* and *in vivo*[23].

2.12 Properties of Tregalizumab

2.12.1 Tregalizumab facilitates activation of regulatory T-cells and inhibits T-cell proliferation

Compared to other anti-CD4 antibodies, Tregalizumab facilitates activation of naturally occurring regulatory T-cells (Tregs) *in vitro*[21,321–323]. However, in comparison to OKT-3, it does not evoke proliferation of effector T-cells (in the presence of autologous PBMCs)[22].

A mixed lymphocyte reaction (MLR) was used to assess the suppressive characteristics of Tregalizumab[23,320]. After allogeneic or antigen-specific stimulation, proliferation of CD4+ and CD8+ effector T-cells and their secretion of cytokines was inhibited to a great extent by Tregalizumab pre-treated regulatory T-cells[22,23,316,323].

Furthermore, secretion of inflammatory cytokines or proliferation of effector T-cells by Tregalizumab was not observed[323]. However, high levels of intracellular cyclic AMP (cAMP) in regulatory T-cells (but not in Teffs) were found after Tregalizumab stimulation[22]. Since elevated levels of cAMP are closely linked with Treg function[122], induction of cAMP via Tregalizumab might represent one activation mechanism. Moreover, upregulation of the latency-associated peptide (LAP) was detected[22], which is usually associated with TGF-β secretion[324]. So, it is speculated if Tregalizumab accounts for release of TGF-β by regulatory T-cells[325].

2.12.2 Tregalizumab does not induce Fc-part effects

Although Tregalizumab belongs to the IgG1 subclass, no typical Fc-part effects were observed. Antibody-dependent cell-mediated cytotoxicity (ADCC) was not seen after incubation of CD4+ T-cells with different concentrations of Tregalizumab[323]. Moreover, compared to other monoclonal antibodies, Tregalizumab did not induce complement dependent cytotoxicity (CDC)[23], which can be activated via classical and non-classical pathways[326]. In addition, Tregalizumab induced no apoptosis in resting or stimulated PBMC[23], which implicates that Tregalizumab is a non-depleting antibody[23,317].

In vitro studies, regarding the influence of IL-1 and IL-6 on the suppressive function of Tregalizumab on the proliferation of effector T-cells, showed no impact of these cytokines[327]. Only high concentrations (50 ng/mL and 100 ng/mL) of TNF-α revealed a little influence on suppression of effector T-cells evoked by Tregalizumab[327].

2.12.3 Anti-CD4 antibodies bind to different domains on CD4

Helling *et al.* analyzed binding of Tregalizumab in comparison to the other anti-CD4 antibodies OKT-3, RPA-T4, SK3, MT310, QS4120, EDU-2, B-A1 and MT441[22]. Measurements revealed that MT441, but none of the other anti-CD4 monoclonal antibodies, vied with Tregalizumab for binding to the CD4 molecule[22]. However, since MT441 recognises a different epitope of D2, Helling *et al*. concluded that Tregalizumab binds to a unique, conformational epitope on D2[322]. This fact is supported by the different binding sites of the following antibodies. Except from MT441, which binds to D2 of CD4[328], all other antibodies bind to other domains of the CD4 molecule: D3 of CD4 is bound by OKT-4[329] and D1 of CD4 is recognized by SK3[329] and RPA-T4[330].

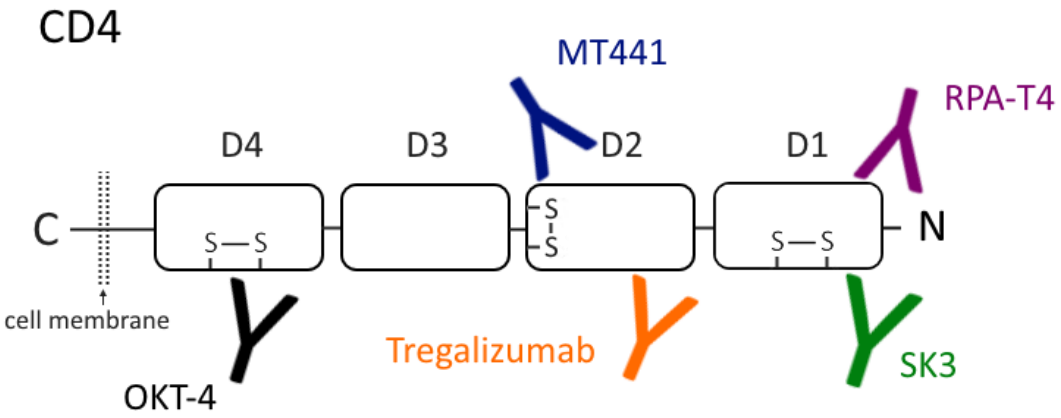

Figure 8: Schematic binding sites of different anti-CD4 antibodies

Tregalizumab binds to a unique, conformational epitope on D2 of the CD4 molecule. On the opposite side of D2, the binding site of MT441 is located. The monoclonal antibodies RPA-T4 and SK3 recognize D1 and OKT-4 bind to D3[22].

3 Aim of this PhD thesis

Many studies indicate that Tregs show functional deficiencies in autoimmune diseases[129,331–333]. New strategies to tackle autoimmune reactions and to re-establish a good immunological balance are the enhancement of activity of CD4+ CD25+ regulatory T-cells. Therefore, anti-CD4 antibodies were investigated emphasizing CD4 as an interesting target[20,21]. As a new therapeutic approach, Tregalizumab has been investigated in eight clinical trials including healthy subjects, RA and psoriasis patients. In the latest phase 2b trial, (TREAT 2b, T-cell Regulating Arthritis Trial 2b, ClinicalTrials.gov Identifier: NCT01999192 and EudraCT No. 2013-000114-38), conducted with patients suffering from RA, the primary endpoint was not reached[23].

A pharmacokinetic-pharmacodynamic model of Tregalizumab, based on clinical data from RA patients and healthy subjects[24], surprisingly showed higher CD4 down-modulation in healthy subjects compared to RA patients. This result may implicate that efficacy of Tregalizumab is higher in healthy population than in RA patients.

Tregalizumab's binding site is in close proximity to the disulfide bridge of D2 of the CD4 molecule, which is a known target for the oxidoreductase Trx1[25]. Structural alterations of the disulfide bridge, which is located in close proximity to the non-linear epitope in the Tregalizumab binding site, were thought to potentially exert influence. This special disulfide bridge is redox active and can be present in the reduced or in the oxidized state in equilibrium[25]. The redox change is selectively performed by Trx1. It is also important to note that redox alterations of this disulfide bridge are essential for entry of human immunodeficiency virus[25,334].

To examine if reduction of the D2 disulfide bridge may be responsible for higher CD4 down-modulation in healthy subjects compared to RA patients, this work further examined the role of Trx1 on Tregalizumab binding to CD4 and the role of Trx1 in RA in general.

Since the influence of conformal changes of D2 of the CD4 molecule (due to physiological factors as Trx1) on Tregalizumab binding, signalling and potency

has not been assessed before, a range of experiments was performed which are described in this thesis. Starting with the unexpected differences in predicted CD4 down-modulation between RA patients and healthy subjects, binding of Tregalizumab to CD4 was again analyzed using three-dimensional modeling.

First, active Trx1 (Trx1-CC) and its inactive thioredoxin mutant (Trx1-SS) should be expressed in M15 *E.coli* cells and purified via affinity chromatography.

Second, it should be evaluated if Trx1 can alter binding of Tregalizumab to the glycoprotein CD4 and recombinant human soluble CD4 (rh sCD4). To investigate if Tregalizumab is the only antibody whose binding is impacted by Trx1, pre-incubation other anti-CD4 antibodies (SK3, RPAT-4, MT441, OKT-4) were analyzed. Since other anti-CD4 antibodies bind to either D1 (SK3, RPAT-4) or to D3 (OKT-4), it was hypothesized that Trx1 pre-treatment induces the strongest impact on binding of Tregalizumab. Like Tregalizumab, MT441 binds also to D2. However, the epitope is not as wide as the epitope of Tregalizumab. So, it was speculated that impact of Trx1 on binding of MT441 is minor. Therefore, binding studies of Tregalizumab to rh sCD4 and CD4 of CD4+ cells after Trx1 pre-treatment should be a particular focus of this work.

Furthermore, the impact of Trx1 in its physiological systems should be evaluated. Trx1 acts under physiological conditions in combination with TrxR and NADPH. So, it should be assessed whether binding of Tregalizumab is affected when pre-treatment of Trx1 under physiological conditions in performed.

Third, the redox state of the CD4 molecule should be evaluated to verify impact of Trx1 on the disulfide bridges of this glycoprotein.

To examine if the disulfide bridge in D2 of the CD4 molecule plays an essential role in binding events, cells should be transfected with mutated CD4 lacking disulfide bridge of D2. D3 does not reveal a disulfide bridge in its domain. Since OKT-4 binds to D3 of the CD4 molecule, it was speculated that binding should be minor affected by Trx1 than binding of Tregalizumab. Therefore, binding of the monoclonal antibodies Tregalizumab and OKT-4 should be assessed.

To evaluate the influence of Trx1 pre-treatment on signalling in T-cells after Tregalizumab stimulation, some signalling experiments were performed. Normally, stimulation of CD4 leads to activation of the lymphocyte-specific protein tyrosine kinase $p56^{Lck}$. Hence, impact of Trx1 on the T-cell signalling pathway induced by Tregalizumab should be assessed.

The results of this work should contribute to a more revised insight into Tregalizumab binding and signalling properties and impact of physiological factors as Trx1. To examine if reduction of the disulfide bridge in D2 of CD4 may be responsible for higher CD4 down-modulation in healthy subjects compared to RA patients (which was seen in the PK-PD model) this thesis should further examine the role of Trx1 on the binding of Tregalizumab to CD4 and the role of Trx1 in RA in general.

4 Material and methods

4.1 Devices

Name	Supplier
-150°C freezer	Thermo Fisher Scientific Inc., Waltham, Massachusetts, USA
-80°C freezer	
Äkta Explorer	GE Healthcare Life Sciences, Freiburg, Germany
Cell incubator Heracell™ 240	Thermo Fisher Scientific Inc., Waltham, Massachusetts, USA
Centrifuge Biofuge Fresco Heraeus™	
Centrifuge Biofuge PrimoR Heraeus™	
Centrifuge Heraeus™ Multifuge 3L-R	
Centrifuge Heraeus™ Pico17	
Clean bench Herasafe	
Conduktometer inoLab (WTW series)	Xylem Water Solutions Deutschland GmbH, Großostheim , Germany
ELISA Washer	Tecan Group AG, Männerdorf, Switerland
Epson perfection V700 Photo	Epson, Suwa, Nagano, Japan
FACS Calibur	Becton Dickinson GmbH, Heidelberg, Germany
FACS Canto II	
Fluorescence microscope IX53	Olympus, Shinjuku, Tokio, Japan
Gel Air Dryer	Bio-Rad Laboratories, Inc., Hercules, California, USA
Heater	VWR International LLC, Radnor, PA, USA
Hemocytometer	LO - Laboroptik Ltd, Lancing, UK
Magnetic stirrer RH basic 2	IKA® -Werke GmbH & Co. KG, Staufen, Germany
Microplate reader Infinite®F200	Tecan Group AG, Männedorf, Switzerland
Microplate reader POLARstar Omega	BMG Labtech, Ortenberg, Germany
Microplate reader Sector Imager 6000	Meso Scale Discovery, Rockville, MD, USA
Microplate reader Sunrise	Tecan Group AG, Männedorf, Schweiz

Microtiter plate shaker MTS 2/4 digital	IKA® -Werke GmbH & Co. KG, Staufen, Germany
Mikroscope Wilovert	Helmut Hund GmbH, Wetzlar, Germany
Multiphor II	GE Healthcare Life Sciences, Freiburg, Germany
Nalgene Cryo 1 Freezing Container	Thermo Fisher Scientific Inc., Waltham, Massachusetts, USA
NuPAGE Blotting system (X Cell II Blot Module) X Cell Sure Lock® Mini-Cell	Thermo Fisher Scientific Inc., Waltham, Massachusetts, USA
NuPAGE electrophoretic system (X Cell Sure Lock mini-Cell)	
Odyssey Imager	LI-COR Biosciences, Lincoln, NE, USA
pH Meter (WTW series)	Xylem Water Solutions Deutschland GmbH, Großostheim, Germany
Power Pac 1000	Bio-Rad Laboratories, Inc., Hercules, California, USA
Power Supply EPS 3501 XL	GE Healthcare Life Sciences, Freiburg, Germany
Refrigerator Comfort no frost	Liebherr, Bulle Switzerland
Scale AT261 Delta Range	Mettler-Toledo, Columbus, OH, USA
Scale CP6201	Satorius AG, Goettingen, Germany
Shaker Polymax 1040	Heidolph Instruments GmbH & Co. KG, Schwabach, Germany
Thermomixer comfort	Eppendorf AG, Hamburg, Germany
Transfection device Nucleofactor™	Lonza, Basel, Switzerland
Ultrasonic bath	VWR International LLC, Radnor, PA, USA
Ultrospec 3100 pro	GE Healthcare Life Sciences, Freiburg, Germany
Water bath SUB Aqua 18	Grant Instruments, Cambridgeshire, GB

4.2 Consumables

Name	Supplier
Cell culture flask	Sarstedt AG & Co, Nümbrecht, Germany
Filter paper Whatman® Schleicher & Schuell®	Sigma-Aldrich, St. Louis, MO, USA
Multichannel pipette	Eppendorf AG, Hamburg, Germany
Nitrocellulose-blotting membrane (Trans Blot Transfer Medium)	Bio-Rad Laboratories, Inc., Hercules, California, USA
Safe lock tubes	Eppendorf AG, Hamburg, Germany
Slide-A-Lyzer™	Thermo Fisher Scientific Inc., Waltham, Massachusetts, USA

4.3 Reagents

Reagent	Supplier	Order number
2-Iodacetamide	Merck KGaA, Darmstadt, Germany	804744
Acetic acid 96 % (for analysis)		100062
AnaTag™ APC Labeling Kit	antibodies-online, Atlanta, GA, USA	ABIN488416
Aqua scrubbing solution Econtainer®	B.Braun Melsungen AG, Meslungen, Germany	0082479E
Pierce™ BCA Protein Assay Kit	Thermo Fisher Scientific, Waltham, Man USA	23225
Bovines serum albumin	Sigma-Aldrich, St. Louis, MO, USA	A9647
Casein	Merck KGaA, Darmstadt, Germany	102241
Caustic soda 1 mol/L (1 N)		1.09137
di-Sodium hydrogen phosphate anhydrous		1.06586
cOmplete™ Protease Inhibitor Cocktail	Sigma-Aldrich, St. Louis, MO, USA	11697498001
Dithiothreitol (99 %)	GE Healthcare Life Sciences, Freiburg, Germany	17-1318-02
Ethanol	Merck KGaA, Darmstadt, Germany	1.00983

Ethylenediaminetetraacetic acid disodium-dihydrate	VWR International LLC, Radnor, PA, USA	20309.296
EZ-Link™ NHS-SS-Biotin	Thermo Fisher Scientific, Waltham, Man USA	31494
FITC Antibody Labeling Kit (Pierce™)		53027
Glutathione	Sigma-Aldrich, Buchs, Switzerland	SLBD9746V
Glycine	Merck KGaA, Darmstadt, Germany	1.04201
Human serum albumin	Sigma-Aldrich, St. Louis, MO, USA	A3782-1G
Human TruStain FcX™	BioLegend, San Diego, CA, USA	422301
Hydrochloric acid 1 mol/L (1 N)	Merck KGaA, Darmstadt, Germany	1.09057
Insulin solution human	Sigma-Aldrich, St. Louis, MO, USA	I9278
Insulin-FITC labelled human		I3661
LB-Broth		L7275
Methanol	Merck KGaA, Darmstadt, Germany	1.06009
$MM(PEG)_{24}$	Thermo Fisher Scientific Inc., Waltham, Massachusetts, USA	22713
NADPH Tetra sodium salt	AppliChem Inc. Omaha, NE, USA	A1395
Potassium Phosphate	Merck KGaA, Darmstadt, Germany	529568
di-Potassium hydrogen phosphate		105101
Recombinant Human CD4	R&D Systems, Minneapolis, MN, USA	514-CD/CF
Sodium dihydrogen phosphate waterless	Merck KGaA, Darmstadt, Germany	1.06586
Sodium dihydrogen phosphate-dihydrate		106345
Sodiumchlorid		1.06400
SULFO TAG labelled Streptavidin	Meso Scale Discovery, Rockville, MD, USA	R32AD-1
Tartrazine	Sigma-Aldrich, St. Louis, MO, USA	86310
Tetramethylbenzidine substrate kit	KPL, Gaithersburg, MD, USA	507700

$TMM(PEG)_{12}$	Thermo Fisher Scientific Inc., Waltham, Massachusetts, USA	22361
Tris(hydroxymethyl)aminomethane	Merck KGaA, Darmstadt, Germany	1.08382
Tris(hydroxymethyl)aminomethane hydrochloride		1.08219
Triton X-100		1.08603

4.4 Cell lines

Cell type	Supplier	Order number	Species	Disease
HPB-ALL	DSMZ	ACC 483	Homo sapiens	T-cell leukemia
U266B1 [U266]	ATCC	ATCC® TIB-196™	Homo sapiens	myeloma; plasmacytoma

4.5 Medium / cell culture

Medium	Supplier	Order number
Dimethylsulfoxide	Sigma-Aldrich, St. Louis, MO, USA	D2438-5x10ML
Dulbecco's Phosphate-Buffered Saline	Thermo Fisher Scientific Inc., Waltham, Massachusetts, USA	14190-094
Fetal calf serum	GE Healthcare Life Sciences, Freiburg, Germany; former: PAA Laboratories GmbH	A15-105
L-Glutamine 200 mM	Lonza, Basel, Switzerland	BE 17-605E
Lymphoflot	Bio-Rad Laboratories, Inc., Hercules, California, USA	824012
RPMI 1640 Medium	Thermo Fisher Scientific Inc., Waltham, Massachusetts, USA	21870-076
Trypanblue 0,4%	Sigma-Aldrich, St. Louis, MO, USA	T8154
Soidum chloride solution 0.9 % (w/v)	B.Braun Melsungen AG, Melsungen, Germany	455534

4.6 Reagents for flow cytometry

Reagent	Supplier	Order number
BD Cytofix™ Fixation Buffer	Becton Dickinson GmbH, Heidelberg, Germany	554655
BD Phosflow™ Perm Buffer III		558050
FACS™ Lysing Solution 10X Concentrate		349202

4.6.1 Antibodies

4.6.1.1 Cross linker

Antibody	Supplier	Order number	Note
Goat anti-human IgG Fc	Thermo Fisher Scientific Inc., Waltham, Massachusetts, USA	H10300	polyclonal
Rabbit anti-Mouse IgG (H+L)		31188	polyclonal

4.6.1.2 Antibodies for flow cytometry

Antibody	Clone	Supplier	Order number	Dilution in end volume	Isotype
Alexa Fluor® 647 Mouse anti-Lck (pY505)	4/LCK-Y505	Becton Dickinson GmbH, Heidelberg, Germany	558577	1:10	Mouse IgG1
anti-human CD3 PerCP	SK7 (= Leu-4)		345766	1:100	Mouse IgG_1, κ
anti-human CD4 PE	SK3		347327	1:52	Mouse IgG1, κ
anti-human CD45 PerCP	2D1		345809	1:520	Mouse IgG1, κ
anti-human CD64 PE	10.1		558592	1:10	Mouse IgG1, κ
BT-061 APC	N/A	Biotest AG, Dreieich, Germany	na	1:3250	Human, IgG1
BT-061 FITC	N/A		na	1:11050	Human, IgG1
PE anti-human CD4	OKT-4	BioLegend, San Diego, CA, USA	317409	1:5	Mouse IgG2b, κ
PE Mouse Anti-Zap70 (Y319)/Syk (Y352)	17A/P-ZAP70	Becton Dickinson GmbH, Heidelberg, Germany	557881	1:8	Mouse IgG1

4.6.1.3 Isotype controls

Antibody	Clone	Supplier	Order number	Isotype
APC Mouse IgG1, κ Isotype control	MOPC-21	Becton Dickinson GmbH, Heidelberg, Germany	555751	Mouse IgG1, κ
APC Mouse IgG2b κ Isotype control	27-35		555745	Mouse IgG2b, κ
Biotin Mouse IgG2b, κ Isotype control	MPC-11	BioLegend, San Diego, CA, USA	400303	Mouse IgG2b, κ
FITC Mouse IgG1 κ Isotype control	MOPC-21	Becton Dickinson GmbH, Heidelberg, Germany	555748	Mouse IgG_1, κ
Isotype control Mouse IgG2b, PE	eBMG2b	eBioscience, Inc. San Diego, CA; USA	9012-4732-025	Mouse IgG2b
PE Mouse IgG1, κ Isotype control	MOPC-21	BioLegend, San Diego, CA, USA	400113	Mouse IgG1, κ

4.6.1.4 Further antibodies

Antibody	Clone	Supplier	Order number	Isotype
anti-human CD4/Biotin	M-T441	Ancell Cooperation, Bayport, MN, USA	148-030	Mouse IgG2b
APC Mouse Anti-Human CD14	M5E2	Becton Dickinson GmbH, Heidelberg, Germany	555399	Mouse IgG2a, κ
Biotin anti-human CD4	OKT-4	BioLegend, San Diego, CA, USA	317405	Mouse IgG2b, κ
Biotin anti-human CD4	SK3		344610	Mouse IgG1, κ
Biotin Mouse Anti-Human CD4	RPA-T4	Becton Dickinson GmbH, Heidelberg, Germany	555345	Mouse IgG1, κ
Tregalizumab (BT-061)	na	Biotest AG, Dreieich, Germany	na	IgG1

4.6.2 Dynabeads

Dynabeads	Supplier	Order number
Dynabeads® Untouched™ Human CD4 T-cell kit	Thermo Fisher Scientific Inc., Waltham, Massachusetts, USA	11346D

4.6.3 Reagents for Western Blot

Reagent	Supplier	Order number
Immunoblot PVDF Membran	Bio-Rad Laboratories, Inc., Hercules, California, USA	162-0174
IRDye®680 RD donkey anti-goat IgG (H+L) 1mg/mL	LI-COR Biosciences, Lincoln, NE, USA	925-68074
IRDye®680 RD donkey anti-rabbit IgG (H+L) 1mg/mL		925-68073
IRDye®680 LT Streptavidin 1 mg/mL		926-68031
Li-COR Blocking Buffer PBS		927-40000
NuPAGE® Transfer buffer (20x)	Thermo Fisher Scientific Inc., Waltham, Massachusetts, USA	NP00061

4.6.4 Reagents for SDS-PAGE

Reagent	Supplier	Oder number
Acetic acid (glacial)100%	Merck KGaA, Darmstadt, Germany	1.00063
Ammonium sulfate		1.01217
Coomassie Brilliant Blue G 250	Sigma-Aldrich, St. Louis, MO, USA	17424
Development Accelerator Reagent	Bio-Rad Laboratories, Inc., Hercules, California, USA	161-0448
Glycerine	VWR International LLC, Radnor, PA, USA	444482V
Image Development Reagent	Bio-Rad Laboratories, Inc., Hercules, California, USA	161-0464
Methanol	Merck KGaA, Darmstadt, Germany	1.06009
N-Ethylmaleimide, Alfa Aesar™	Thermo Fisher Scientific Inc., Waltham, Massachusetts, USA	40526
NuPAGE® Sample Reducing Agent (10x)		NP0004
NuPAGE® LDS Sample Buffer (4x)		NP0007
NuPAGE® MOPS SDS Running Buffer (20x)		NP0001
NuPAGE™ Novex™10 4-12 % Bis-Tris Protein Gel, 1.5 mm, 10-well		NP0335BOX
NuPAGE™ Novex™10% Bis-Tris Protein Gel, 1.0 mm, 10-well		NP0301BOX
ortho-Phosphoric acid 85%	Merck KGaA, Darmstadt, Germany	1.00552

Reduction Moderator Solution	Bio-Rad Laboratories, Inc., Hercules, California, USA	161-0463
SeeBlue® Plus 2 Pre-stained Protein Standard (1x)	Thermo Fisher Scientific Inc., Waltham, Massachusetts, USA	LC5925
Silver Complex Solution	Bio-Rad Laboratories, Inc., Hercules, California, USA	161-0462
Silver Stain Plus Kit		161-0449

4.6.5 Manufacturing of thioredoxin

Reagent	Supplier	Order number
B-Per™ Bacterial Protein Extraction Reagent	Thermo Fisher Scientific Inc., Waltham, Massachusetts, USA	78248
HiTrap® Chelating HP	GE Healthcare Life Sciences, Freiburg, Germany	17-0408-01
Human Thioredoxin Assay Kit – IBL	IBL, Gumma, Japan	27417
Imidazole	Merck KGaA, Darmstadt, Germany	1.04716. 0050
Nickel(II) sulfat hexahydrat		106727
Thioredoxin reductase	Sigma-Aldrich, St. Louis, MO, USA	T9698
Zeba™ Spin Desalting Columns, 7K MWCO, 0.5 mL	Thermo Fisher Scientific Inc., Waltham, Massachusetts, USA	89882

4.6.6 Blood, plasma

Reagent	Supplier	Remark
Blood	Blood donation center	healthy subjects
Plasma	BioRad, Dreieich, Germany	healthy subjects
Human Plasma EDTA K2	SeraLab, London, GB	Rheumatoid Arthritis patients

4.6.7 Reagents for transfection

Reagent	Supplier	Order number
Cell Line Optimization 4D-Nucleofector™ X Kit	Lonza, Basel, Switzerland	V4XC-9064

4.6.7.1 Vectors

Reagent	Supplier
hCD4	GeneART®, Thermo Fisher Scientific Inc., Waltham, Massachusetts, USA
hCD4 cys mut	

4.6.8 Buffer/Solutions

All buffers are manufactured using distilled water if not further specified.

4.6.8.1 SDS-APGE buffer

Buffer	**Reagents**	
Coomassie Brilliant Blue destaining solution	0.1 % (w/v)	Coomassie Brilliant Blue 250
	2 % (v/v)	orthophosphoric acid 85%
	15 % (w/v)	Ammonium sulfate
Fixation solution	7 % (v/v)	Acetic acid (glacial)100%
	37 % (v/v)	Methanol
Fast destaining solution	22.5 % (v/v)	Methanol
	10 % (v/v)	Acetic acid (glacial)100%
Running buffer	5 % (v/v)	NuPAGE® SDS MOPS Running Buffer (20x)
Slow destaining solution	25 % (v/v)	Methanol

4.6.8.2 Western blot buffer

Buffers for PVDF membrane	**Reagents**	
Transfer buffer	5 % (v/v)	NuPAGE® Transfer buffer (20x)
	10 % (v/v)	Methanol
Washing buffer	0.1% (v/v)	Tween 20
	ad 100 % (v/v)	Dulbecco's Phosphate-Buffered Saline

4.6.8.3 Lyse buffer

Buffer	**Reagents**	
Tris-buffered-saline	10 mM	TRIS hydrochloride
	150 mM	Sodium chloride
Lyse buffer	1% (w/v)	Triton-X-100
	1 tablet	cOmplete™ Protease Inhibitor Cocktail
	ad 100 % (v/v)	Tris-buffered-saline

4.6.8.4 Purification buffer

Buffer	**Reagents**	
Wash buffer (Trx1) pH 8.0	50 mM	Sodium dihydrogen phosphate dihydrate
	300 mM	Sodium chloride
	20 mM	Imidazole

Elution buffer (Trx1) pH 8.0	50 mM	Sodium dihydrogen phosphate dihydrate
	300 mM	Sodium chloride
	1 M	Imidazole

4.6.8.5 Electrochemoluminescence buffer

Buffer	**Reagents**	
Wash buffer	150 mM	Sodium chloride
	50 mM	Tris(hydroxymethyl)aminomethane
	0.05 % (v/v)	Tween 20
Assay buffer	1 % (w/v)	Bovine serum albumin
	ad 100 % (v/v)	Dulbecco's Phosphate-Buffered Saline
Blocking buffer	2 % (w/v)	Bovine serum albumin
	ad 100 % (v/v)	Dulbecco's Phosphate-Buffered Saline

4.6.9 Miscellaneous

Name	**Reagents**	
TE buffer pH 7.5	50 mM	Tris(hydroxymethyl)aminomethane hydrochloride
	2 mM	EDTA Disodium-dihydrate
PE buffer pH 6.5	100 mM	K_2HPO_4/ KH_2PO_4
	2 mM	EDTA Disodium-dihydrate
LB Medium	25 g/L	LB-Broth in Aqua dest.

4.7 Cell culture

The suspension cell lines were cultured at 37°C, 5 % CO_2 in an incubator. Cells were split twice a week and seeded in warmed-up RPMI 1640 enriched with fetal calf serum and 2 mM L-glutamine. According to the requirements of cell lines, different concentrations of FCS were added:

Table 1: Cultivation condition of different cell lines

Cell line	Cell density at seeding [cells/mL]	Percentage of FCS [%]
HPB-ALL	$5*10^5$	20
U266	$2*10^5$	15

Sterile conditions were ensured by using a laminar air flow bench.

4.8 Cryopreservation of cells

For long term storage cells were pelletized and resuspended in 90% fetal calf serum enriched with 10% dimethyl sulfoxide. Cells were seeded according to optimal cell count (see below). By means of Nalgene® Cryo 1°C Freezing Containers cells were frozen for 24 hours at -80°C. Afterwards cells were transferred into the -150°C freezer.

Table 2: Cell lines used for experiments

Cell line	Cell density for cryopreservation [cells/mL]
HPB-ALL	$3*10^6$
U266	$3*10^6$

4.9 Determination of cell count

Cell count was determined using a hemocytometer. 0.2 % trypane blue / 0.9 % (w/v) sodium chloride were used to detect death cells. After pre-dilution of cells, viability (formula 1, [%]) and cell count (formula 2, [cells/mL]) were calculated as follows:

$$Viability = \frac{living\ cells}{livving\ cells + death\ cells} \quad (1)$$

$$Cell\ count = \frac{cell\ dilution\ factor\ \times\ cell\ count\ \times 10^4}{number\ of\ counted\ quadtrates} \quad (2)$$

4.10 Isolation of peripheral blood mononuclear cell from whole blood

Whole blood was gained from BioRad's blood donation centre in Dreieich, Germany. Peripheral blood mononuclear cell were isolated from citrated blood of healthy subjects using Leucospe^{TM} tubes. For this purpose, 15 mL warmed Lymphoflot separation medium was poured into the tubes and centrifuged for 1 minute at 1000 x g and room temperature (switched brakes) until the fluid was under the porous barrier. 25 mL blood were filled into 50 mL tubes and centrifuged for 25 minutes at 1000 x g and room temperature without brakes. The buffy coated was collected using a sterile serological pipette, transferred into a new tube and washed with D-PBS. Samples were centrifuged for 10 minutes at 250 x g and room temperature. The washing procedure was repeated once. Cells were seeded to $1*10^7$ cells/mL with RPMI 1640 enriched with 10 % fetal calf serum and 2 mM L-glutamine. PBMCs were stored at 37°C, 5% CO_2 until usage.

4.11 Cell lysate

$1*10^6$ cells in D-PBS were incubated with 150 nM TrxR, 1 mM NADPH and 5 µM Trx1 over night. Afterward, cells were washed for three times with D-PBS and lysed using lysing buffer (TBS, 1% Triton-X-100, Complete Protease Inhibitor) for 2 hours at 2-8°C. Supernatant was collected after centrifugation (10 minutes at 13000 U/rpm (Biofuge fresco) at 2-8°C) and incubated with LDS sample buffer 4x enriched with 200 mM NEM. The sample was denaturized at 70°C for 30 seconds. Preparation of $MM(PEG)_{24}$ was performed according to the manufacturer's instructions. Pegylation was conducted by addition of 30 mM $MM(PEG)_{24}$ (250 mM stock solution) to the lysing buffer.

4.12 SDS-PAGE

SDS-PAGE was performed using a NuPAGE X Cell Sure Lock mini-Cell system. If possible, samples were diluted to 1 mg/mL with distilled water. For analysis of a reduced or non-reduced SDS-PAGE samples ware prepared as follows:

- Non-reduced SDS-PAGE: one part N-ethylmaleimide (NEM, 400 mM) was mixed with one part LDS sample buffer 4x (*NR mix*ture). The sample

was diluted at a ratio of 1:2 with the *NR mixture* and denaturized by heating for 30 seconds at 70°C.

- Reduced SDS-PAGE: 2.5 parts of LDS sample buffer 4x were mixed with 1 part of Sample Reducing Agent 10x (*R mixture*). The sample was diluted at a ratio of 1:2 with the R mixture and denaturized by heating for 10 minutes at 70°C.

5 -25 µL of samples were pipetted into a ready to use NuPAGE 4 - 12 % Bis – Tris gel, respectively NuPAGE 10% Bis-Tris gel. The gel was run for 50 minutes at 200 Volts by means of power supply. Protein weight was determined by using the SeeBlue® Plus 2 Prestained Standard.

Pegylation of rh sCD4 was performed as follows: preparation of $TMM(PEG)_{12}$ was performed according to the manufacturer's instructions. Pegylation was conducted by addition of $TMM(PEG)_{12}$ (250 mM stock solution) to rh sCD4 ± DTT, rh sCD4 ± Trx1, rh sCD4 ± Trx1/TrxR/NADPH respectively, according to the manufacturer's instructions. Subsequent incubation for 2 hours at 2-8°C followed. Non-reduced SDS-PAGE was performed as described above. However, instead of NEM, D-PBS was used.

4.13 Coomassie staining

To fix the proteins, the gel was incubated for 45 - 60 minutes in fixation buffer before staining with Coomassie staining solution for 3 ± 1 hours. Afterwards, the gel was treated with fast destaining solution for 1 minute and with slow destaining solution for 18 ± 2 hours.
The gel was scanned via Epson Perfection V700 Photo scanner and incubated in 1% (w/v) glycerine after the decolouration process. By means of cellophane the gel was preserved.

4.14 Silver Staining

Silver staining was performed using the Silver Stain Plus Kit (Bio-Rad) according to the manufacturer's instructions.
To fix the proteins the gel was incubated for 30 minutes at 20 rpm in fixation buffer subsequently after electrophoresis. The gel was washed for two times

with distilled water for 20 minutes at 20 rpm on the laboratory flat shaker before staining with silver staining solution. Staining was performed for 5-15 minutes. The staining procedure was stopped using 5 % acetic acid in distilled water and the gel was washed again for three times à 10 minutes with distilled water. After scanning via Epson Perfection V700 Photo scanner and incubation in 1% (w/v) glycerine) for 1 hour the gel was preserved in cellophane.

4.15 Western Blot

Western Blot was performed using a PVDF membrane for fluorescence labelled antibodies. The PVDF membrane was pre-wetted for one minute in methanol. After an equilibration period of 10 minutes in transfer buffer the SDS-PAGE gel was blotted for 60 minutes at constant 30 Volts via X Cell II Blot Module (Expected current: start ~ 170 mA, end: ~ 110 mA). The PVDF membrane was blocked for 60 minutes or over night for 18 ± 2 hours at 4°C with Odyssey blocking buffer. Afterwards, the membrane was incubated with primary antibody for one hour and treated with washing buffer for 5 minutes for four times. Incubation with fluorescence labelled antibody followed for one hour. The membrane was again washed for four times (à 5 minutes) with washing buffer before incubation in distilled water for 5 minutes two times. Infrared light was recorded by an infrared imagining system (Odyseey®CLx). After drying of the membrane for 30 minutes in the gel air dryer (37°C), the membrane was scanned (Odyssey instrument, settings: Focus F = 0.02 µm, Scan resolution µ = 84 µM, Scan quality Q = medium, Channel intensity A = automatic).

4.16 Electrochemiluminescence ELISA

96 well standard microtiter plates (MSD) were coated with 50 µL rh sCD4/carrier free (2 µg/mL, 100 ng/well) and incubated for 20 ± 4 hours at 2-8°C.

The plates were washed by means of a plate washer (Tecan) for three times, using 300 µL/well washing buffer 1x, after the coating procedure. Plates were dried by shaking.

200 µL/well of blocking buffer were filled in each well and plate was incubated for 75 ± 15 minutes at room temperature. Another washing step followed (300 µL/well washing buffer, three times).

50 µL of different concentrations of Trx1 or DTT were added and incubated for 30 ± 15 minutes at room temperature. Tregalizumab was biotinylated by means of EZ-Link™ NHS-SS-Biotin according to the manufacturer's instructions.
Before addition of biotinylated Tregalizumab or other biotinylated antibodies (each 50 µL), the plate was washed again for three times. Solutions were mixed for 90 ± 10 minutes using a plate shaker (500-700 rpm). 50 µL/well streptavidin conjugated with sulfo-TAG (1 µg/mL, STS) were added and incubated for 60 ± 15 minutes at 500-700 rpm and room temperature. After washing, 150 µL/well *Read Buffer T* (diluted in a ratio 1:2 with distilled water) were added to the samples. Sector Imager 6000 was used for detection of signals.

4.17 Determination of protein concentration via OD-280

To determine the concentration of protein samples a photometric OD280nm analysis was performed. Samples were diluted in a ratio of 1:11 with distilled water, respectively D-PBS, and measured at 280 nm using a photometer. Measurements were compared to blank and human serum albumin was used an internal control. Concentrations were calculated applying the Lambert-Beer law.
The following extinction coefficients were used:

Table 3: Extinction coefficients of used reagents

Sample	Extinction coefficients ε
Tregalizumab	1,48
Trx1	0,67

4.18 Determination of protein concentration via BCA assay

To verify the concentration of Trx1, a bicinchoninic acid assay (BCA™ Protein Assay Kit, Pierce) was used according to manufacturer's instructions. BSA served as standard. Extinction was measured at 570 nm via a photometer (Tecan sunrise).

4.19 Trx1: Expression and purification

Recombinant human thioredoxins (wild type Trx1-CC(CCC), Trx1-CC(AAA) and inactive mutant Trx1-SS(AAA)) were provided by the Redox Regulation group of the DKFZ, Heidelberg, Germany.

Cultivation of bacteria suspension was performed by the Redox Regulation group (A160) at the DKFZ in Heidelberg. Purification was performed at Biotest AG, Dreieich. *E.coli* M15 cells were transformed using a pQE-60 vector to gain Trx1. LB culture medium was enriched with ampicillin (100 µg/mL) and kanamycin (25 µg/mL) and bacteria culture was incubated over night at 37°C. Bacteria culture was diluted in a ratio of 1:10 with new LB medium and seeded up to 0.6 – 0.8 OD at the shaker. Expression was induced by adding 1 mM IPTG. After four till five hours the culture was centrifuged for 15 minutes at 6000 x g and 4°C (Sorval Evolution RC). The pellet was resuspended in B-Per Bacterial Protein Extraction reagent enriched with 10 mM imidazole and inverted for 10 minutes. Suspension was centrifuged for 20 minutes at 20,500 rpm and 4°C (Sorval Evolution RC). Trx1 was stored at -80°C up to next processing step or directly purified using an Äkta^{TM} explorer (GE Healthycare). HiTrap columns (GE Healthcare) loaded with Nickel (II) sulfate were used to purify thioredoxins from bacteria extracts. After purging with washing buffer, proteins were eluted via imidazole gradient elution (10 mM – 500 mM imidazole). Fractions were analysed for protein using the chromatogramme and SDS-PAGE. Fractions containing thioredoxin were pooled and dialyzed using D-PBS as dialysis solution and a Slide-A-Lyzer^{TM} dialysis cassette according to manufacturer's instructions. Thioredoxin was divided into aliquots and stored at 4°C.

4.20 Determination of activity of thioredoxin and thioredoxin reductase

Determination of activity of Trx1 and TrxR was performed according to *Arnér und Holmgreen* 2001[300].

4.20.1 Determination of activity of thioredoxin

Activity of Trx1 was measured with dithiothreitol (DTT) and insulin in a 96 well plate. A master mixture consisting of 160 µM insulin in 100 mM potassium

phosphate enriched with 2 mM EDTA buffer (PE buffer, pH 6.5) was confected. 1 mM DTT and 1 µM or 5 µM Trx1 were added to the master mixture and absorption was measured immediately at 620 nm (Tecan Infinite) for 20 minutes. In addition, controls without DTT respectively Trx1, were measured.

4.20.2 Determination of activity of thioredoxin reductase

Activity of TrxR was analyzed by measuring NADPH consumption. A master mixture consisting of 160 µM insulin and 150 µM NADPH in 50 mM Tris*Cl and 2 mM EDTA buffer (TE buffer) were mixed with 20 µM Trx1 and 5 nM or 100 nM TrxR. Consumption of NADPH was measured via photometric measurement at 340 nm (POLARstar Omega). The reaction was performed in TE buffer.

4.21 Reduction of Trx1 via DTT

Trx1 was stored in D-PBS containing 5 mM DTT. Additionally, Trx1 was reduced (10 minutes at room temperature) with 5 mM DTT before each experiment in order to prevent oxygen induced inactivity of Trx1. Zeba spin desalting columns (7 MWCO) were used according to the manufacturer's instructions to separate DTT: columns were purged from storage solution by centrifugation for one minute at 1500 x g. Afterwards samples were added and DTT was removed by centrifugation for two minutes at 1500 x g. Trx1 was used subsequently after reduction.

4.22 Determination of Trx1 levels in plasma samples

Trx1 levels in plasma of RA patients and healthy subjects were measured using a Trx1 ELISA (Human Thioredoxin Assay Kit, IBL) according to the manufacturer's instructions. RA plasma was purchased by Sera Laboratories International Ltd, UK or obtained from Biotest study 986 (TREAT 2B). Plasma of healthy donors was gathered from fresh blood of volunteers from BioRad's blood donation centre, Dreieich, Germany. Blood was centrifuged at 1000 x g for 30 minutes at room temperature. Subsequently, supernatant excluding the erythrocytes was centrifuged for 15 minutes at 2576 x g (4000 U/min) at room temperature. The supernatant was sterile filtered (0.2 µm, Satorius), filled in aliquots and stored at – 80°C until use.

4.23 Flow cytometry

Antibodies were titrated for optimal staining prior to use. Labelling of Tregalizumab with APC was performed using AnaTag™ APC Labelling Kit according to the manufacturer's instructions. Cell suspension was stained with fluorochrome-labelled antibody for 30 minutes on ice in the dark. Staining was stopped using FACS Lysing solution 1x. Cells were incubated for at least 15 minutes and measurement started afterwards.

Results were obtained using a four-colour FACS Calibur (BD Biosciences) with the BD CellQuest™ Software. Mean fluorescence intensity was evaluated by means of FlowJo data analysis software (Tree Star Inc.).

4.24 Transfection

Vector DNA of human CD4 and mutated human CD4 (cysteines in D2 were replaced by alanine) were generated by geneART®. Plasmid maps are shown in Figure 9. Sequences of CD4 and mutated CD4 can be found in the appendix (chapter 8).

U266B1 cells were transfected via electroporation using Amaxa®Cell Line optimizing Solution Box (Lonza). 675 µL SF solution were mixed with 150 µL supplement. $5*10^5$ cells were centrifuged at for 10 minutes at 250 x g and room temperature. Pellet was resuspended in 20 µL supplemented SF solution. 4 µg DNA were added to the cell suspension, which was afterwards transferred into a 16-well Nucleocuvette™ Strip (Lonza). An eGFP (*pmaxGFP*) served as positive control.

Transfection was performed by Nucleofector™ (Lonza) applying programme No. DY-100. Due to regeneration reasons, cells were diluted 1:5 with pre-warmed RPMI 1640 medium after transfection procedure and incubated for 10 minutes at 37°C and 5% CO_2. Afterwards, cells were transferred into a 24 well culture plate and incubated in 500 µL RPMI 1640 + 10 % FCS + 2 mM L-glutamine.

Transfection efficacy was observed using fluorescence microscopy by green fluorescence of eGFP control.

A

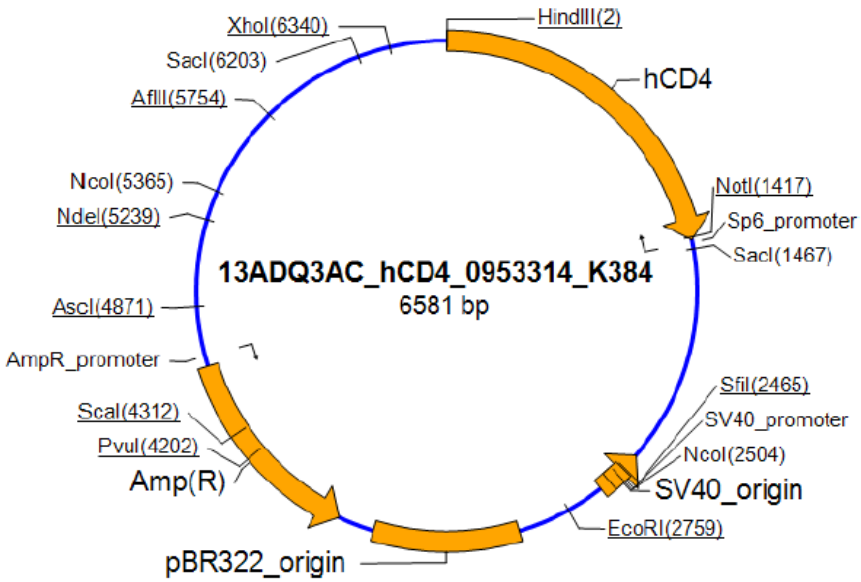

B

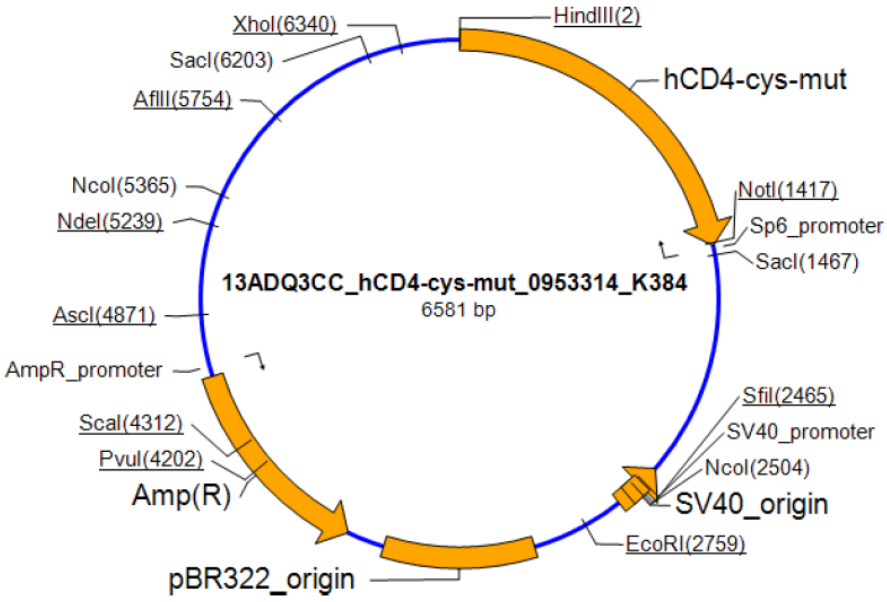

Figure 9: Plasmid maps of human CD4 and mutated human CD4 expression vectors

Expression vectors of human CD4 (**A**) and mutated human CD4 (**B**) (cysteines in D2 were replaced by alanine) were generated by GeneArt Gene Synthesis service. Therefore, synthetic oligonucleotidies and/or PCR product were used to assemble the synthetic gene. The fragment was cloned into *0953314_K384* by means of HindIII and XBaI cloning sites. Purification of the plasmid DNS was performed to separate transformed bacteria. Concentration was measured by means of UV spectroscopy. Sequencing was applied to verify the final construct. Promotors in front of inserts are not shown.

4.25 Labelling of Tregalizumab with allophycocyanin

Tregalizumab was labelled with allophycocyanin (APC) via AnaTag™ APC Labeling Kit (antibodies-online) according to manufacturer's instructions. To desalt Tregalizumab afterwards, Zeba spin desalting columns (7MWCO) were use.

4.26 CD4 down-modulation

$3*10^5$ PBMC were treated with different concentrations of Tregalizumab and incubated for 3 hours ± 10 minutes in RMPI 1640 medium supplemented with 2 mM L-glutamine and 10 % FCS at 37°C, 5% CO_2. The cells were centrifuged for 10 minutes, 1500 U/min at room temperature and stained with anti-CD4 PE (SK3, BD Biosciences), anti-CD45 PerCP (BD Biosciences), anti-CD3 APC (BD Biosciences) and BT-061 FITC (Biotest AG) and the mean fluorescence (MFI) was measured by flow cytometry using a BD FACS Calibur (BD Biosciences).
The lymphocyte population was identified by gating of cell size and granularity (FSC/SSC). Gating of CD45+ CD3+ showed T-cells, expression of CD3+ CD4+ represented T helper cells (Figure 10).

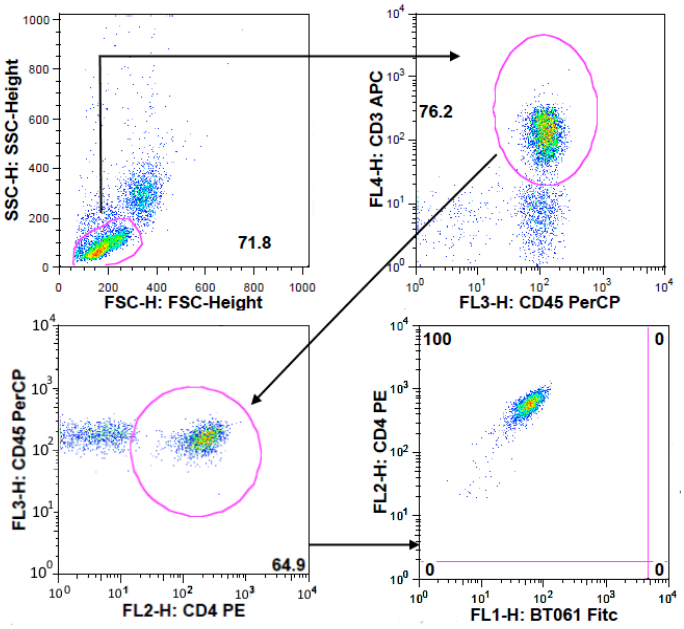

Figure 10: Gating strategy to determine CD4 down-modulation:

The lymphocyte population was identified by gating of cell size and granularity (FSC/SSC). Gating of CD45+ CD3+ shows T-cells, expression of CD3+ CD4+ represented T helper cells. CD4 expression levels were determined by using an anti-CD4 PE antibody.

A non treated control was set to 100% and the CD4 down-modulation of each sample was calculated. Data was determined using FlowJo data analysis software (Tree Star Inc.).

4.27 Determination of binding of Tregalizumab to CD4+ cells after Trx1 treatment

To analyze the impact of Trx1 and its physiological system, the CD4+ HPB-ALL cell line and fresh isolated PBMCs were used. Two incubation time periods were tested.

4.27.1 HPB-ALL were incubated for 60 minutes or over night incubation with Trx1

In order to assess binding of Tregalizumab to Trx1 treated CD4+ cells, the human T-cell leukemia cell line HPB-ALL was used. Trx1 was pre-reduced by 5 mM DTT to prevent oxygen induced inactivity of Trx1 (as described above). 10^5 cells gathered from cell culture were incubated with D-PBS containing 1 mM NADPH, 300 nM or 500 nM TrxR and 10 µM Trx1 in a 96 well U-bottom plate at 37°C, 5% CO_2 for one hour. After incubation, cells were centrifuged at 220 x g for 10 minutes at room temperature and washed for three times using D-PBS. HPB-ALL cells were stained with BT-061 APC. Mean fluorescence was determined by flow cytometry (FACS Calibur).

4.27.2 Assessment of over night incubation of Trx1 and HPB-ALL cells and PBMCs

For binding experiments of Tregalizumab to CD4+cells over night, HPB-ALL cells as well as PBMC were used. PBMC were isolated from citrated blood according to the Ficoll-Hypaque density separation protocol as described above.

Trx1 was pre-reduced by 5 mM DTT to prevent oxygen induced inactivity of Trx1 (as described above). $1*10^5$ cells were incubated with 1 mM NADPH, 150 nM TrxR and 5 µM Trx1 in a 96 well U-bottom plate at 37°C, 5 % CO_2 for 15 ± 2 hours over night. The redox inactive mutant Trx1-SS served as control. Here, the active site residues Cys(32) and Cys(35) were substituted by serine, and the additional non-active cysteines were replaced by alanine. PBMC were

incubated in RPMI 1640 + 10 % FCS + 2 mM L-glutamine, HPB-ALL cells in D-PBS. For assessment of impact of GSH on CD4, PBMCs were pre-treated with 10 mM reduced GSH and incubated overnight for 15 ± 2 hours at 37°C, 5 % CO_2. Cells were centrifuged at 220 x g for 10 minutes at room temperature and washed for three times using D-PBS.

PBMCs were stained with fluorochrome-labelled antibodies against CD3 (anti-CD3 PerCP (BD Biosciences) and CD4 (BT-061-APC; Biotest AG).

Monocytes were gated according to their size and granularity (FSC/SSC). Mean fluorescence intensity (MFI) of anti-CD64 PE (BD Biosciences) was analyzed by means of flow cytometry (BD FACSCalibur™). HPB-ALL cells were stained with BT-061-APC. Mean fluorescence was determined by flow cytometry (BD FACSCalibur™).

4.28 Analysis of signalling of CD4+ cells by phosphorylation of proteins

Intracellular phosphorylation of lymphocyte-specific protein tyrosine kinase $p56^{Lck}$ and Zeta-chain-associated protein kinase 70 (ZAP-70) was determined after stimulation with Tregalizumab or OKT3 using fluorochrome-labelled antibodies (Alexa Fluor® 647 anti-Lck (pY505)) and PE anti-Zap70 (Y319)/Syk (Y352, all BD Biosciences).

For this purpose, CD4+ cells were isolated from human PBMC using Dynabeads® Untouched™ Human CD4 T-Cells Kit according to manufacturer's instructions. $1*10^5$ cells were incubated with 5 µM Trx1, 150 nM TrxR and 1 mM NADPH over night for 15 ± 2 hours at 37°C, 5% CO_2. Cells were washed three times with D-PBS and resuspended in RPMI 1640 enriched with 10 % FCS and 2 mM L-glutamine. Tregalizumab (1 µg/mL) and OKT3 (1 µg/mL), respectively, were added and incubated on a plate shaker (300 rpm) for 30 minutes at room temperature. Afterwards, cells were washed with D-PBS/3% FCS.

Cells stimulated with Tregalizumab were cross-linked with 20 µg/mL polyclonal anti-human IgG, OKT3 stimulated cells were cross-linked with 10 µg/mL of anti-murine IgG, respectively, for 10 minutes at 37°C, 5% CO_2. Pre-warmed 100 µL fixation buffer was added to each sample and cells were incubated for 10 minutes at 37°C and 5% CO_2. After washing with D-PBS/3 % FCS, cells

were treated with cold Perm Buffer III, incubated for 30 minutes on ice and washed again. Cells were stained for 30 minutes on ice. Afterwards, cells were washed and resuspended in 200 µL D-PBS/3% FCS. Mean fluorescence intensity was determined using a FACSCanto™ (FACSDiva™ Software, BD Biosciences).

The mean fluorescence intensity of the measured value was divided by the mean fluorescence intensity of the untreated control referring to the fold induction.

The inactive mutant Trx1-SS served as control. Trx1 treated cells were compared to Trx1-untreated the sample.

4.29 Evaluation of clinical data from Biotest studies 979 and 985

Binding of BT-061-FITC and anti-CD4 (SK3) PE to lymphocytes was measured using flow cytometry (Biotest Study 979, EudraCT: 2010-018485-24, Biotest study 985, EudraCT Number: 2011-004956-20).

Resulting MFI values of gated CD4+ T-cells (SK3 PE (BD Biosciences) and BT-061 FITC were divided through MFI values of CD4- T-cells referring to the ratio [SK3+/CD4-], [BT-061+/CD4-], respectively. Relative binding of Tregalizumab in relation to total CD4 on the cell surface of T-cells was determined by dividing [BT-061+/CD4-] through [SK3+/CD4-].

All clinical studies were carried out in accordance with the international guidelines on Good Clinical Practice (ICH-GCP) and in compliance with applicable national regulations. It is confirmed that the studies were carried out and documented in accordance with the corresponding study protocol accepted by regulatory authorities and ethic committees. A signed informed consent was obtained from all subjects.

4.30 Gating strategies

The binding of PBMC to CD4 was determined by gating on lymphocytes according to cell size and granularity (FSC/SSC) and then within the gate on CD3+ BT-061+ cells. The monocyte population was identified by gating of cell

size and granularity (FSC/SSC). Within the gate the fluorescence of the PE-labelled anti-CD64 (BD Biosciences) was analyzed.

Binding of HPB-ALL cells to CD4 was determined by gating on lymphocytes according to cell size and granularity (FSC/SSC) and then within the gate on APC-labelled BT-061+ cells.

Binding of transfected U266B1 cells to CD4 was determined by gating according to cell size and granularity (FSC/SSC) and then within the gate on CD4+ cells (APC-labelled BT-061+ cells and PE-labelled OKT-4+ cells).

4.31 Statistical analysis

All data are described as mean ± SD. Normal distribution of data was checked using a Kolmogorov-Smirnov test or a Shapiro-Wilk test. Accordingly, the significance was calculated using an unpaired student's t-test or a Mann-Whitney test or paired t-test, Wilcoxon matched-pairs signed rank test, respectively. P-Values and statistic were assessed using Prism 6.02 (GraphPad Software, La Jolla, USA). Significance is shown as p-values: *$p<0.05$, **$p<0.01$, ***$p<0.001$, **** $p< 0.0001$.

5 Results

The first step of the mode-of-action of Tregalizumab is binding to the CD4 molecule via its Fab fragment. This is followed by a cross-link of Tregalizumab's Fc-part with the Fcγ I receptor (CD64) on monocytes activating a signalling cascade[28]. As outcome, regulatory T-cells are activated and CD4 molecules on regulatory and effector T-cells bound by Tregalizumab are internalized. This does-dependent pharmacodynamic effect arises quickly after administration of Tregalizumab and remains a few days, depending on the dose administered[23]. As described, flow cytometry can be used to measure the CD4 down-modulation via a fluorochrome-labelled anti-CD4 antibody. Since this effect is a surrogate for the potency of Tregalizumab, the CD4 down-modulation assay was performed in several clinical studies. For a better understanding of the dose-response effects of Tregalizumab in patients, a pharmacokinetic-pharmacodynamic (PK-PD) model was established predicting the CD4 down-modulation of several populations[24]. It was developed using the down-modulation of the CD4 molecule on the T-cell surface as pharmacodynamic marker. The PK-PD model, based on clinical data from RA patients and healthy subjects, surprisingly showed higher CD4 down-modulation in healthy subjects (Figure 11, yellow curve), compared to RA patients (Figure 11, orange curve).

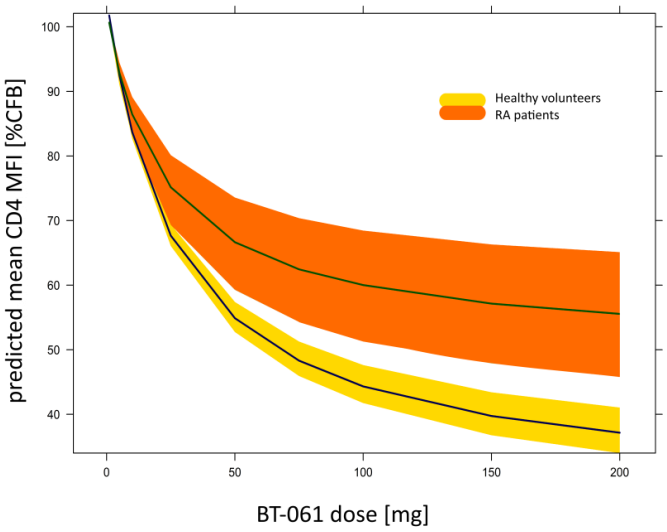

Figure 11 Predicted CD4 modulation after first dosing SC (mean +/- 95%CI)

The theoretical down-modulation of the cell surface protein CD4 after Tregalizumab administration as predicted by a PK-PD-model is depicted after the first SC dosing (predicted mean values +/- the 95% confidence interval). The predicted CD4 down-modulation is higher in healthy subjects (yellow curve) compared to patients with rheumatoid arthritis (orange curve).

This result implicates that efficacy of Tregalizumab is higher in the healthy population than in RA patients.

The binding site of Tregalizumab in close proximity to the disulfide bridge of D2 of the CD4 molecule (Figure 12, Figure 13 and Figure 4), which is a known target for the oxidoreductase Trx1[25].

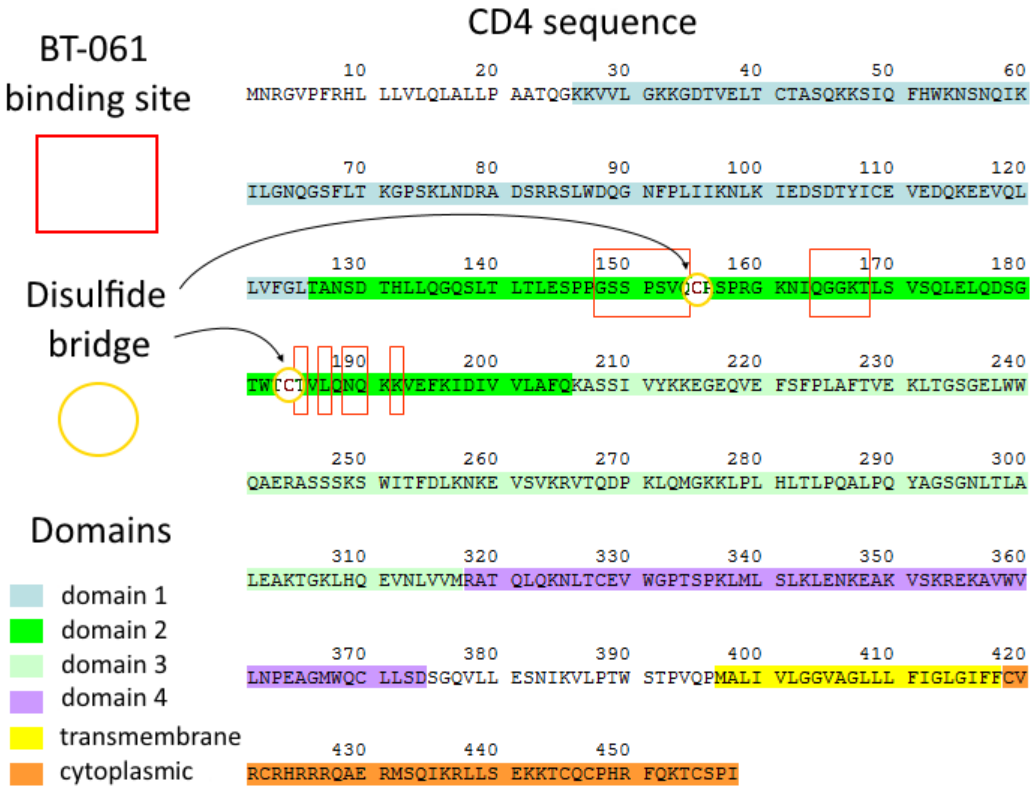

Figure 12: Sequence of the CD4 molecule with binding sites of Tregalizumab.

Tregalizumab binds in close proximity to the D2 disulfide bridge of CD4. This disulfide bridge is susceptible for reduction by Trx1.

This special disulfide bridge is redox active and can be present in the reduced or in the oxidized state in equilibrium[25]. The redox change is selectively performed by Trx1. It is also important to note that redox alterations of this disulfide bridge are essential for entry of human immunodeficiency virus[25,334].

To examine if reduction of this disulfide bridge may be responsible for higher CD4 down-modulation in healthy subjects compared to RA patients, this thesis further examined the role of Trx1 on the binding of Tregalizumab to CD4 and the role of Trx1 in RA in general.

As an overview the following work was performed:

- Binding of Tregalizumab to CD4 was again analyzed using three-dimensional modelling
- Trx1 (Trx1-CC) and its inactive thioredoxin mutant (Trx1-SS) was expressed in M15 *E.coli* cells and purified via affinity chromatography.
- The redox state of the CD4 molecule was evaluated after Trx1 pre-treatment
- Other anti-CD4 antibodies (SK3, RPAT-4, MT441, OKT-4, L120) were analyzed with regard to their binding to rh sCD4
- Binding studies of Tregalizumab to rh sCD4 and CD4+ cells after thioredoxin pre-treatment were conducted
- The impact of Trx1 and its physiological partners TrxR and NADPH on CD4+ HPB-ALL cells and PBMC was evaluated
- CD4 and mutated CD4 transfected cells were generated to analyse the binding of Tregalizumab (compared to OKT-4) to CD4 lacking the disulfide bridge in D2
- Influence of Trx1 pre-treatment on signalling (ZAP-70 and $p56^{Lck}$) in T-cells after Tregalizumab stimulation was assessed
- Data from two clinical studies were analyzed retrospectively concerning the binding of Tregalizumab to CD4
- Plasma levels of Trx1 were analyzed retrospectively to gain more insights of a possible correlation between Trx1 levels in RA patients from the last clinical study and efficacy of Tregalizumab

5.1 Tregalizumab binds in close proximity to the CD4 disulfide bridge in domain D2

Looking for a possible explanation for the decreased CD4 down-modulation of RA patients compared to healthy subjects, consideration went back to the Tregalizumab-CD4 interaction. Protein crystallography revealed that Tregalizumab binds to D2 of CD4 to a conformational epitope that is not recognized by other anti-CD4 mAbs[22]. The epitope is near to an intermolecular disulfide bridge (Figure 13). Distances from Cys(155) and Cys(184) to Tregalizumab's tyrosine 105 (Tyr105) carbon atoms were calculated to be 7.0 - 11.0 Å. For more details see Table 4.

Table 4: Distances between Tregalizumab's Tyrosin(105) and CD4 Cys(155) and Cys(184)

Distance [Å]		Tregalizumab –Tyr(105)						
		Cα	Cβ	Cγ	Cδ1,2	Cε1,2	Cζ	Oη
CD4 – Cys(155)	Cα	10,0	8,5	6,9	7,0	7,3	7,4	8,0
CD4 – Cys(184)	Cα	11,0	9,5	8,9	8,7	8,5	8,4	8,5

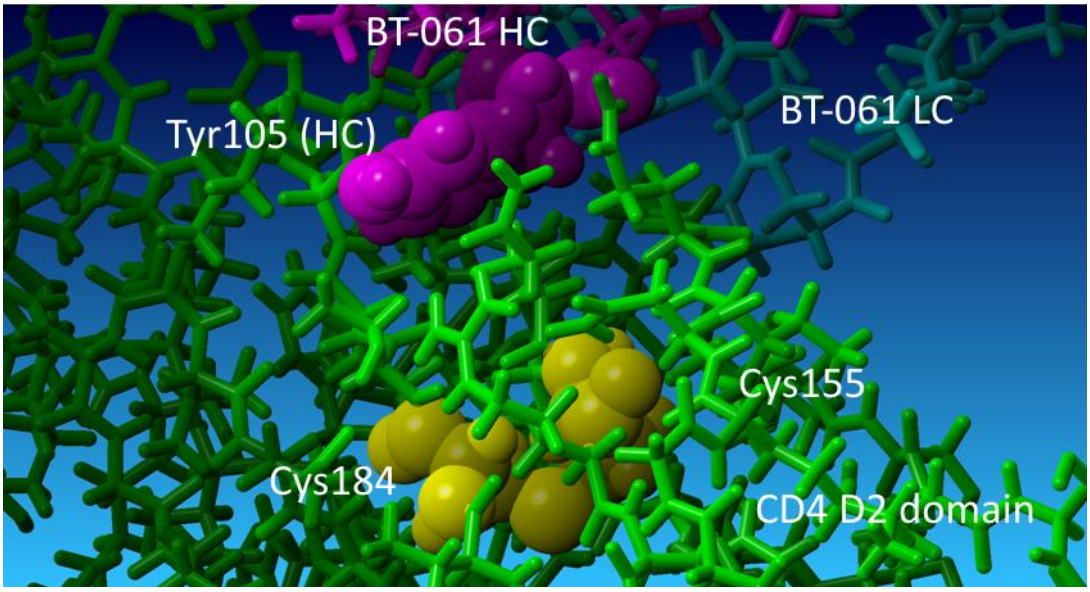

Figure 13: Space-filling model of binding of Tregalizumab to D2 in close proximity to the disulfide bridge.

Crystal structure of the Tregalizumab-CD4-interaction. The D2 disulfide bond (marked in yellow) is in close proximity to the Tregalizumab binding sites (Tregalizumab heavy chain in purple, light chain in cyan). Amino acid tyrosine 105 (Tyr(105)) displayed as space fill model is important for the Tregalizumab-CD4-interaction.

Since this disulfide bond between cysteines Cys(155) and Cys(184) is in very close proximity to the binding interface of Tregalizumab to CD4, it is likely to influence the binding characteristics between both entities. Moreover, the disulfide bridge has been described to be selectively reduced by Trx1[25].

5.2 Force field calculation of Tregalizumab – CD4 complex

Moreover, impact of disulfide-bridge on binding energy of Tregalizumab was calculated by CONDOR Scientific Computing & Consulting. Therefore, binding energy was minimized by means of YASARA View software system[335] using the NOVA force field (s. Figure 14).

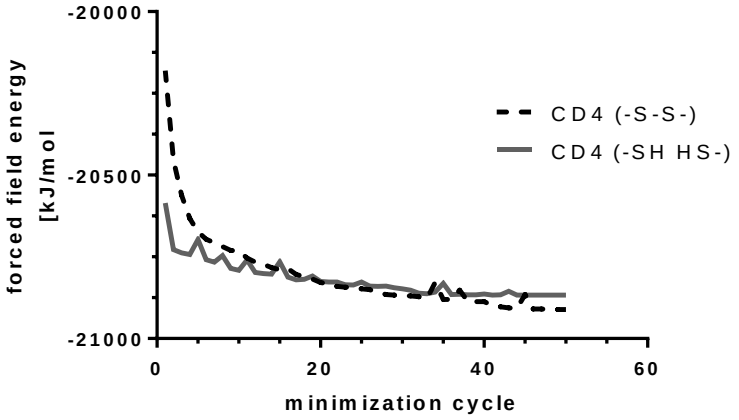

Figure 14: Tregalizumab-CD4 binding energy.

Course of energy minimization for the Tregalizumab –CD4 complex and separate constituents with and without D2-disulfide bridge in CD4 is shown. Calculations have been performed with the YASARA software system using the NOVA force field. *Modified*: Dr. Holger Wallmeier – CONDOR Scientific Computing & Consulting.

Calculation of binding energy was performed using the following formulas:

$$Binding\ energy\ (-S-S-) = energy\ (CD4{:}Tregalizumab\ complex) - [enregy\ (CD4_{-S-S-}) + energy\ (Tregalizumab)]$$

$$Binding\ energy\ (-SH\ HS-) = energy\ (CD4{:}Tregalizumab\ complex) - [enregy\ (CD4_{-SH\ HS-}) + energy\ (Tregalizumab)]$$

Graphs implicated fluctuations between very similar energy conformations (multiple minima problem). So, significant difference in binding energy between CD4 and Tregalizumab with and without the D2-disulphide bridge could not

concluded. Possibly, the binding energy of CD4 (including free thiols) is a little more stable compared to CD4 exhibiting the D2 disulfide bridge. However, since force field calculations only involve internal energy U (corresponds to enthalpy H), entropy contribution was not taken into account and the impact of disulfide bridge in D2 and binding of Tregalizumab had to be further elucidated.

5.3 Expression and purification of thioredoxins

To analyze the impact of Trx1 on binding of Tregalizumab to CD4, purification of different types of Trx1 was performed after expression in *E.coli* M15 cells. Thioredoxin1-CC-(CCC), thioredoxin1-CC-(AAA) and the inactive mutant Trx1-SS-(AAA) were purified by means of an Äkta™ Explorer (GE Healthcare) using a HiTrap column to catch the histidine tagged Trx1 (Figure 15).

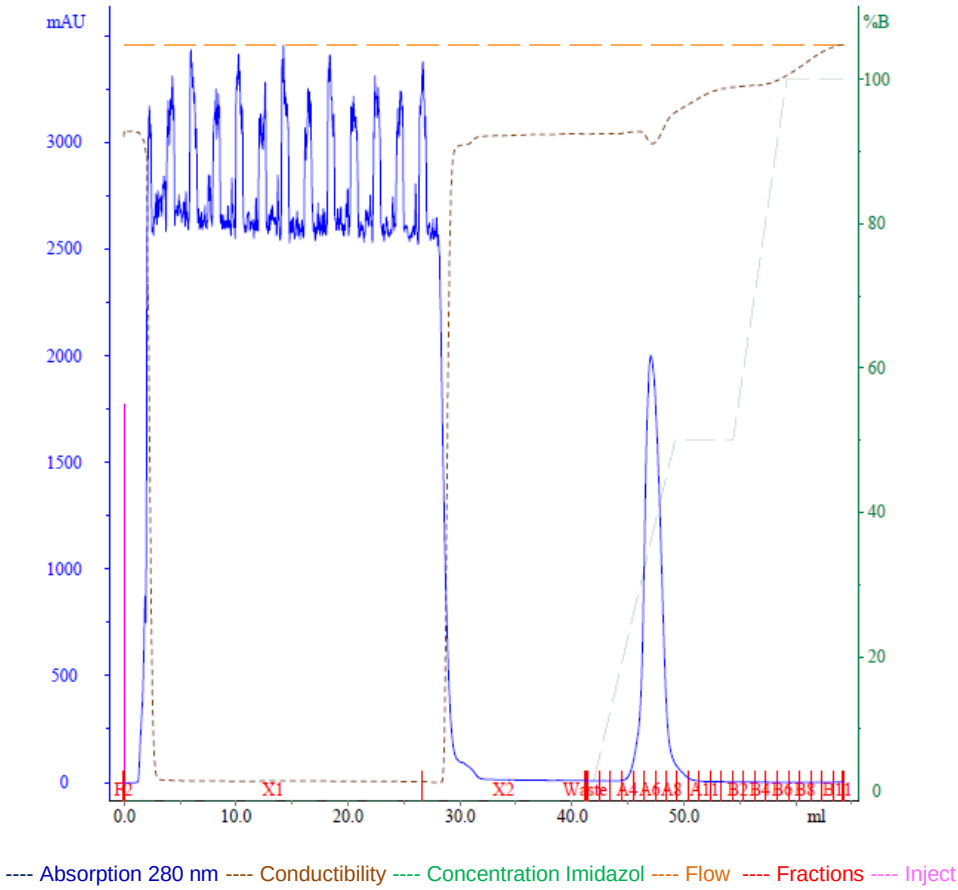

Figure 15: Chromatogram of thioredoxin1-CC-(AAA) via his-tag affinity chromatography

Purification of hexahistidine-SBP- tagged Trx1-CC-(AAA) was performed via an Äkta™ Explorer. The bacterial lysate was loaded on the HiTrap column (pink line), which was washed with washing buffer containing imidazole. Protein was eluted with increasing concentrations of imidazole (lime green line). Protein elution was measured via UV absorption at 280nm (dark blue line). Fractions A4-A9 (red line) were pooled to be analyzed via SDS-PAGE.

Additionally, in the most purified batches, a streptavidine-binding-protein (SBP) tag is cloned to the Trx1 molecule. However, this SBP-tag was not used for purification. The chromatogram of purification of Trx1-CC-(AAA) is shown as an example (Figure 15).

After elution, the fractions were collected and analyzed via SDS-PAGE (Figure 16) in order to identify fractions containing protein (in this example: fractions A4 –A9). Afterwards, fractions comprising the protein were combined and the pool was desalted using a Slide-A-Lyzer™ dialyses cassette. The concentration of the protein was determined by means of a photometric analysis (OD280). After adding 5 mM DTT, the pool was split in aliquots and stored at 2-8°C.

5.4 Analysis of thioredoxin purification fractions

Human Trx1 reveals a molecular weight of approximately 12 kDa[221]. A reducing SDS-PAGE was performed to analyze the quality of affinity chromatography purified fractions to determine the protein content (Figure 16).

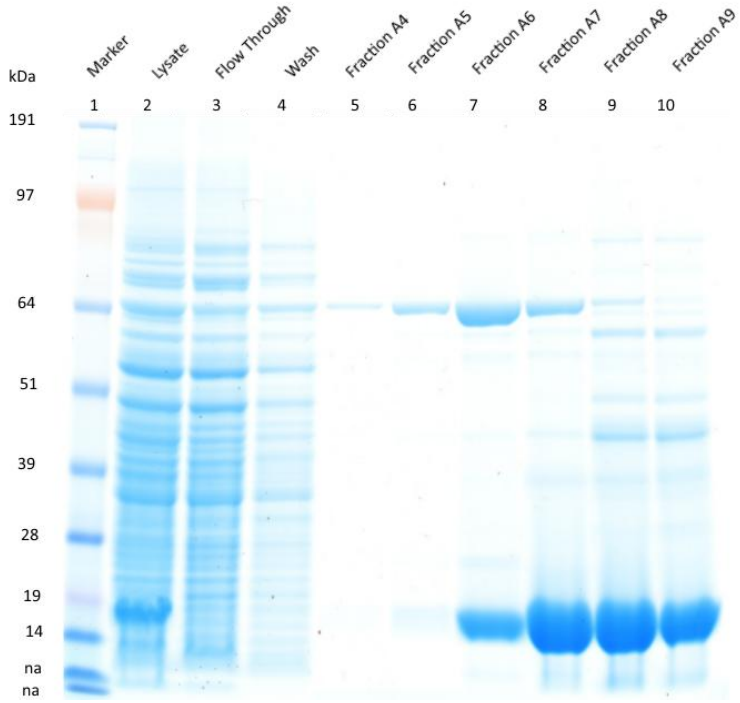

Figure 16: SDS-PAGE of Trx1 purification fractions

The different fractions of purification of Trx1 were analyzed by reducing SDS-PAGE to verify their quality. The size of the See Blue Plus® Pre-stained Protein Standard marker is shown in [kDa] on the left side of the gel. Lysate, flow through and wash fractions were analyzed via SDS-PAGE as well as fractions A4 – A9. Protein was detected with Coomassie staining. SBP-tagged Trx1-His_6- was found at approximately 17 kDa.

Trx1 was expressed as hexahistidine tagged molecule with a streptavidin-binding peptide (SBP)-tag exhibiting a lager molecular weight (approximately 17kDa) than non-tagged Trx1 (12kDa). See Blue®Plus Prestained Protein Standard was used as marker. The corresponding bands of the molecular weight marker are depicted in lane 1 in [kDa] (Figure 16). Lane 2 exhibited the bacterial lysate. Flow through fraction was applied in lane 3. Here, it was clear to see that the SBP- tagged Trx1-hexahistidine band (17 kDa) disappeared due to binding to the nickel sulfate column. Furthermore, no band of Trx1 was seen in lane 4 revealing the wash fraction. Fractions A4 (lane 5, Figure 16) to fraction A9 (lane 10, Figure 16) showed different concentrations of protein. The highest amount of Trx1 was found in fraction A7 (lane 8, Figure 16) and A8 (lane 9, Figure 16). Fraction A6 (lane 7, Figure 16) featured an impurity at approximately 64 kDa, which can be a tetramer of Trx1 and which was not reduced by reducing SDS-PAGE conditions. However, it is more likely to be another host cell protein binding to the column. Moreover, fraction A7 (lane 8) revealed the impurity at 64 kDa in smaller quantity. For this reason, only fractions A7 to A9 were pooled and used for further experiments.

5.5 Analysis of Trx1 activity

The activity of the purified Trx1 can be determined via reduction of insulin, which displays the protein substrate. Thereby, insulin is reduced very fast by Trx1 (Figure 17 A, red line) resulting in precipitation. In return, reduction of insulin catalyzed by DTT is much slower. However, recuperation of Trx1 by DTT takes place in a faster manner than reduction of insulin by DTT. The precipitated reduced insulin can be determined by turbidimetric analysis at 650 nm and correlates with activity of the tested $Trx1^{300}$. The active Trx1 (here Trx1-CC-(CCC) is shown as an example, (Figure 17 A). Activity of Trx1-CC-(CCC) was compared to the inactive mutant Trx1-SS-(AAA) (Figure 17 B). Thus, the active form of thioredoxin Trx1-CC-(CCC) (5 µM) catalyzed the reduction of insulin faster than 1 µM thioredoxin Trx1-CC-(CCC) (Figure 17 A) The mutant Trx1-SS-(AAA) did not reveal reduction of insulin showing that this thioredoxin protein is inactive (Figure 17 B). As expected, the blank controls of both experiments did not demonstrate any major increase of absorption (Figure

17 A and B). The first blank represented a test approach with DTT and without Trx1. The second blank contained only the tested Trx1 without DTT. There was a little increase of blank 1 control due to the fact that DTT is also capable to reduce insulin resulting in a small amount of precipitated insulin.

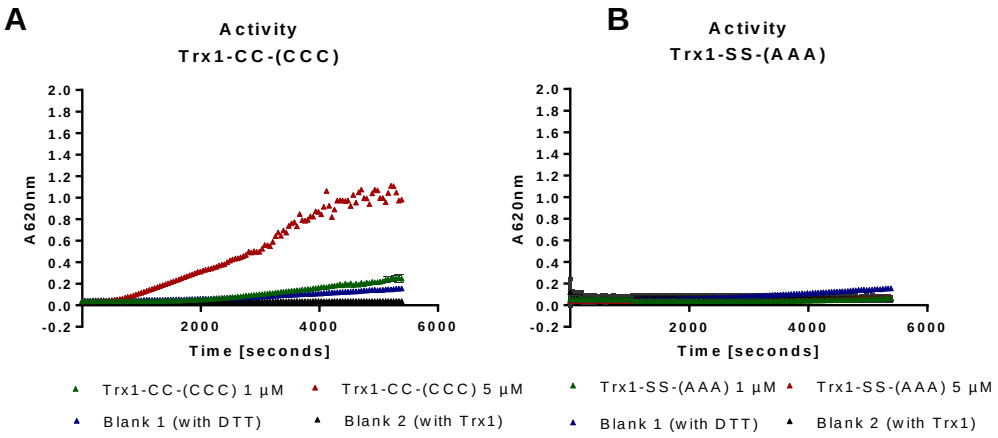

Figure 17: Determination of Trx1 activity via reduction of insulin by Trx1

Insulin was reduced by Trx1 to determine the activity of the purified Trx1.
(**A**) 5 µM Trx1-CC-(CCC) was able to reduce insulin resulting in the precipitated form, which can be measured by turbidimetric analysis at 650 nm. 1 µM Trx1-CC-(CCC) reduces insulin in a slower manner. The experiment was measured in triplicates.
(**B**) As expected, neither 5 µM nor 1 µM of the inactive mutant Trx1-SS-(AAA) did reveal any activity resulting in no precipitated insulin. The experiment was measured in triplicates.

5.6 Analysis of thioredoxin reductase activity

After determination of Trx1 activity, enzymatic activity of TrxR from rat liver was analyzed.

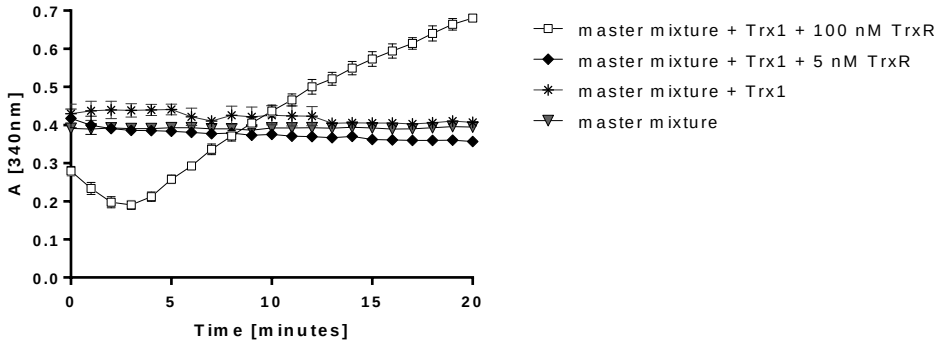

Figure 18: Determination of activity of TrxR from rat liver with insulin assay

Two concentrations of TrxR (5 nM and 100 nM) were incubated with 160 µM insulin, 150 µM NADPH and 20 µM Trx1 in TE buffer. The absorbance was measured at 340 nm. The initial linear phase depicted consumption of NADPH as a decrease of the curve showing activity of TrxR. After the initial phase, insulin B chains started to precipitate - which can be seen in the increase of the curve. The experiment was measured in triplicates.

Activity of TrxR (5 nM and 100 nM) was measured via consumption of NADHP as the initial linear phase, which can be seen as a decrease of absorbance. A photometric measurement at 340 nm revealed that 100 nM TrxR is active since consumption of NADPH was observed. However, 5 nM TrxR showed no effect, which can be explained by short sample time (Figure 18). After the primary phase the curve rose due to precipitation of the reduced insulin B chains.

5.7 Higher Trx1 levels in RA plasma compared to healthy subjects

Many studies display that Trx1 levels are augmented in patients suffering from Rheumatoid Arthritis or other diseases like heart[336–338], lung[339–341] and liver complaints[342,343]. To confirm these facts, Trx1 concentrations in plasma of RA patients and healthy subjects were examined by an enzyme linked immunosorbent assay (Human Thioredoxin Assay Kit, Figure 19).

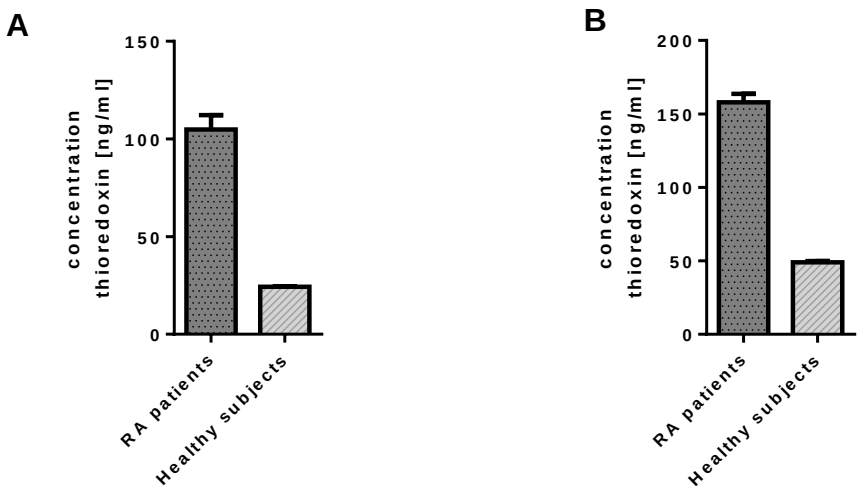

Figure 19: Measurement of the concentration of Trx1 in plasma of RA patients and healthy subjects

Plasma of Rheumatoid Arthritis patients was compared to healthy subjects for their levels of Trx1. ELISA measurement was used to analyse the Trx1 concentration in samples by comparison with a Trx1 standard curve. Two experiments (**A** and **B**) are shown and mean of six individually measured samples are depicted (measured in duplicates).

Since the colour intensity is proportional to the Trx1 concentration, the Trx1 levels in plasma samples were quantified with help of a Trx1 standard curve. The results of measurement revealed that plasma of RA patients contained higher levels (Figure 19 A, 104.8 ± 7.4 ng/mL; B, 157.9 ± 5.8 ng/mL) of Trx1 than healthy donors (Figure 19 A, 24.4 ± 0.2 ng/mL; B, 49.0. ± 0.9 ng/mL).

These tests confirm the literature observations that Trx1 levels are increased in RA patients.

5.8 Trx1 is able to reduce recombinant human soluble CD4

Trx1 is described to be able to selectively reduce CD4 D2 disulfide bond, which can exist in the reduced and in the oxidized state[25,334]. To verify this fact, a SDS-PAGE was performed to determine, if recombinant human soluble CD4 (rh sCD4) can be reduced by purified thioredoxins and to analyze the redox state of CD4. Trx1-SS was used a negative control. Determination of reduction was shown by labelling of rh sCD4 thiols with (Methyl-PEG_{12})$_3$-PEG4-maleimide ($TMM(PEG)_{12}$) representing a methyl-containing, polyethylene glycol substance with a molecular mass of approximately 2.6 kDa (Figure 20). Covalent pegylation of sulfhydryls can be achieved by an activated maleimide group, which reacts with thiols[344]. The arising labelled thiols reveal a bigger molecule size due to attached pegylation agent.

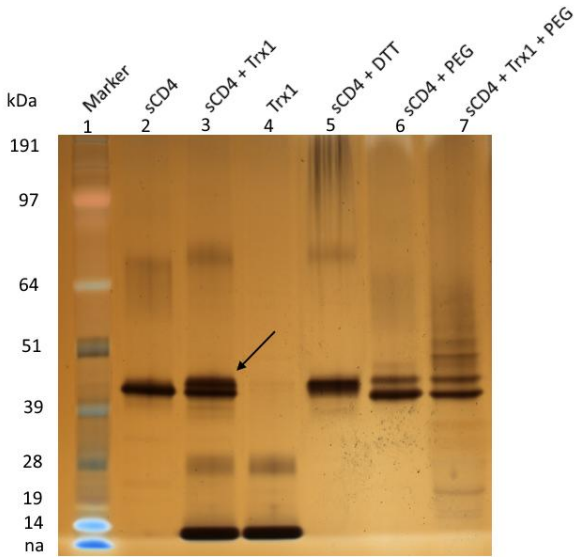

Figure 20: Impact of Trx1 on rh sCD4

A non-reducing SDS-PAGE (4-12% Bis-Tris gel) was performed to analyze the influence of Trx1 on rh sCD4. $TMM(PEG)_{12}$ a methyl- containing, polyethylene glycol substance with a molecular mass of approximately 2.6 kDa was used to form covalent pegylation of thiol groups of rh sCD4. Silver staining was used to visualize protein. 62.5 ng rh sCD4 (~ 40 kDa) were pre-incubated with 2.5 µM Trx1 (~ 12 kDa) (lane 3) or 25 mM DTT (lane 5). After incubation of rh sCD4 with $TMM(PEG)_{12}$ an additional band appeared representing pegylated free thiols (lane 6). Trx1 pre-treatment and pegylation resulted in two extra bands (lane 7) indicating that one disulfide bridge of rh sCD4 was reduced by Trx1. The size markers in [kDa] are depicted on the lift side of the gel. Trx1 (lane 4) and rh sCD4 (lane 2) were used as controls. PEG = $TMM(PEG)_{12}$.

Recombinant human sCD4 was found at approximately 40 kDa at a non-reducing SDS-PAGE (Figure 20, lane 2). Lane 3 represented rh sCD4, which was incubated which 2.5 µM Trx1 whereat, Trx1 appeared at 12 kDa (Figure 20, lane 3 and 4). After treatment with reduced Trx1 (Figure 20, lane 3) or 25 mM DTT (Figure 20, lane 5) an additional rh sCD4 band arose, representing reduced rh sCD4 with a lower mobility in the gel. After pegylation with TMM(PEG)$_{12}$ a second band was detected next to the rh sCD4 band (Figure 20, lane 6). Moreover, after pre-incubation with Trx1 and subsequent pegylation two additive bands emerged, representing labelled thiols. In addition, Trx1 was pegylated causing a pale band at approximately 22 kDa (Figure 20, lane 7). Bands at about 28 kDa delineated dimers of Trx1.

Moreover, the impact of the complete Trx1/TrxR/NADPH system on rh sCD4 was determined using a non-reducing SDS-PAGE analysis (Figure 21).

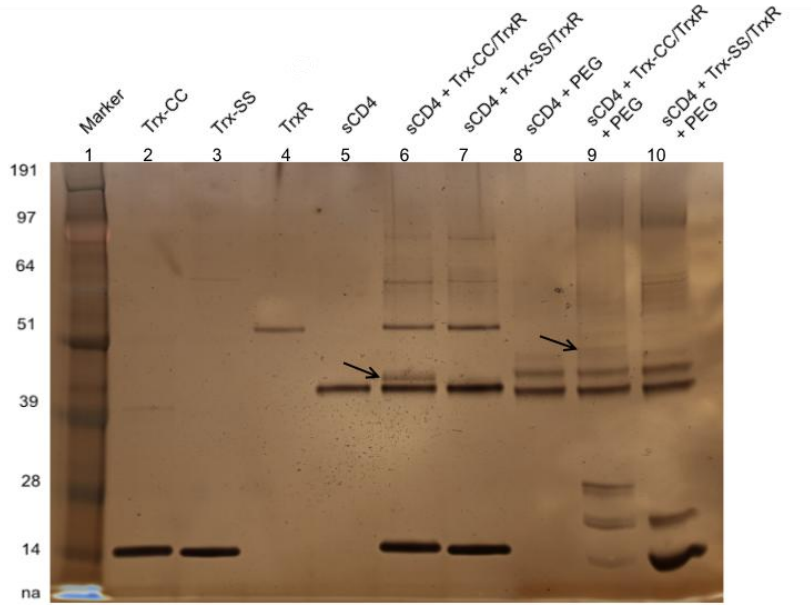

Figure 21: Impact of Trx1 and TrxR on rh sCD4

Impact of Trx1 and TrxR/NADPH to rh sCD4 was analyzed using a non-reducing SDS-PAGE (10% Bis-Tris gel). Proteins were visualised by silver staining. Hexahistidine-SBP-tagged Trx1-CC and Trx1-SS can be found at approximately 17 kDa (lane 1 and 2). TrxR exhibited a molecular weight of 55 kDa (lane 4) and rh sCD4 of about 40 kDa (lane 5). Pre-incubation with 5 µM Trx1-CC, 150 nM TrxR and 1 mM NADPH (over night at 2-8°C) caused an additional band next to the rh sCD4 band (lane 6, see arrow), which was not observed after incubation with 5 µM Trx1-SS, 150 nM TrxR and 1 mM NADPH (lane 7). Pegylation of rh sCD4 using TMM(PEG)$_{12}$ evoked two extra bands (lane 8). Pre-incubation of rh sCD4 with 5 µM Trx1-CC, 150 nM TrxR and 1 mM NADPH showed four bands (lane 9) of which one is extra (see arrow), compared to rh sCD4 (lane 8). However, the fourth band was not detected after Trx1-SS/TrxR/NADPH pre-incubation (lane 10). Since Trx1 was not removed, three Trx1-CC band pairs were observed after pegylation (lane 9) ≤ 28 kDa. PEG = TMM(PEG)$_{12}$.

Here, Trx1-SS was also included as negative control. Pre-incubation of rh sCD4 with 5 µM Trx1-CC, 150 nM TrxR and 1 mM NADPH showed a similar extra band at approximately 43 kDa (Figure 21, lane 6) compared to rh sCD4 without pre-treatment (Figure 21, lane 5).

The inactive Trx1-SS protein did not alter the band pattern and only the rh sCD4 band at 40kDa was observed as expected (Figure 21, lane 7). Pegylation of sulfhydryl groups using TMM$(PEG)_{12}$ revealed two additional bands regarding the rh sCD4 protein (Figure 21, lane 8).

Pre-treatment of rh sCD4 with Trx1-CC, TrxR, NADPH also evoked an additional band (Figure 21, lane 9). This band was not seen using 5 µM Trx1-SS, 150 nM TrxR and 1 mM NADPH (Figure 21, lane 10).

In conclusion, Trx1 as well as the Trx1/TrxR/NADPH system is able to reduce a disulfide bond in the rh sCD4 molecule.

5.9 Trx1 shows no observable impact on the native CD4 molecule on CD4+ HPB-ALL cells

Having confirmed the impact of Trx1 on rh sCD4, the native CD4 molecule on CD4+ HPB-ALL cells was examined by western blotting. 10^6 CD4+ HPB-ALL cells were incubated over night with 150 nM TrxR, 1 mM NADPH and 5 µM Trx1-CC, respectively 5 µM Trx1-SS.

Cells were lysed in buffer with and without MM$(PEG)_{24}$ pegylation agent. MM$(PEG)_{24}$ is a methyl-containing, polyethylene glycol substance with a molecular mass of approximately 1.2 kDa. Similar to TMM$(PEG)_{12}$, the methyl-PEG-Maleimide reagent is able to form covalent pegylation of thiol groups. The supernatant was analysed by SDS-PAGE and subsequently immunoblotted against anti-CD4 (Figure 22).

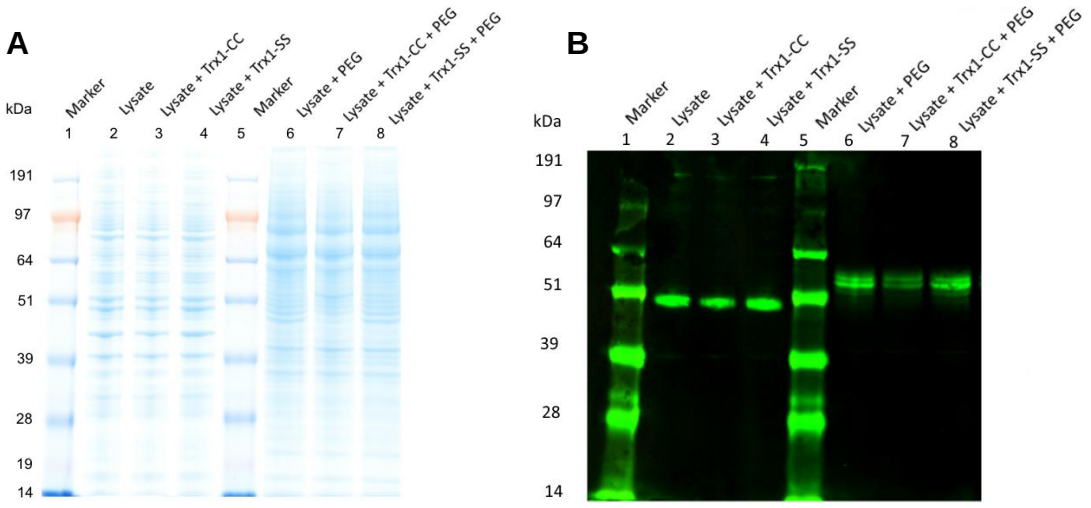

Figure 22: SDS-PAGE and western blot of HPB-ALL lysate

(**A**) HPB-ALL cells were analyzed via reducing SDS-PAGE to determine impact of Trx1 on CD4 surface protein. After over night incubation of HBP-ALL cells with 5 µM Trx1-CC or 5 µM Trx1-SS, 150 nM TrxR and 1 mM NADPH cells were lysed by means of lysing buffer containing either $MM(PEG)_{24}$ (lane 6-8) or no labelling agent (lane 2-4). SDS-PAGE was subsequently blotted $MM(PEG)_{24}$ against CD4.
(**B**) Western blotting was conducted to examine the impact of Trx1 on CD4+ HPB-ALL cells. After over night incubation of HBP-ALL cells with 5 µM Trx1-CC or Trx1-SS, 150 nM TrxR and 1 mM NADPH cells were lysed by means of lysing buffer containing $MM(PEG)_{24}$ (lane 6-8) or no (lane 2-4). The PVDF membrane was incubated with polyclonal goat anti-human CD4 antibody (R&D Systems) and donkey anti-goat IRDye®800 (LI-COR), which was used as secondary antibody. Infrared fluorescence was used to visualize the results. PEG = $MM(PEG)_{24}$.

Overall, infrared fluorescence measurement revealed no additional bands. However, since the bands of lysed CD4+ cells treated with Trx1-CC and $MM(PEG)_{24}$ are difficult to detect, it is possible that additional bands are existing but can not be visualized. Moreover, a possible reason for this is that the anti-CD4 antibody is not able to detect CD4 after incubation with $MM(PEG)_{24}$. In conclusion, Trx1 revealed no observable impact on the native CD4 molecule on CD4+ HPB-ALL cells.

5.10 Trx1 binding experiments to rh sCD4

Trx1 is described to selectively reduce D2 of the CD4 molecule[25], which is in close proximity to the Tregalizumab binding site. In order to asses if binding of Tregalizumab is influenced by Trx1-driven reduction of the D2 disulfide bridge, some binding studies were performed. Recombinant human sCD4 and CD4+ cells were pre-incubated with Trx1 and binding of Tregalizumab was determined (Figure 23 and Figure 24).

5.10.1 Trx1 reduces Tregalizumab binding to rh sCD4

First, the binding of Tregalizumab to rh sCD4 was assessed after pre-incubation (for 30 minutes) with pre-reduced Trx1. An electrochemiluminescent assay was performed to elucidate the effect of Trx1. As shown in Figure 23 A, binding of Tregalizumab to rh sCD4 was significantly decreased to 34.3 ± 15.2 % in relation to the non-treated control after pre-treatment with 20 µM Trx1.

5.10.2 Impact of Trx1 depends on its concentration

Moreover, it was explored if binding of the monoclonal antibody is influenced by Trx1 in a concentration dependent manner. Recombinant human sCD4 was incubated with different Trx1 concentrations and binding of Tregalizumab was determined by electrochemiluminescence (Figure 23).

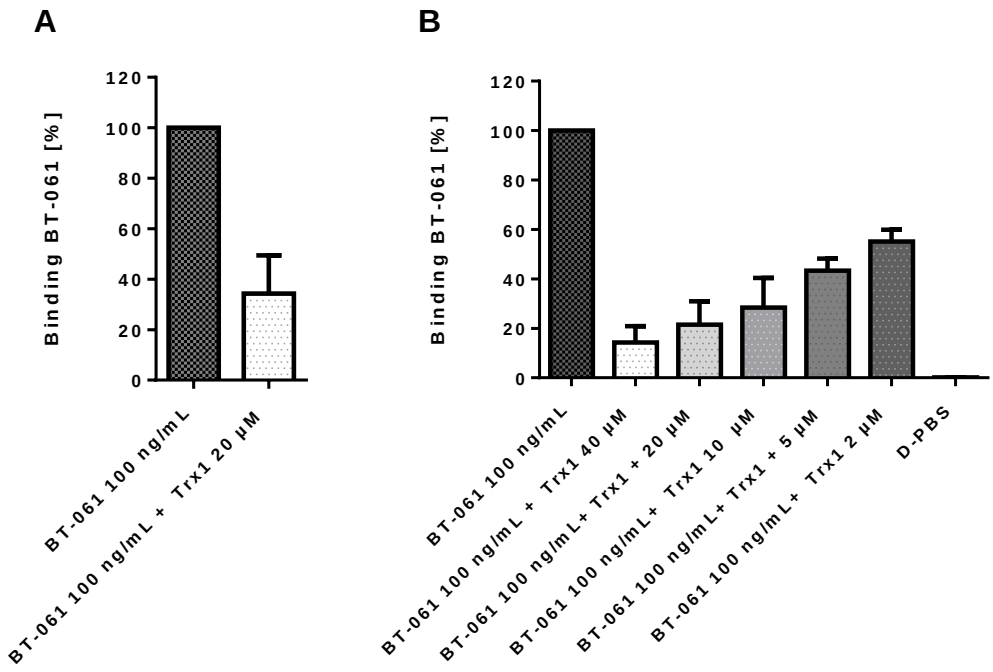

Figure 23: Impact of Trx1 on binding of Tregalizumab to rh sCD4

(**A**) Rh sCD4 was incubated with 20 µM Trx1 for 30 ± 5 minutes. After three washing steps, binding of Tregalizumab to rh sCD4 was measured using an electrochemiluminescence ELISA. Data represent results from three independent experiments measured in triplicates. Error bars indicate the standard deviation. P-values were calculated by means of a Wilcoxon matched-pairs signed rank test.
(**B**) Different concentrations of Trx1 were incubated with rh sCD4. Binding of Tregalizumab was measured by means of electrochemiluminescence. A concentration dependent decrease of Tregalizumab binding was observed. Data represent results from one experiment measured in triplicates. Error bars indicate the standard deviation.

The analysis demonstrated that the concentration of Trx1 influences binding of Tregalizumab to rh sCD4 differently. 40 µM Trx1 showed a reduction of about 86% to 14.2 ± 6.6%, 20 µM Trx1 revealed a remaining binding of 21.5 ± 9.5%. Furthermore, 10 µM Trx1 caused a decline to 28.4 ± 12.0%, 5 µM Trx1 incubation resulted in retained binding of 43.3 ± 4.9%. 55.1 ± 4.8% binding remained after pre-treatment of rh sCD4 with 2 µM Trx1. D-PBS served as negative control. No signal was observed as expected (Figure 23 B).

5.10.3 Trx1 reduces binding of Tregalizumab and other anti-CD4 antibodies to rh sCD4

Impaired binding of Tregalizumab to rh sCD4 caused by Trx1 is potentially entailed by structural changes of the CD4 molecule after reduction of the D2 disulfide bridge. To examine whether other anti-CD4 antibodies are also affected by Trx1, the other monoclonal antibodies SK3, RPAT-4, OKT-4 and MT441 were also analyzed using the electrochemiluminescence assay (Figure 24).

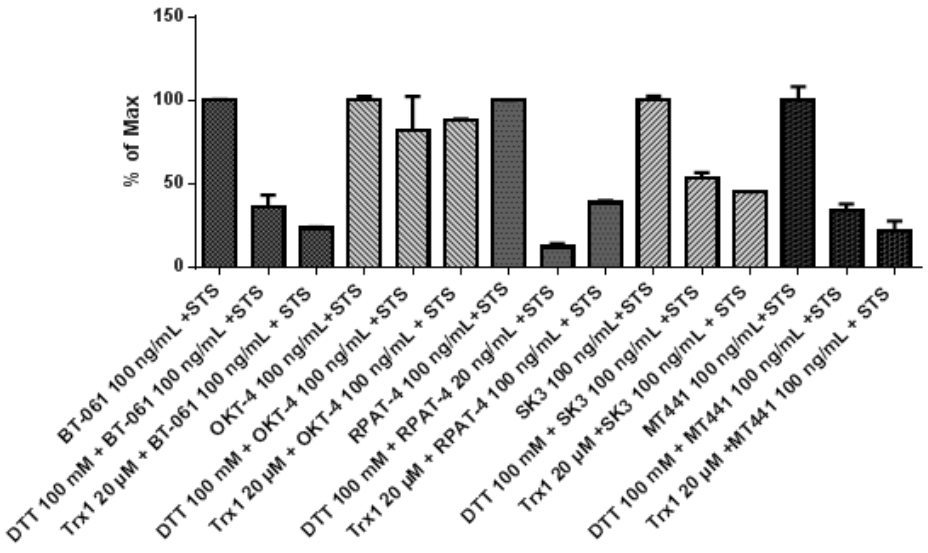

Figure 24: Impact of Trx1 on various CD4 antibodies

Tregalizumab (BT-061), SK3, RPAT-4, MT441 and OKT-4 were analyzed for binding to rh sCD4 using an electrochemiluminescence assay. Trx1 impacts also other anti-CD4 antibodies: Binding of Tregalizumab and MT441 was affected by 20 µM Trx1 to a comparable extent. Similar effects were seen with regard to RPA-T4 and SK3. However, impact of Trx1 treatment resulted in a less decline of binding to rh sCD4 compared to Tregalizumab and MT441. No decrease in binding was detected for OKT-4 after pre-treatment with 20 µM Trx1. 100 mM DTT served as positive control due to its reducing properties. Data represent results from one experiment measured in triplicates. Error bars indicate the standard deviation. STS = sulfo-tag labelled streptavidin.

100 mM DTT served as positive control due to its reducing properties. Measurements revealed that Trx1 impacts also other anti-CD4 antibodies: Binding of Tregalizumab and MT441 was affected by 20 µM Trx1 to a comparable extent. Similar effects were seen with regard to RPA-T4 and SK3. However, pre-incubation of rh sCD4 with Trx1 resulted in a less decline of binding to rh sCD4 of these antibodies compared to Tregalizumab and MT441.No decrease in binding was detected for OKT-4 after pre-treatment with 20 µM Trx1. These effects may result from different binding sites of each antibody to the different domains of CD4. Since D3 of the CD4 molecule contains no disulfide bridge[55], impact of Trx1 on OKT-4 (which bins to D3) is negligible. Binding of RPA-T4 and SK3, which bind to D1, are also impacted by Trx1 pre-treatment. However, binding of antibodies, which target D2, seemed to be influenced to the highest extent by Trx1. Regarding influence of DTT, it can be concluded that impact of Trx1 on binding of all antibodies was higher compared to DTT, except RPA-T4. Here, DTT caused a higher decline of binding of this monoclonal antibody to CD4.

5.11 Labelling of Tregalizumab with allophycocyanin

Due to power of Trx1 to decrease the binding of Tregalizumab to rh sCD4, additional studies with CD4+ cells were performed to scrutinize if binding of Tregalizumab to CD4+ cells is also impacted. For this purpose, flow cytometry experiments with fluorochrome-labelled Tregalizumab should be conduced. Therefore, fluorescence labelled Tregalizumab had to be generated for use in the following experiments. Allophycocyanin (APC, Figure 25) was selected due to its excitation maximum at 650 nm and an emission maximum at 660 nm[345].

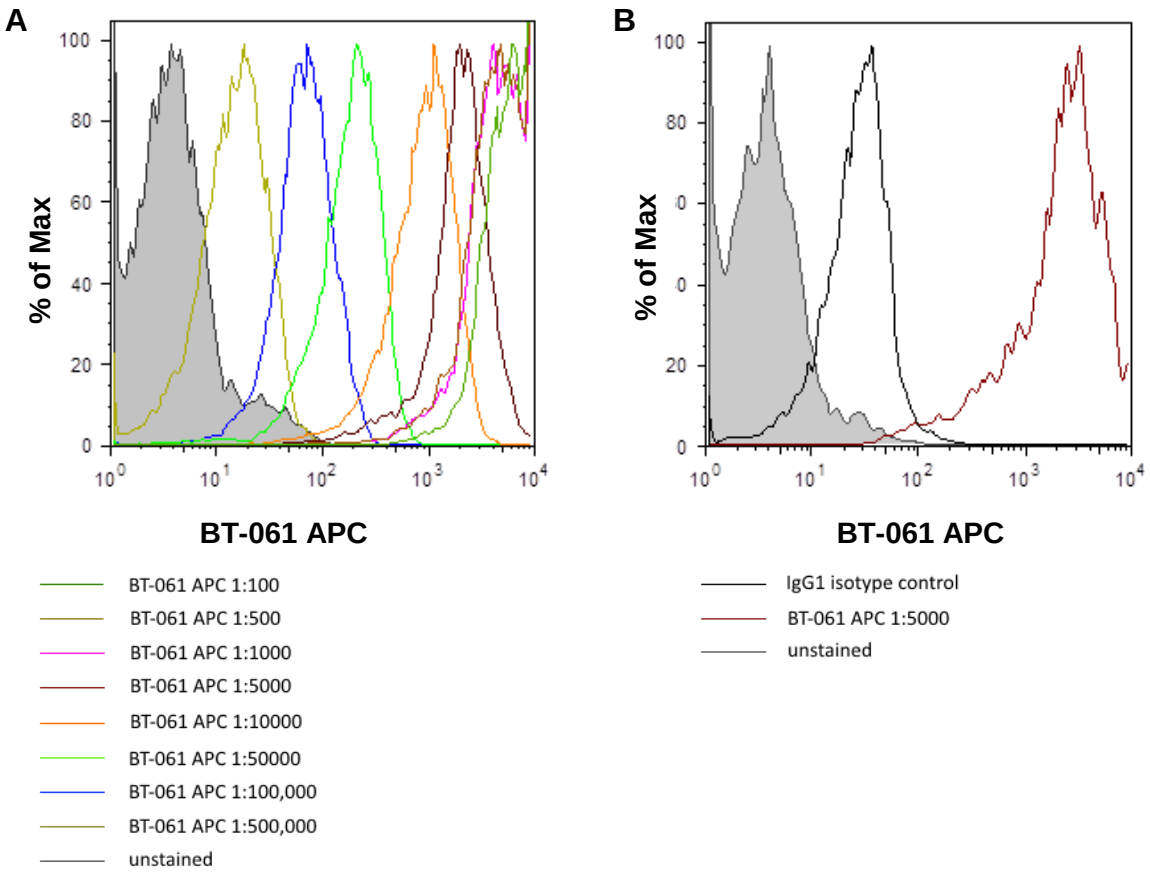

Figure 25: Labelling of Tregalizumab with allophycocyanin

(**A**) Tregalizumab (BT-061) was labelled with allophycocyanin (APC). The efficacy was tested by flow cytometry using CD4+ HPB-ALL cells. Different dilutions were tested from 1:100 to 1:500,000. A suitable concentration of 1:5,000 was identified and used in further experiments.
(**B**) To confirm the specificity of the BT-061-APC antibody, a mouse IgG1 APC-labelled antibody was used as isotype control. Both, the isotype control and BT-061-APC were diluted to the same concentration and mean fluorescence intensity was detected by flow cytometry. No unspecific binding of Tregalizumab was seen.

After preparation of APC-labelled Tregalizumab with help of a commercially available kit, the binding properties of the conjugate was tested applying CD4+ HBP-ALL cells and mouse IgG1 as isotype control (Figure 25, B). The optimal dilution of Tregalizumab-APC (1.5 mg/mL) was tested to be approximately 1:5,000 corresponding to 15 µg antibody (since 50 µL cell suspension were stained with 80 µL of 1:5,000 pre-diluted antibody), which was used in further experiments (Figure 25, A).

5.12 Binding of Tregalizumab to CD4+ cells is reduced by the Trx1/TrxR/NADPH physiological system

Trx1 is present in low nanomolar concentrations in the blood plasma[346]. However, in some autoimmune diseases elevated Trx1 levels occur[15,16,18,210]. In some tissues Trx1 concentrations can reach up to 10 µM[347] and its expression is up-regulated after activation of different cells[309]. Expression and secretion of Trx1 is even higher in human regulatory T-cells compared to effector T-cells[213].

In order to evaluate the impact of Trx1 and its physiological partners on binding of Tregalizumab to CD4+ HPB-ALL cells, binding studies were performed. HPB-ALL cells represent a human T-cell line, which was established from a Japanese boy suffering from acute lymphoblastic leukaemia and thymoma[348]. Moreover, PBMC were analysed. Flow cytometry studies should elucidate the physiological influence of Trx1/TrxR/NADPH on binding of Tregalizumab to these cells.

In the cellular environment Trx1 exerts its reduction function with help of the flavoenzyme TrxR and NADPH[221]. Thereby, TrxR keeps Trx1 in the reduced and active state. In the conducted experiments CD4+ cells were pre-incubated with Trx1, TrxR and NADPH. During reduction of one CD4 molecule by one molecule Trx1 the Trx1 gets oxidized and remains inactive. In order to recycle Trx1 to the active state, TrxR was added. The recycled Trx1 is then able to subsequently reduce another CD4 molecule and the redox cycle starts again. Therefore, high concentrations of Trx1 are necessary for reduction, since HPB-ALL cells express high levels of CD4.

5.12.1 Short term treatment with Trx1 reduces binding of Tregalizumab to CD4+ HPB-ALL cells

Two incubation periods of HPB-ALL cells with the Trx1/TrxR/NADPH system were tested. A short time incubation of 60 minutes was compared to over night incubation (15 ± 2 hours), simulating the physiological conditions of the organism. Moreover, two different concentrations of TrxR were analyzed to identify the adequate concentration of the enzyme in this assay (Figure 26).

5.12.1.1 Treatment with 300 nM TrxR, 10 µM Trx1 and 1 mM NADPH

10^5 CD4+ HPB-ALL cells were incubated with and without 300 nM TrxR and 10 µM Trx1 for one hour (n = 5). Cells incubated without Trx1 served as negative control. Compared to the non-treated control (1579 ± 573 MFI), pre-treatment with Trx1 showed a little reduction of Tregalizumab binding to CD4 (n = 5), which was not significant: 10 µM Trx1 in combination with 300 nM TrxR and 1 mM NADPH caused a decreased binding of Tregalizumab of around 20% (1278 ± 344 MFI). Moreover, incubation of CD4+ cells without the enzyme showed also a reduction of approximately 20% (1281 ± 621 MFI; Figure 26 A).

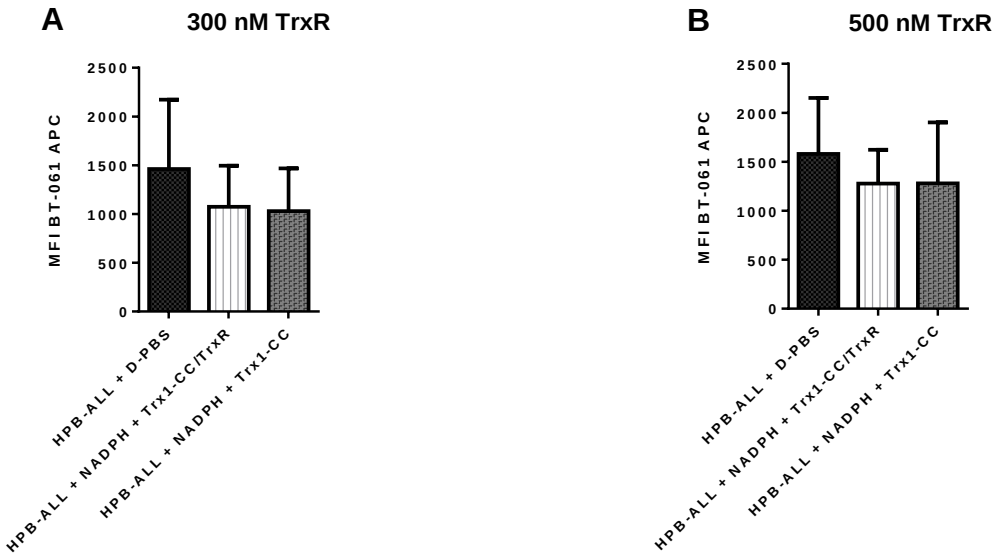

Figure 26 Short term pre-treatment of CD4+ HBP-ALL cells with Trx1 and impact on binding of Tregalizumab to CD4+ HPB-ALL cells

10^5 cells were incubated with 10 µM Trx1 and either 300 nM TrxR (**A**) or 500 nM TrxR (**B**) and 1 mM NADPH for 60 ± 5 minutes. Data represent results from five independent experiments performed in duplicates. Error bars indicate the standard deviation. P-values were calculated by means of Wilcoxon matched-pairs signed rank test since data is not normally distributed.

5.12.1.2 Treatment with 500 nM TrxR, 10 µM Trx1 and 1 mM NADPH.

Incubation of CD4+ cells with 500 nM TrxR in combination with 10 µM Trx1 showed similar results (n = 5): Compared to the non-treated control (1461 ± 712 MFI) pre-incubation of CD4+ cells with 500 nM TrxR, 1 mM NADPH and 10 µM Trx1 resulted in a reduced binding of around 26% (1075 ± 420 MFI). Trx1 without TrxR showed a decline to 71% binding (1031 ± 438 MFI, Figure 26 B).

5.12.2 Trx1 incubation overnight impacts binding of HPB-ALL cells significantly

To simulated more physiological conditions HPB-ALL cells were pre-treated with different concentrations of Trx1, 150 nM TrxR and 1 mM NADPH and incubated over night (Figure 27). On the one hand, CD4+ cells were incubated with the active protein in combination with or without TrxR. On the other hand, an inactive Trx1 mutant (Trx1-SS) served as negative control. Binding of Tregalizumab was measured using flow cytometry and fluorochrome-labelled Tregalizumab.

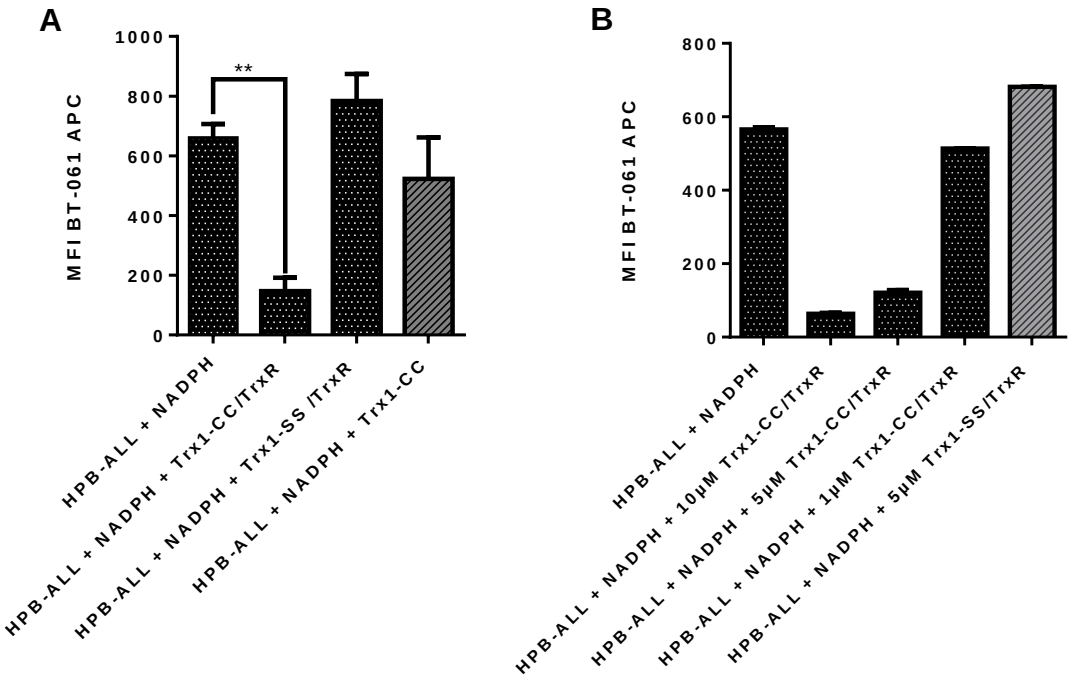

Figure 27: Impact of Trx1 on binding of Tregalizumab to CD4+ HPB-ALL cells

A) CD4-positive T-cell leukaemia cells (HPB-ALL) were incubated with 5 µM Trx1, 150 nM TrxR and 1 mM NADPH for 15 ± 2 hours over night. Binding of Tregalizumab to CD4 was measured using flow cytometry. The redox inactive thioredoxin1-SS-mutant (Trx1-SS) served as control. Mean fluorescence intensity (MFI) of BT-061-APC is shown.
Data represent results from four independent experiments performed in duplicates. Error bars indicate the standard deviation. P-values were calculated by means of a paired t-test since the data is normally distributed. Significance is shown as p-value: ** p< 0.01.
B) HPB-ALL cells were incubated with either 1 µM, 5 µM or 10 µM Trx1, 150 nM TrxR and 1 mM NADPH for 15 ± 2 hours over night. Impact of Trx1 on binding of Tregalizumab to CD4 depends on Trx1 concentration. Data represent results from one experiments performed in duplicates.

HPB-ALL cells incubated with 150 nM TrxR, 5 µM Trx1 and 1 mM NADPH over night resulted in a significantly reduced binding of Tregalizumab from 661 ± 91 to 147 ± 45 mean fluorescence intensity units (MFI) of the BT-061-APC staining ($p < 0.0041$). This corresponds to a reduction of binding of 78 % compared to

the non-treated control (Figure 27 A). Incubation with 5 µM Trx1 alone without TrxR displayed a less pronounced reduction of binding of Tregalizumab. This is expected since Trx1 without TrxR is not recycled and can facilitate the disulfide reduction process only once per molecule. As expected, the inactive control Trx1-SS was not able to reduce the Tregalizumab binding to CD4.

The influence of Trx1 on binding of Tregalizumab to CD4 depends on the concentration of Trx1 (Figure 27 B).

When HPB-ALL cells were incubated with 5 µM Trx1, 150 nM TrxR and 1 mM oxidized NADP+ for 15 ± 2 hours over night no decrease of binding of Tregalizumab was observed (data not shown).

5.12.3 Trx1 decreases binding of Tregalizumab to PBMC

The results of impact of Trx1 on HPB-ALL cells were confirmed using peripheral blood mononuclear cells (PBMCs) isolated from healthy subjects (Figure 28). Pre-treatment of PBMC with Trx1/TrxR/NADPH resulted in a significant ($p < 0.0007$) decrease of 71 % of Tregalizumab binding to CD4+ cells compared to untreated cells (from 479 ± 73 to 140 ± 75 MFI of the BT-061-APC staining), whereas the inactive mutant showed no significant decline of Tregalizumab binding. Pre-incubation of PMBC with Trx1 without TrxR also revealed a less pronounced diminished binding of Tregalizumab comparable to the result observed on HPB-ALL cells (Figure 28).

5.13 Glutathione showed no impact on Tregalizumab binding

Beside Trx1, other molecules are able to modulate the redox potential in the blood, such as GSH, which represents a physiologically relevant reducing agent[27]. The intracellular concentrations of GSH range from 0.5 mM to 10 mM in mammalian cells. However, much lower levels can be detected in the blood plasma[27]. To investigate a potential influence of GSH on the stability of the CD4 disulfide bridges and the interaction between Tregalizumab and CD4, further binding experiments were performed. Even when using GSH concentrations up to 10 mM, no significant effect on binding of Tregalizumab to CD4+ cells from PBMCs was observed (Figure 28).

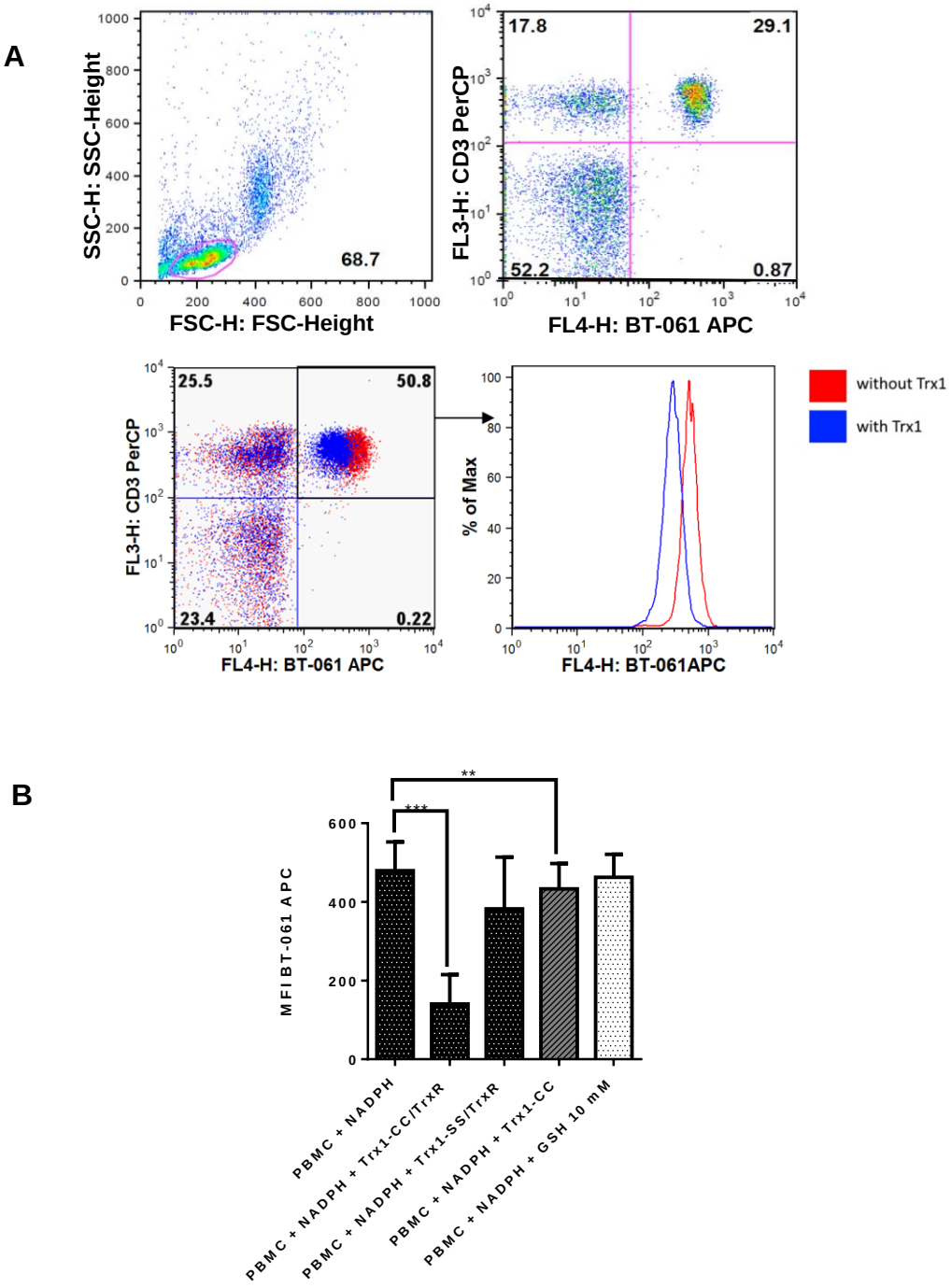

Figure 28: Impact of Trx1 on binding of Tregalizumab to peripheral blood mononuclear cells

(**A**) The gating strategy is illustrated: lymphocytes were selected according to cell size and granularity (FSC/SSC) and the binding of Tregalizumab to CD4 was determined in the CD3+ CD4+ gated cells. A representative dot plot (lower left) and histogram (lower right, [% of max]) of CD3+ CD4+ (BT-061+) cells is depicted with (blue) and without (red) Trx1/TrxR pre-incubation.
(**B**) Impact of the Trx1 system on binding of Tregalizumab to isolated PBMCs expressing CD4. PBMC were incubated with 5 µM Trx1, 150 nM TrxR and 1 mM NADPH over night. The inactive mutant Trx1-SS served as negative control. Data represent results from five independent experiments performed in duplicates. Error bars indicate the standard deviation. P-values were calculated by means of a paired t-test since data is normally distributed. Significance is shown as p-value: ** p< 0.01, *** p< 0.001.

These results demonstrate that recombinant and cellular CD4 can be selectively reduced by Trx1 and this reduction diminishes the binding of Tregalizumab to the CD4 receptor. The other physiologically relevant reducing agent GSH does not influence binding of Tregalizumab to CD4.

5.14 Trx1 has no influence on CD64 expression on monocytes

The pharmacological effect of CD4 down-modulation after Tregalizumab stimulation can only occur when the Fc part of Tregalizumab is cross-linked with the Fc-gamma receptor 1 (FcγRI, CD64) on monocytes[28]. Regarding CD64, no disulfide bridges are described for the CD64 receptor[349]. It can be possible that the observed higher CD4 down-modulation in healthy subjects compared to RA patients is caused either by a decreased binding of Tregalizumab's Fab part to CD4 or by diminished expression or modification of the FcγRI (CD64). To test a potential influence on CD64 binding of Tregalizumab, PBMCs encompassing monocytes were incubated with the Trx1/TrxR/NADPH system and binding to CD64 on monocytes was determined by flow cytometry using a specific anti-CD64 antibody. Moreover, influence of 10 mM GSH on Tregalizumab – CD64 interaction was tested in these experiments (Figure 29).

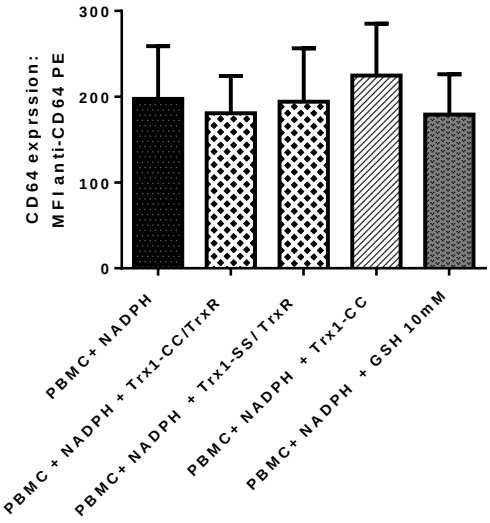

Figure 29: Impact of Trx1/TrxR and GSH on Fc-gamma receptor 1 (CD64) expression

PBMC were incubated with either 5 µM Trx1, 150 nM TrxR, 1 mM NADPH or 10 mM GSH, 1 mM NADPH for 15 ± 2 hours over night. After three washing steps binding of fluorochrome-labelled anti-CD64 antibody was measured via flow cytometry (n = 5, duplicates). Monocytes were gated according to their size and granularity (FSC/SSC). Mean fluorescence intensity (MFI) of anti-CD64 PE is shown. Error bars indicate the standard deviation.

Untreated monocytes revealed a mean fluorescence intensity of 197.5 ± 61.4. Trx1-CC /TrxR/NADPH pre-incubated monocytes showed a relative expression of CD64 of 180.8 ± 43.2 MFI. 194.2 ± 62.1 mean fluorescence activity was observed after incubation with the inactive Trx1-SS mutant and TrxR.

Treatment of cells with pre-reduced Trx1-CC without TrxR revealed relative expression of 224.7 ± 60.5 MFI. Furthermore, GSH did not show any affect: 179.1 ± 47.1 MFI remained after pre-incubation of PBMC with this tripeptide.

Neither the thioredoxin system nor reduced GSH influenced expression of CD64 or binding of anti-CD64 antibody to the FcγRI on monocytes. Overall, no significant difference in CD64 expression was observed after Trx1 pre-treatment or GSH pre-incubation, respectively. Binding of Tregalizumab to CD64 via the Fc-part of the antibody was not evaluated und can, therefore, not be excluded.

5.15 Transfection of CD4- U266B1 cells

To gain more insights and to confirm that the D2 disulfide bridge plays a role in binding of Tregalizumab to the CD4 molecule, CD4- U266B1 cell were transfected with human CD4 (wild-type) and mutated human CD4 (without D2 disulfide cysteines) vector. U266B1 cells represent a human B lymphocyte cell line, which was gathered from a 53 years old man suffered from plasmacytoma[350].

Synthetic oligonucleotides were used to assemble synthetic genes of human CD4 and mutated human CD4. The disulfide bridge of D2 of the CD4 molecule was removed by mutation of cysteine residues to alanine resulting in a mutated D2 CD4 variant DNA. After cloning of constructs into Biotest expression vector, U266 B1 cells were transfected with hCD4 and hCD4 mut DNA using electroporation. Transfected cells were analyzed by light and fluorescence microscopy. As transfection control *pmax GFP,* which leads to expression of the green fluorescent protein (GFP) protein after successful cell transfection, was used. An example transfection with *pmax GFP* is displayed in Figure 30 as transmission light and corresponding fluorescence image. Approximately 30 % of the cells were transfected, which can be seen by fluorescence of green fluorescent protein (Figure 30, B).

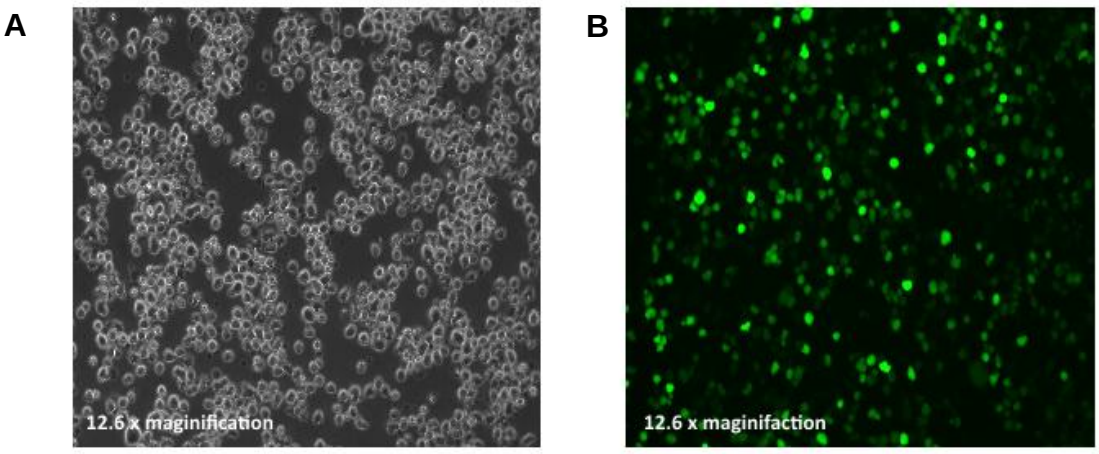

Figure 30: Transfection of U266B1 cells with hCD4 and mutated hCD4

CD4 negative U266B1 cells were transfected with hCD4 and mutated hCD4 DNA using electroporation (Amaxa Nucleofector®-Kit Program-DY-100, SF Solution). Cells were inspected 24 hours post Nucleofection® using transmission light (**A**) and a fluorescence filter (**B**). Green fluorescent protein is used as transfection control (**B**).

5.15.1 Lack of the D2 disulfide bridge affects binding of Tregalizumab and OKT-4

hCD4 transfected U266B1 cells were examined for binding of Tregalizumab and OKT-4 (Figure 31).

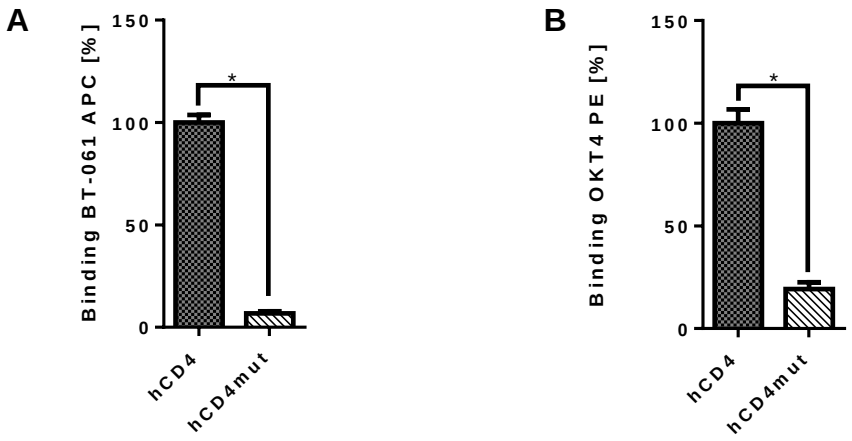

Figure 31: Binding of Tregalizumab and OKT-4 to transfected U266B1 cells

U2661 B1 cells were transfected with either hCD4 DNA or mutated hCD4 DNA. The mutated CD4 variant lacks the D2 disulfide bridge (cysteins were replaced by alanine, Cys/Ala variant).
(**A**) Binding of Tregalizumab (BT-061) was measured via flow cytometry using fluorochrome-labelled Tregalizumab (n = 2, triplicates). Binding of Tregalizumab is significantly decreased when the disulfide bridge is missing. A decline to 6.8 ± 1.1 % binding was observed when cells were transfected with the mutated CD4 DNA.
(**B**) Binding of OKT-4 to transfected U266B1 was examined using flow cytometry (n = 2, triplicates). Fluorochrome-labelled OKT-4 was used to determine its binding to human CD4 and to the mutated D2 Cys/Ala variant. Lack of the D2 disulfide bridge resulted in a significantly decline to 19.2 ±3.3 %. Error bars indicate the standard deviation. P-values were calculated by means of a Wilcoxon matched-pairs signed rank test. Significance is shown as p-value: * $p < 0.05$.

For this purpose, binding of APC-labelled Tregalizumab and PE-labelled OKT-4 was analyzed using flow cytometry. Cells transfected with human CD4 served as control. The mean MFI value of the CD4 transfected cells was set to 100 %. Binding of Tregalizumab or PE-labelled OKT-4 to the mutated D2 Cys/Ala CD4 variant was calculated in relation to this control.

A reduced binding of Tregalizumab to CD4 was observed when the two cysteines, forming the disulfide bridge in D2, were mutated. This led to a significant decrease of binding of Tregalizumab to CD4 (6.8 ± 1.1 %), representing a reduction of approximately 93 % (Figure 31 A).

As a control, it was investigated if another antibody, which does not bind to D2, is also impaired by the mutation. The monoclonal antibody OKT-4 binds to D3 of the CD4 molecule, which does not exhibited a disulfide bridge[329]. So, OKT-4 was tested for binding to transfected U266B1 cells. Binding to human CD4 and to the mutated D2 Cys/Ala variant of CD4 was examined by flow cytometry using fluorochrome-labelled antibody OKT-4. The MFI mean value of OKT-4 was utilized for normalization and binding of OKT-4 to the mutated variant was calculated in relation in percentage. Analysis revealed that binding of OKT-4 was also significantly diminished to 19.2 ±3.3 % (Figure 31 B).

5.15.2 Binding of Tregalizumab is stronger affected by lack of the D2 disulfide bridge compared to OKT-4

Since binding of both antibodies was weaker to mutated CD4, it can not be excluded that both CD4 variants are expressed differently in U266B1 cells. To compare binding of Tregalizumab and binding of OKT-4 to CD4, Tregalizumab was depicted in relation to OKT-4, which was set to 100 % (Figure 32). Using this evaluation, binding of Tregalizumab was declined to 40 %, representing a significant difference between the two monoclonal antibodies.

Therefore, it can be concluded that binding of Tregalizumab is stronger affected by lack of the D2 disulfide bridge compared to OKT-4.

Thus, it can be hypothesized that the D2 disulfide bridge is directly influencing binding of Tregalizumab. In contrast, Trx1 has much weaker effects on binding of the control antibody OKT-4, which binds to D3 of the CD4 molecule.

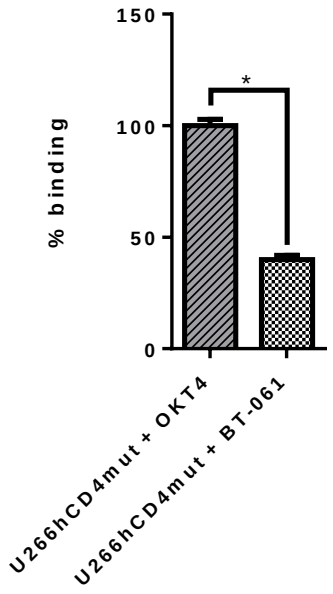

Figure 32: Comparison of Tregalizumab and OKT-4 binding to transfected U266B1 cells

Comparison of Tregalizumab (BT-061) and OKT-4 according to their binding properties to the mutated Cys/Ala D2 CD4 variant (hCD4 mut). MFI values of OKT-4 were set to 100 % and binding of BT-061 was calculated. Data represent results from two independent experiments performed in triplicate. Error bars indicate the standard deviation. P-values were calculated by means of a Wilcoxon matched-pairs signed rank test. Significance is shown as p-value: * $p < 0.05$.

5.16 CD4 signalling of Tregalizumab is affected by Trx1

Stimulation of CD4 results in signalling events of the lymphocyte-specific protein tyrosine kinase p56^{Lck} [351]. In addition, phosphorylation of zeta-chain-associated protein kinase 70 can be detected after activation of the TRC-CD3 complex[351].

Helling et al. reported that binding of Tregalizumab to the T-cell receptor induces a unique signalling in T-cells via the CD4 molecule[22]. To assess how signal transduction, provoked by Tregalizumab, is influenced by Trx1 and its physiological partners, phosphorylation of p56^{Lck} and ZAP-70 was analyzed. As in former studies no significant differences in phosphorylation patterns of regulatory T-cells and effector T-cells were observed after Tregalizumab stimulation[22], only CD4+ T-cells isolated from PBMC were analyzed.

CD4+ cells were incubated with Trx1, TrxR and NADPH over night. Intracellular staining with fluorochrome-labelled antibodies against p56^{Lck} (pY505) and ZAP-70/Syk (pY319/pY352) was used to detected phosphorylation of the relevant signal molecules by flow cytometry.

After stimulation with Tregalizumab or OKT-3 and cross-linking with anti-human IgG (Tregalizumab), respectively anti-murine IgG (OKT-3), phosphorylation was measured. The cross-link duration was set to 10 minutes due to the maximal the extent of phosphorylation at this time point[317].

The inactive mutant Trx1-SS served as negative control. Fold induction of phosphorylation versus the untreated control was calculated. Trx1 treated cells were compared to the untreated control.

Phosphorylation of the human p56^{Lck} peptide after stimulation of cells with cross-linked Tregalizumab yielded the following results (Table 5 and Figure 33): pre-incubation of CD4+ cells with the active Trx1 resulted in a significant decrease of fold induction (1.2 ± 0.2 fold induction compared to the untreated control which showed 2.1 ± 0.3 fold induction). However, the inactive Trx1-SS control (2.1 ± 0.5 fold induction) did not change fold induction significantly.

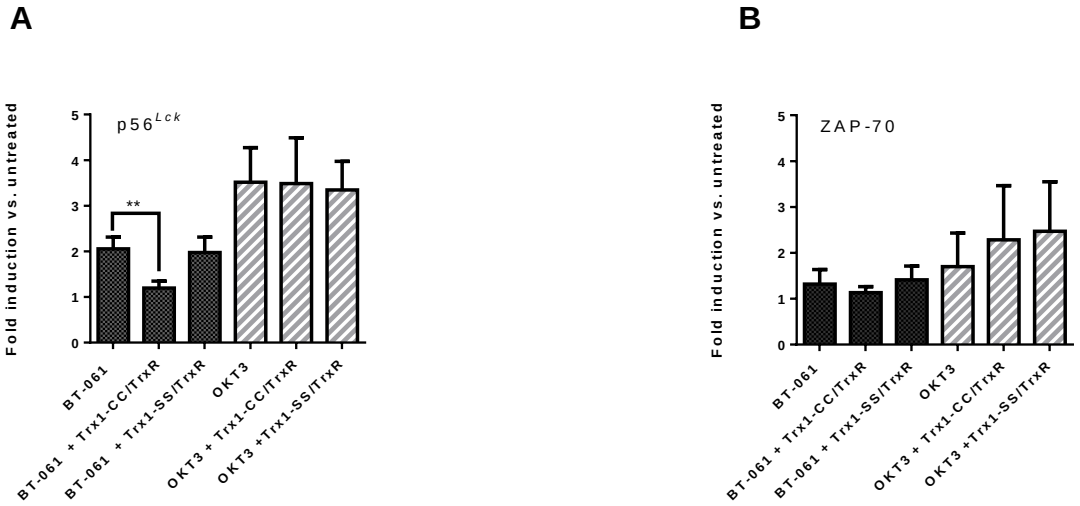

Figure 33: Impact of the Trx1 system on TCR signalling

10^5 CD4+ cells were isolated from PBMCs and incubated over night with 150 nM TrxR and 1 mM NADPH and either 5 µM active Trx1-CC or the inactive mutant Trx1-SS. Untreated cells were used as negative control. After the washing procedure, CD4+ cells were stimulated with either Tregalizumab (BT-061) or OKT3. Both antibodies were cross-linked with anti-human IgG (BT-061) or anti-murine IgG (OKT3). All data represent results from four independent experiments performed in duplicates.
(**A**) Phosphorylation of lymphocyte-specific protein tyrosine kinase p56^{Lck} (pY505) was measured after intracellular staining by flow cytometry using anti-lck(pY505) antibody.
(**B**) ZAP-70 phosphorylation was determined after intracellular staining by flow cytometry with anti-ZAP-70/Syk (pY319/pY352) antibody.
Error bars indicate the standard deviation. P-values were calculated by means of a paired t-test since data is normally distributed. Significance is shown as p-value: ** p< 0.01.

Table 5: Impact of Trx1 on Tregalizumab and OKT-3 induced $p56^{Lck}$ and ZAP-70 phosphorylation in CD4+ cells

		Fold induction of phosphorylation versus untreated		
Parameters	**Treatment**	**without Trx1**	**+ Trx1-CC**	**+ Trx1-SS**
$p56^{Lck}$	BT-061 + ahIgG	2.1 ± 0.3	1.2 ± 0.2	2.1 ± 0.5
	OKT-3 + amIgG	3.5 ± 0.8	3.5 ± 1.0	3.3 ± 0.6
ZAP-70	BT-061 + ahIgG	1.3 ± 0.3	1.1 ± 0.1	1.4 ± 0.3
	OKT-3 + amIgG	1.7 ± 0.7	2.3 ± 1.2	2.5 ± 1.1

n = 4, measured in duplicates

Anti-murine cross-linked OKT-3 stimulation of CD4+ cells revealed a fold induction of 3.5 ± 0.8. Active Trx1 pre-incubation showed no significant change in fold induction (3.5 ± 1.0). Furthermore, Trx1-SS displayed no altered fold induction (3.3 ± 0.6).

In contrast to $p56^{Lck}$, Trx1 pre-treatment showed no significant impact on ZAP-70 phosphorylation. Here, the Tregalizumab treated control revealed a fold induction of 1.3 ± 0.3. Trx1 pre-incubation did not result in a significant change in phosphorylation (1.1 ± 0.1) after stimulation with Tregalizumab. Moreover, compared to the Tregalizumab treated cells, an invariant fold induction (1.4 ± 0.3) was observed when cells were pre-treated with the inactive mutant Trx1-SS before stimulation with cross-linked Tregalizumab.

Besides Tregalizumab, differently Trx1 treated CD4+ PBMC cells were stimulated with cross-linked OKT-3, which resulted in a fold induction of phosphorylation of 1.7 ± 0.7. Trx1-CC treatment elicited no significant increase of phosphorylation (2.3 ± 1.2), which was also observed for the inactive Trx1 control Trx1-SS (2.5 ± 1.1).

It can be concluded that phosphorylation of $p56^{Lck}$ (after stimulation by Tregalizumab) is impaired by Trx1 pre-treatment in contrast to OKT-3 (Figure 34). However, ZAP-70 phosphorylation is not affected by the small oxidoreductase regarding both antibodies.

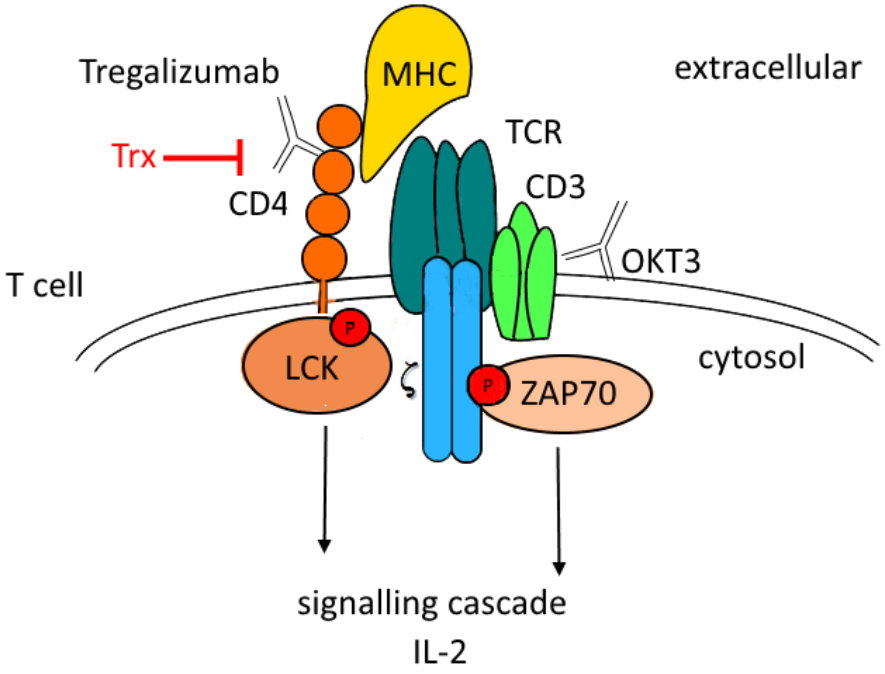

Figure 34: Induction of phosphorylation of p56^{Lck} and ZAP-70 after Tregalizumab and OKT3 stimulation

Tregalizumab and OKT3 induce phosphorylation of different signalling molecules after binding to CD4, respectively CD3. Trx1 is able to decrease binding and signalling of Tregalizumab.

5.17 Binding of Tregalizumab is decreased in RA patients compared to healthy subjects

Having established the effect of reduction of the D2 disulfide bond on Tregalizumab binding to CD4 *in vitro*, this work evaluated, if the increased levels of Trx1 in RA patients lead to the same effect *in vivo*. Data from two clinical studies were analyzed retrospectively, concerning the binding of Tregalizumab to CD4 (Figure 35).

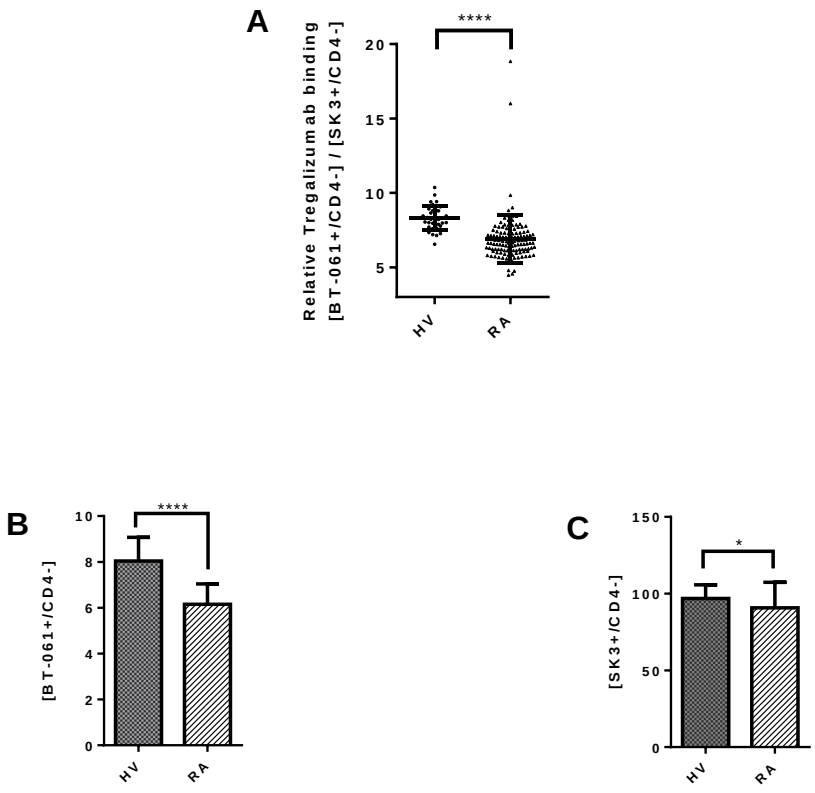

Figure 35 Tregalizumab binding to CD4 is lower in RA patients compared to healthy subjects

Data from two clinical studies (Biotest RA Study 979, EudraCT: 2010-018485-24; Biotest healthy subjects Study 985, EudraCT: 2011-004956-20) were analyzed retrospectively relating to binding of Tregalizumab to CD4. Binding of Tregalizumab to CD4-positive T-cells was measured by flow cytometry using non-competing fluorochrome-labelled anti-CD4 antibodies (BT-061-FITC and SK3-PE). 35 healthy subjects (Biotest study 985) and 127 RA patients (Biotest study 979) were analyzed by the same central laboratory. The MFI values of BT-061-FITC and SK3-PE were used to calculate the relative binding of BT-061 in relation to the total CD4 expression (SK3 antibody).
(A) Population-related relative binding of Tregalizumab in healthy subjects (HV) and RA (RA) patients is depicted to show distribution of individual responses.
(B) Mean relative binding of BT-061 to CD4 is depicted as a bar graph. Error bars indicate the standard deviation. P-values were calculated by means of an unpaired t-test since the data is normally distributed.
(C) Mean relative binding of anti-CD4 antibody SK3 to CD4 is shown as a bar graph.
Error bars indicate the standard deviation. P-values were calculated by means of a Mann-Whitney test. Significance is shown as p-value: * $p < 0.05$, **** $p < 0.0001$.

In total, results of 127 RA patients (Biotest Study 979, EudraCT: 2010-018485-24) and 35 healthy subjects (Biotest study 985, EudraCT: 2011-004956-20) were evaluated. Relative Tregalizumab binding in relation to the total CD4 molecules on T-cells was analyzed.

As shown in Figure 35A, relative binding of Tregalizumab (ratio of MFIs between BT-061 and the non-competing anti-CD4 antibody SK3) in RA patients is significantly ($p < 0.0001$) lower (6.9 ± 1.6, $n = 127$) compared to healthy subjects (8.3 ± 0.8, $n = 35$).

The observed difference in binding is caused by the difference in mean binding of Tregalizumab to CD4 ([BT-061+/CD4-]), which is significantly lower in RA patients compared to healthy subjects (Figure 35B). Ratios of BT-061+ cells compared to CD4- cells revealed a significant higher value for RA patients and for healthy subjects (6.1 ± 0.9 versus 8.0 ± 1.0, $p < 0.0001$).

In contrast, the overall CD4 expression ([CD4+/CD4-]) in general is slightly lower in RA patients compared to healthy subjects. (Figure 35C, $p = 0.0484$, RA = 90.7 ± 16.6, HV = 96.9 ± 8.9).

5.18 Plasma Trx1 levels do not correlate with ACR score of RA patients after Tregalizumab administration

To search for a correlation between Trx1 levels and clinical efficacy of Tregalizumab, plasma samples of responder (improvement of ACR score after treatment of Tregalizumab) and non-responder (no improvement of ACR score after treatment of Tregalizumab) patients from study 986 (TREAT 2b, T-cell Regulating Arthritis Trial 2b, ClinicalTrials.gov Identifier: NCT01999192 und EudraCT No. 2013-000114-38) were analyzed by ELISA, retrospectively. For this purpose a human thioredoxin ELISA was performed according to the manufacturer's instructions (Human Thioredoxin Assay Kit). The analysis included samples of patients treated with 100 mg and 200 mg Tregalizumab collected at week 0 before weekly Tregalizumab administration (baseline).

Figure 36 shows the Trx1 levels at week 0 of 38 patients with an improvement of ACR score after Tregalizumab treatment at week 12 (responder) compared to Trx1 levels of 38 patients with no improvement of the clinical score. ELISA

measurement revealed Trx1 plasma levels of 37.4 ± 105.4 ng/mL regarding responder and 33.3 ± 71.6 ng/mL for non-responder (n = 38, Figure 36 A). The group, which has been treated with 100 mg Tregalizumab, revealed Trx1 plasma levels of 32.7 ± 65.4 ng/mL for responder and 43.7 ± 97.5 ng/mL for non-responder (n = 19, Figure 36 B). Non responder exhibited Trx1 plasma levels of 42.1 ± 136.1 ng/mL, and responder showed Trx1 levels of 23.0 ± 28.2 ng/mL with respect to administration of 200 mg Tregalizumab (n = 19, Figure 36 C).

Generally, the distribution of Trx1 plasma concentrations at week 0 was very similar between RA patients with or without clinical improvement. Using a Mann-Whitney test, no significant difference in Trx1 levels could be observed between patient populations, responder versus non-responder, independently of the administrated dose. Therefore, a correlation between ACR score of RA patients after Tregalizumab treatment and Trx1 levels could not be concluded.

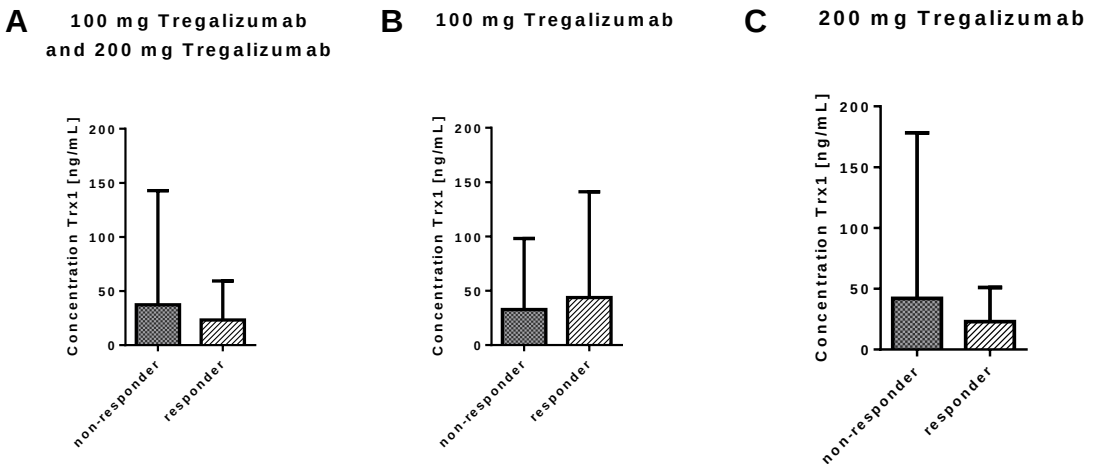

Figure 36: Plasma Trx1 levels do not correlate with ACR score of RA patients after Tregalizumab treatment

Responder and non-responder of Biotest study 986 (TREAT 2b) were analyzed with regard to Trx1 plasma levels by means of an anti-Trx1 ELISA. Patients were treated with 100 mg and 200 mg (A), 100 mg (B) or 200 mg (C) Tregalizumab. Data from 38 individually measured samples is depicted (measured in duplicates). Error bars indicate the standard deviation. P-values were calculated by means of a Mann-Whitney test.

6 Discussion

Oxidative stress is considered to be one possible activator in the development and disease activity of rheumatoid arthritis[11,12,197,198,352]. Moreover, it plays an important role in other pathogenic mechanism, e.g. of diabetes mellitus[353], neurodegenerative diseases[354,355] as well as in hypertension and atherosclerosis[356,357]. One option of the organism to counteract high levels of oxidative metabolites is to use the activity of the small oxidoreductase thioredoxin (Trx1), which is involved by the organism and operates at the site of inflammation[214,358,359].

The 12 kDa Trx1 represents one of the major players in redox processes as it is able to reduce oxidized proteins, thereby, maintaining redox homeostasis. The highly conserved active site of Trx1 comprises the typical thioredoxin fold consisting of the amino acid sequence -Cys-Gly-Pro-Cys-, which can also be found in other proteins belonging to the thioredoxin superfamily[218].

6.1 Role of Trx1 with regard to RA, Trx1 levels are augmented in RA

Because of the unequivocal relationship between high Trx1 levels and oxidative stress, numerous studies have investigated the impact of Trx1 on the pathogenesis of RA[15,16,18,210]. These studies revealed that Trx1 protein and activity levels were augmented in patients suffering from RA[15–19]. Serum and plasma Trx1 levels were found to be elevated in RA compared to osteoarthritis patients. Moreover, the synovial fluid (SF) of RA patients revealed a higher Trx1 concentration than those of osteoarthritis patients[17,19]. Furthermore, it could be demonstrated that RA disease activity correlated with elevated Trx1 plasma levels and with Trx1 activity respectively[17,18]. In addition, one study described that levels of the Trx1 related molecule, peroxiredoxin-2, in lymphocytes of RA patients were also increased and that these levels correlated with the extent of inflammation[360].

Tregalizumab (BT-061) is a humanized monoclonal antibody, which is developed by Biotest AG, Dreieich, Germany. As Tregs can be selectively activated by Tregalizumab *in vitro* (Tregalizumab does not invoke Teffs)[22], the antibody was investigated as a novel approach for the treatment of RA. To

elucidate tolerability, safety and efficacy of Tregalizumab, the antibody has been investigated in overall eight clinical trials of which four studies involved patients with rheumatoid arthritis and healthy subjects. A PK-PD model was established to characterize the correlation between the CD4 down-modulation after Tregalizumab administration and the dose[24]. This PK-PD model, based on clinical data from RA and healthy subject trials, surprisingly revealed higher CD4 down-modulation in healthy subjects compared to patients suffering from RA. Moreover, a reason why the latest study TREAT2b with Tregalizumab did not demonstrate efficacy in RA patients has not yet been found. This thesis illustrates research undertaken to elucidate the described occurrence of a higher CD4 down-modulation in healthy subjects compared to RA patients.

Since Tregalizumab binds to D2 of CD4[22,23], which can be selectively reduced by Trx1[25], this work examined the role of the oxidoreductase with regard to binding of Tregalizumab to CD4. Plasma levels of Trx1 were found to be between 25.5 ±12 ng/mL and 122 ± 21 ng/mL in different *in vitro* and clinical studies resulting - in an average of about 88 ng/mL[15–18]. These values are comparable with experiments shown in this thesis revealing a range of Trx1 levels between approximately 100 ng/mL and 150 ng/mL Trx1 in plasma of RA patients, compared to healthy subjects revealing levels between 25 ng/mL and 50 ng/mL. So, consistent with the literature, increased levels of Trx1 in RA plasma compared to plasma of healthy subjects were measured. It is also interesting to note, that impaired T-cell function in RA patients was analyzed by Maurice *et al.*[15]. They discovered that the dysfunction of T-cells is associated with low intracellular GSH levels and increased Tx1 concentration in the SF referring to as hyporesponsiveness of SF T-cells. This hyporesponsiveness goes along with protein modifications caused by ROS due to oxidative stress[208] and displacement of LAT from the membrane[205,207]. Thus, these results also suggest the fact, that high Trx1 levels play an essential role in the RA disease process.

6.2 Trx1 reduces rh sCD4 shown via SDS-PAGE

Based on literature search, this thesis investigated, whether high Trx1 levels are able to affect Tregalizumab binding to CD4, since its predicted CD4 down-modulation in RA patients compared to healthy subjects did not behave according to the expectations.

Since Trx1 is able to selectively reduce the disulfide bridge in D2 of the CD4 molecule[25], which is in close proximity to the binding site of Tregalizumab, it might be possible that its binding is impaired in patients possessing augmented Trx1 concentrations.

To verify if the disulfide bridge in D2 of the CD4 molecule is affected by Trx1 reduction, a SDS-PAGE analysis of rh sCD4 was performed and an additional band after Trx1 and Trx1/TrxR pre-incubation in the experiments appeared. Moreover, a second band arose next to the rh sCD4 band after pegylation and pre-incubation with Trx1 and subsequent pegylation created two additive bands representing labelled thiols. However, reduction of CD4 by Trx1 treated CD4+ cells lysate could not be concluded since the bands of lysed CD4+ were difficult to detect. It is possible that additional bands exist but were not able to be visualized. Effects of Trx1 on sCD4 are indeed described in the literature. As shown by Harris *et al*., reduction of soluble CD4 by DTT resulted in a shift of the reduced band to apparent higher molecular values comparable with results of this work[53]. The reduced form of rh sCD4 seems to migrate not as good as the non Trx1 pre-reduced form through the gel. This might be due to interruption of the protein structure caused by reduction of the texturing disulfide bridge. As a reduction agent DTT is able to reduce disulfide bridges[361]. However, buried disulfide bridges seem to be difficultly to be accessed by DTT and so, Matthias *et al*. demonstrated no reduction of sCD4 using 5 µM DTT. However, Trx1 was able to reduce sCD4, which can exist in the reduced and oxidized state on the cell surface[25].

6.3 Disulfide bridge in D2 of CD4 possess important allosteric properties, comparison of binding of different anti-CD4 antibodies via ELISA

The so-called "–RHS staple" disulfide bridge in D2 of the CD4 molecule plays a major role in many physiological processes due to its allosteric properties[362]. Apart from the fact that Trx1 induced dimerization of CD4 is necessary for MHCII recognition by the T-cell receptor, human immunodeficiency virus entry process is closely linked to redox changes in this disulfide bond[25,63,334,346,363].

This thesis addressed the question how binding of Tregalizumab is affected when the disulfide bridge of CD4 D2 is reduced by Trx1. For this purpose, several binding experiments were performed applying electrochemiluminescence and flow cytometry analysis. Since the anti-CD4 antibody MT441 recognises a different epitope of D2 compared to Tregalizumab, Helling *et al*. concluded that Tregalizumab binds to a unique, conformational epitope on D2[322]. One of the three binding pockets of Tregalizumab involves Tyr(105)[22], whose position maybe altered by the reduction of the CD4 disulfide bridge, resulting in a broadening of the binding pocket and a decrease in binding of Tregalizumab. To gain a detailed view on binding energy of the Tregalizumab - CD4 complex, forced filed calculations (performed with YASARA software system using the NOVA force field) were conducted. However, calculations revealed no difference in binding energy between CD4 with and without the D2-disulphide bridge. But, since force field calculations only involve internal energy U (corresponds to enthalpy H) entropy contribution was not taken into account and impact of the disulfide bridge on Tregalizumab had to be further elucidated *in vitro*.

Hence, measurements of thesis work should analyse if Trx1 is able to influence Tregalizumab. Binding studies, using an electrochemiluminescence assay, revealed that binding of Tregalizumab to rh sCD4 is affected by pre-treatment with Trx1 and decreases binding in a dose dependent manner.

Moreover, other anti-CD4 antibodies, which bind to CD4, were analyzed after pre-treatment of CD4 with Trx1 to scrutinize, if Trx1 evokes alteration of the binding positions of each antibody. Helling *et al*. analyzed binding of Tregalizumab in comparison to the following other anti-CD4 antibodies: OKT-3,

RPA-T4, SK3, MT310, QS4120, EDU-2, B-A1 and MT441. Measurements showed that MT441, which bind to D2 of CD4[322,328], but none of the other anti-CD4 monoclonal antibodies, competed with Tregalizumab for binding to the CD4 molecule[22]. This goes along with results of this work, since binding of Tregalizumab and MT441 was affected by Trx1 to a comparable extent. This implicates that conformal change of the disulfide bridge in D2 of CD4 impacts these two antibodies most powerful. Except from Tregalizumab and MT441 all other antibodies recognises other domains of the CD4 molecule[329,330]. Trx1 induced similar, but less pronounced effects, with regard to RPA-T4 and SK3; even if, binding of antibodies, which target D2, are influenced to the highest extent. Since D1 of CD4 is recognized by SK3[329] and RPA-T4[330] a conformational change may also effect these two antibodies.

After pre-treatment with Trx1 no decrease in binding was detected for OKT-4, which seems to be associated with its binding to D3[329] where no disulfide bridge is located[55]. Since D3 of the CD4 molecule contains no disulfide bridge, impact of Trx1 on OKT-4 might be negligible.

Regarding influence of DTT on CD4, it can be concluded that impact of Trx1 on binding of all antibodies was little higher compared to DTT, except RPA-T4. DTT caused a higher decline of binding of this monoclonal antibody to CD4.
So, Trx 1 effects, regarding the extent of binding of each antibody to rh sCD4, are different, which might result from diverse binding sites of each antibody to the domains of CD4 and therefore, different distances from the conformational changes.

6.4 Tregalizumab shows less binding to mutated CD4 compared to OKT-4

Based on the results obtained, it is reasonable to assume that alterations of the disulfide bridge in CD4 D2 may have an influence on the antibodies binding. To gain more insights into the relevance of the disulfide bridge in D2, with regard to binding capability of Tregalizumab, transfectants lacking this CD4 disulfide bridge were generated. Since OKT-4 was not influenced by Trx1 pre-treatment as much compared to Tregalizumab, this antibody was selected for comparison. Flow cytometry studies revealed that binding of Tregalizumab to the CD4

mutant is reduced and this reduction is major when compared to OKT-4. This finding emphasizes the importance of the disulfide bridge for Tregalizumab binding and is in good agreement with the results obtained from the electrochemiluminescence ELISA investigations.

6.5 Trx1 decreases binding of Tregalizumab to CD4 on cells

Starting with the unexpected differences in predicted CD4 down-modulation between RA patients and healthy subjects, results demonstrated that the disulfide bridge in D2 of the CD4 molecule is important for the Tregalizumab - CD4 interaction regarding rh sCD4. Tests also revealed that Trx1 is able to diminish binding of Tregalizumab to CD4 on the cell surface of the T-leukaemia cell line HPB-ALL and on peripheral blood mononuclear cells.

For these cell experiments, different Trx1 concentrations were used. TrxR and NADPH were added in excess. Trx1 incubation times of 60 minutes versus over night incubation were compared to mimic physiological conditions. Over night pre-incubation of CD4+ HPB-ALL cells and PBMC with the Trx1/TrxR system demonstrated a significant decrease of the binding of Tregalizumab to the cells. Moreover, it was shown, that that decrease depends on the Trx1 concentration. This goes along with the binding studies using rh sCD4. However, 60 minutes incubation of cells with 10 µM Trx1 in combination with 300 nM or 500 nM TrxR showed only little reduction of the binding of Tregalizumab to CD4 - in comparison to over night incubation. This can be possibly explained by the short time frame which might not have been sufficient to reduce all CD4 on the cell's surface.

Regarding over night incubation, Trx1 alone at a concentration of 5 µM was able to significantly decrease Tregalizumab binding but much stronger effects were observed using the physiological Trx1 system including TrxR and NADPH. This is expected since Trx1 without the reductase is not recycled and can facilitate the disulfide reduction process only once per molecule. Moreover, the influence of Trx1 on binding of Tregalizumab to CD4 depends on the concentration of Trx1. When HPB-ALL cells were incubated with Trx1, TrxR and the oxidized cofactor NADP+ over night no decrease of binding of Tregalizumab

was observed (data not shown). This indicates that only the physiological system (Trx1, TrxR and reduced NADPH) is able to decrease binding of Tregalizumab to CD4+ HPB-ALL cells.

Although the Trx1 concentration exceeds the published levels in plasma or synovial fluid of 1–5 nM[346], the local Trx1 concentration at the cell surface of T-cells might be higher. This can be assumed since expression and secretion of Trx1 is noticeably enhanced by some cells types like macrophages, dendritic and monocytes cells after activation[309]. Gromer *et al*. even reported Trx1 tissue concentrations between 1 and 20 µM and calculated intracellular levels of TrxR of 1 µM[347] illustrating physiological relevance of the used Trx1 concentration.

6.6 GSH does not decreases binding of Tregalizumab to CD4 on cells

To scrutinize if another redox protein, GSH, is also able to diminish Tregalizumab binding to CD4, influence of GSH was analyzed using GSH pre-incubated PBMC. As GSH levels normally reach values between 0.5 mM and 10 mM in the cell[27], PBMC pre-incubated with 10 mM GSH were examined. However, no significant decrease in binding of Tregalizumab to PBMC was observed^, which underlines the special role of Trx1 influencing the binding behaviour of Tregalizumab. Therefore, reduction of the CD4 D2 disulfide bridge by Trx1 seems to be one of the relevant processes *in vivo,* as the second redox active molecule, reduced GSH, which is present extracellular in high amounts *in vivo*[27], was not able to influence Tregalizumab binding in physiological concentrations up to 10 mM.

6.7 Impact of Trx1 on CD4 down-modulation

Based on the demonstrated effect that binding of Tregalizumab is declined by Trx1 *in vitro* and *in vivo,* it can be assumed that the CD4 down-modulation, as a read-out of Tregalizumab's efficacy, might be also decreased. The pharmacological effect of CD4 down-modulation can only occur when the Fc part of Tregalizumab is cross-linked with the Fc-gamma receptor 1 (FcγRI, CD64) on monocytes[28]. It might be possible, that the higher CD4 down-modulation in healthy subjects compared to RA patients is caused either by a decreased binding of Tregalizumab's Fab part to CD4, by diminished

expression or by modification of the FcγRI CD64. To evaluate the possibility that the necessary cross-link to Fc gamma receptor on monocytes with the Fc part of Tregalizumab is negatively impacted by Trx1, influence of Trx1 to CD64+ monocytes was also tested. Since the expression of CD64 is not affected by Trx1 and no disulfide bridges are described for the CD64 receptor[349], Trx1 can only influence binding of Tregalizumab to CD4 and the CD64 receptor on monocytes is not affected.

Tregalizumab binding, or "receptor occupancy", was monitored *ex-vivo* during the clinical studies by using a fluorescently labeled Tregalizumab, which binds to the remaining free (non Tregalizumab bound) CD4, while a non-competitive anti-CD4 antibody was used to quantify the total amount of CD4 molecules. The results showed that receptor occupancy correlates with the CD4 down-modulation with similar kinetics. This is in line with the data from *in vitro* studies and sets a correlation between Tregalizumab binding and CD4 down-modulation. However, analyzes failed to measure the CD4 down-modulation after Trx1/TrxR pre-treatment *in vitro* for the following reason. The anti-CD4 antibody SK3 binding, which measures the entire CD4 population and which is used for determination of CD4 down-modulation, seems to be also impacted by the implications caused by Trx1. Therefore, reasonable determination of CD4 down-modulation was not possible *in vitro* (data not shown). FACS measurement of CD4 down-modulation revealed normal CD4 PE (SK3) mean fluorescence intensities (MFI) for Tregalizumab treated PBMC. However, MFI values after Trx1/TrxR/NADPH over night pre-incubation demonstrated approximately half the signal. Similar effects have been observed for the binding of SK3 to rh sCD4. These conditions make determination of Tregalizumab induced CD4 down-modulation challenging and seem to be responsible for the observed differences in the CD4 down-modulation.

6.8 Impact of Trx1 on CD4 signalling

As a substitute for the CD4 down-modulation signalling of T-cells was determined. Therefore, phosphorylation of lymphocyte-specific protein tyrosine kinase ($p56^{Lck}$) and zeta-chain-associated protein kinase 70 (ZAP-70) was

analyzed representing the direct signalling molecule after activation of CD4 and TCR, respectively.

Stimulation of the CD4 molecule induces signalling events via p56$^{Lck\ 351,364}$. Moreover, phosphorylation of ZAP-70 can be detected after activation of the T-cell receptor –CD3 (TCR-CD3) complex[351]. Helling *et al.* reported that binding of Tregalizumab to the T-cell receptor induces a unique signalling in T-cells via the CD4 molecule[22]. The impact of Trx1 on CD4 signalling was assessed on the phosphorylation of p56^{Lck} and ZAP-70 as the first molecules of the signalling cascade triggered after activation of CD4. As a control, the antibody OKT3, was used. Since Helling and coworkers showed no difference in the phosphorylation signals of Teffs and Tregs, the present work only used CD4+ T-cells[317]. Results demonstrated that Trx1 pre-incubation resulted in a significant decrease of p56^{Lck} phosphorylation stimulation with Tregalizumab, confirming the impact of Trx1 on Tregalizumab induced signalling. It is also possible that this observation has a direct impact on activation of Tregs by Tregalizumab.

Helling and coworkers also showed that binding of Tregalizumab induces a specific intracellular signaling with phosphorylation of diverse proteins in Treg and Teff[22]. In addition, impairment of the intracellular signaling prohibits the CD4 down-modulation[316]. For example, inhibition of CD4 down-modulation was demonstrated after treatment of PBMCs with Tregalizumab in the presence of Src kinase inhibitor PP1[23], which is able to suppress the CD4 associated kinase p56$^{Lck\ 365}$. The same inhibitor was shown to block the Tregalizumab-mediated activation of Tregs[23]. In contrast to p56^{Lck}, incubation of PBMC with active Trx1 revealed no significant influence on ZAP-70 phosphorylation after Tregalizumab or OKT3 stimulation.

These findings implicate, that Trx1 also directly influences CD4-initiated signalling events and therefore, might responsible for decreased subsequent CD4 internalization as seen in the PK-PD model.

6.9 Possible Impact of Trx1 on Tregalizumab in clinical study

In the latest double-blind, randomized, placebo-controlled, Phase IIb study (TREAT2b) Tregalizumab did not reach the primary endpoint: compared to placebo no significant improvement of ACR20 was shown[23].

Since Treg function depends on a functional T-cell signalling[366], high levels of Trx1 might have an influence on Tregalizumab in general or on regulatory T-cell function in particular. Using *in vitro* assays, it was shown, that Tregalizumab is able to activate Tregs selectively *in vitro* in contrast to other CD4 antibodies[22]. As described before, Tregalizumab targets a unique epitope on D2 of the CD4 molecule, which results in phosphorylation of signaling molecules in CD4+ T cells[22]. This special phosphorylation pattern was associated with activation of suppressive Treg function[22]. By decreasing binding of Tregalizumab to CD4 and reducing the T-cell activation signal by Trx1, this unique phosphorylation signalling might be affected, which probably lead to a declined activation of T-cells in general via influencing binding of the antibody to cell surface CD4. However, use of CD4 modulation as a PD marker confirmed the activity of Tregalizumab in this clinical trial[23].

6.10 Correlation between Trx1 levels and efficacy of Tregalizumab in RA patients

Since elevated Trx1 levels did impair binding of Tregalizumab to CD4 *in vitro*, Trx1 levels in plasma samples of RA patients were determined retrospectively, to find a correlation between Trx1 levels and clinical efficacy. To address this property of Trx1, plasma samples of responder and non-responder patients were analyzed retrospectively, using samples from the latest Phase 2b study (TREAT 2b). However, determination of Trx1 concentration in RA plasma samples did not show any significant correlation between Trx1 plasma levels and ACR score by using an anti-Trx1 ELISA. It is important to note that Trx1 is actively secreted by a so-called "leaderless" secretory pathway by activated T cells and monocytes[235] and operates at the site of inflammation where those cells are abundant[214,358,359]. Since only levels of plasma Trx1 were able to be analyzed by ELISA, local Trx1 concentrations at the inflammation site can be much higher. Moreover, exposure to an antigen-specific T cells triggers Trx1

release from monocyte-derived human dendritic cells (DCs), which interact with T-cells[309]. Therefore, high local Trx1 levels maybe present on the cell surface and cannot be detected in the plasma. In addition, it was shown that Trx1 expression and secretion is higher in human Tregs compared to other CD4-postive T-cells[213]. Since the RA synovium is enriched with CD4+ CD25+ Tregs[367], a Trx1 secretion by these cells might enhance the survival of autoreactive synovial fluid T-cells due to inhibition of apoptosis by Trx1. This potentially results in aggravation of RA. However, synovial fluid was not analyzed during any clinical trials with Tregalizumab. Therefore, no measurement of Trx1 in this tissue is available. But, it has been described in the literature that Trx1 levels are elevated in synovial fluid of RA patients[15,16,210]. For this reason, it can be hypothesized that binding of Tregalizumab might be decreased at the synovial inflammatory site. Since Tregalizumab interacts with CD4+ CD25+ Tregs[23], which secrete high amounts of Trx1, it can be speculated that Trx1 might also negatively impact the binding and signalling of Tregalizumab in the synovium of RA patients.

6.11 Impact of Trx1 on CD4 binding in RA patients

This thesis hypothesised that elevated Trx1 levels in RA patients are a reason for the observed reduced CD4 down-modulation in RA patients compared to healthy subjects. In addition, it predicts decreased binding of Tregalizumab to CD4 in RA patients due to higher Trx1 concentrations. A retrospective analysis of Biotest clinical studies 979 and 985 determined relative binding of Tregalizumab to CD4 and showed that it was indeed significantly lower in RA patients compared to healthy subjects. However, the CD4 expression was comparable in both populations. Ratio of [CD4+/CD4-] cells was high comparable in the two populations indicating that RA patients and healthy subjects exhibited similar amounts of CD4+ cells. However, statistics show a little difference between healthy subjects and RA patients: binding of SK3 is little lower in RA patients compared to healthy subjects. This finding emphasizes that binding of Tregalizumab to CD4 is impaired in a particular way in RA patients.

7 Conclusion

The present thesis revealed that, elevated Trx1 levels in RA patients negatively influence Tregalizumab binding characteristics to the CD4 molecule and Tregalizumab induced signalling in T-cells. This study investigated the reason for the reduced CD4 down-modulation after Tregalizumab stimulation in RA patients compared to healthy subjects. The observations support the idea that elevated Trx1 levels in RA patients contribute to diminished binding of Tregalizumab to CD4+ target cells and question whether this effect might also contribute to the clinical efficacy of Tregalizumab in the latest trial.

In conclusion, this thesis reports that high Trx1 levels diminish binding of Tregalizumab to CD4 and alter the CD4-induced signalling pathway via the protein kinase $p56^{Lck}$. So, the results point to a relevant connection between oxidative stress in RA patients and impaired binding of Tregalizumab in this context.

The influence of Trx1 on the activity of Tregalizumab should be taken into account in other clinical indications where oxidative stress plays a role. As Trx1 triggered dimerization of CD4 and followed domain swapping in $D2^{64,368}$ was not a topic of this work, influence of this circumstance should be further evaluated with special regard to Tregalizumab. Moreover, since CD4 is also a favoured target for T-cell pharmacological regulation in general (e.g. by depleting CD4+ cells or down-modulating of CD4) high levels of Trx1 can potentially impact other anti-CD4 antibodies, which bind in close proximity to the D2 disulfide bridge.

Further investigations on binding of Tregalizumab to its epitope, including the allosteric disulfide bond in D2 of CD4, would help to better understand the mode of action and the efficacy of this monoclonal antibody.

8 Sequences

8.1 Human CD4 (wild type) CD4

Atgaaccggggagtccctttaggcacttgcttctggtgctgcaactggcgctcctcccagcagccactcaggg
aaagaaagtggtgctgggcaaaaaaggggatacagtggaactgacctgtacagcttcccagaagaagag
catacaattccactggaaaaactccaaccagataaagattctgggaaatcagggctccttcttaactaaaggtc
catccaagctgaatgatcgcgctgactcaagaagaagcctttgggaccaaggaaactttcccctgatcatcaa
gaatcttaagatagaagactcagatacttacatctgtgaagtggaggaccagaaggaggaggtgcaattgct
agtgttcggattgactgccaactctgacacccacctgcttcaggggcagagcctgaccctgaccttggagagc
ccccctggtagtagcccctcagtgcaatgtaggagtccaaggggtaaaaacatacagggggggaagaccc
tctccgtgtctcagctggagctccaggatagtggcacctggacatgcactgtcttgcagaaccagaagaaggt
ggagttcaaaatagacatcgtggtgctagctttccagaaggcctccagcatagtctataagaaagaggggga
acaggtggagttctccttcccactcgcctttacagttgaaaagctgacgggcagtggcgagctgtggtggcagg
cggagagggcttcctcctccaagtcttggatcacctttgacctgaagaacaaggaagtgtctgtaaaacgggtt
acccaggaccctaagctccagatgggcaagaagctcccgctccacctcaccctgccccaggccttgcctca
gtatgctggctctggaaacctcaccctggcccttgaagcgaaaacaggaaagttgcatcaggaagtgaacct
ggtggtgatgagagccactcagctccagaaaaatttga

8.2 Human CD4 (mutated) CD4 Cys-mut

Atgaaccggggagtccctttaggcacttgcttctggtgctgcaactggcgctcctcccagcagccactcaggg
aaagaaagtggtgctgggcaaaaaaggggatacagtggaactgacctgtacagcttcccagaagaagag
catacaattccactggaaaaactccaaccagataaagattctgggaaatcagggctccttcttaactaaaggtc
catccaagctgaatgatcgcgctgactcaagaagaagcctttgggaccaaggaaactttcccctgatcatcaa
gaatcttaagatagaagactcagatacttacatctgtgaagtggaggaccagaaggaggaggtgcaattgct
agtgttcggattgactgccaactctgacacccacctgcttcaggggcagagcctgaccctgaccttggagagc
ccccctggtagtagcccctcagtgcaagctaggagtccaaggggtaaaaacatacagggggggaagacc
ctctccgtgtctcagctggagctccaggatagtggcacctggacagccactgtcttgcagaaccagaagaag
gtggagttcaaaatagacatcgtggtgctagctttccagaaggcctccagcatagtctataagaaagaggggg
aacaggtggagttctccttcccactcgcctttacagttgaaaagctgacgggcagtggcgagctgtggtggcag
gcggagagggcttcctcctccaagtcttggatcacctttgacctgaagaacaaggaagtgtctgtaaaacggg
ttacccaggaccctaagctccagatgggcaagaagctcccgctccacctcaccctgccccaggccttgcctc
agtatgctggctctggaaacctcaccctggcccttgaagcgaaaacaggaaagttgcatcaggaagtgaacc
tggtggtgatgagagccactcagctccagaaaaatttga

9 References

1. Schütt, C. & Bröker, B. *Grundwissen Immunologie*. (Spektrum, Akad. Verl, 2009).
2. Resch, K., Martin, M. U. & Kaever, V. *Immunpharmakologie: 48 Tabellen*. (Ulmer, 2010).
3. Baecher-Allan, C., Brown, J. A., Freeman, G. J. & Hafler, D. A. CD4+CD25high regulatory cells in human peripheral blood. *J. Immunol. Baltim. Md 1950* **167,** 1245–1253 (2001).
4. Sakaguchi, S. *et al.* Immunologic tolerance maintained by CD25+ CD4+ regulatory T cells: their common role in controlling autoimmunity, tumor immunity, and transplantation tolerance. *Immunol. Rev.* **182,** 18–32 (2001).
5. Jonuleit, H. *et al.* Infectious tolerance: human CD25(+) regulatory T cells convey suppressor activity to conventional CD4(+) T helper cells. *J. Exp. Med.* **196,** 255–260 (2002).
6. Sakaguchi, S. *et al.* Foxp3+ CD25+ CD4+ natural regulatory T cells in dominant self-tolerance and autoimmune disease. *Immunol. Rev.* **212,** 8–27 (2006).
7. Feldmann, M., Brennan, F. M. & Maini, R. N. Rheumatoid arthritis. *Cell* **85,** 307–310 (1996).
8. Lee, D. M. & Weinblatt, M. E. Rheumatoid arthritis. *Lancet Lond. Engl.* **358,** 903–911 (2001).
9. Klareskog, L., Padyukov, L., Lorentzen, J. & Alfredsson, L. Mechanisms of disease: Genetic susceptibility and environmental triggers in the development of rheumatoid arthritis. *Nat. Clin. Pract. Rheumatol.* **2,** 425–433 (2006).
10. McInnes, I. B. & Schett, G. The pathogenesis of rheumatoid arthritis. *N. Engl. J. Med.* **365,** 2205–2219 (2011).
11. Veselinovic, M. *et al.* Oxidative stress in rheumatoid arthritis patients: relationship to diseases activity. *Mol. Cell. Biochem.* **391,** 225–232 (2014).
12. Hassan, S. Z. *et al.* Oxidative stress in systemic lupus erythematosus and rheumatoid arthritis patients: relationship to disease manifestations and activity. *Int. J. Rheum. Dis.* **14,** 325–331 (2011).
13. Filippin, L. I., Vercelino, R., Marroni, N. P. & Xavier, R. M. Redox signalling and the inflammatory response in rheumatoid arthritis. *Clin. Exp. Immunol.* **152,** 415–422 (2008).
14. Lu, J. & Holmgren, A. The thioredoxin antioxidant system. *Free Radic. Biol. Med.* **66,** 75–87 (2014).
15. Maurice, M. M. *et al.* Evidence for the role of an altered redox state in hyporesponsiveness of synovial T cells in rheumatoid arthritis. *J. Immunol. Baltim. Md 1950* **158,** 1458–1465 (1997).
16. Maurice, M. M. *et al.* Expression of the thioredoxin-thioredoxin reductase system in the inflamed joints of patients with rheumatoid arthritis. *Arthritis Rheum.* **42,** 2430–2439 (1999).
17. Jikimoto, T. *et al.* Thioredoxin as a biomarker for oxidative stress in patients with rheumatoid arthritis. *Mol. Immunol.* **38,** 765–772 (2002).
18. Lemarechal, H. *et al.* High redox thioredoxin but low thioredoxin reductase activities in the serum of patients with rheumatoid arthritis. *Clin. Chim. Acta Int. J. Clin. Chem.* **367,** 156–161 (2006).

19. Yoshida, S. *et al.* Involvement of thioredoxin in rheumatoid arthritis: its costimulatory roles in the TNF-alpha-induced production of IL-6 and IL-8 from cultured synovial fibroblasts. *J. Immunol. Baltim. Md 1950* **163,** 351–358 (1999).
20. Becker, C., Bopp, T. & Jonuleit, H. Boosting regulatory T cell function by CD4 stimulation enters the clinic. *Front. Immunol.* **3,** 164 (2012).
21. Becker, C., Kubach, J., Wijdenes, J., Knop, J. & Jonuleit, H. CD4-mediated functional activation of human CD4+CD25+ regulatory T cells. *Eur. J. Immunol.* **37,** 1217–1223 (2007).
22. Helling, B. *et al.* A specific CD4 epitope bound by tregalizumab mediates activation of regulatory T cells by a unique signaling pathway. *Immunol. Cell Biol.* **93,** 396–405 (2015).
23. König, M., Rharbaoui, F., Aigner, S., Dälken, B. & Schüttrumpf, J. Tregalizumab - A Monoclonal Antibody to Target Regulatory T Cells. *Front. Immunol.* **7,** 11 (2016).
24. Dokoupilova, E. *et al.* Use Of a Biologic Marker For An Integrated Pharmacodynamic and Clinical Analysis To Inform Further Clinical Development, Including Dose Selection For The Phase 2b Trial - Treat 2b - Of Tregalizumab In Rheumatoid Arthritis. *Arthritis Rheum.* **65,** (Supplement 10), S596 (2013).
25. Matthias, L. J. *et al.* Disulfide exchange in domain 2 of CD4 is required for entry of HIV-1. *Nat. Immunol.* **3,** 727–732 (2002).
26. Lushchak, V. I. Glutathione homeostasis and functions: potential targets for medical interventions. *J. Amino Acids* **2012,** 736837 (2012).
27. Meister, A. & Anderson, M. E. Glutathione. *Annu. Rev. Biochem.* **52,** 711–760 (1983).
28. Vogel, S. *et al.* Antibody induced CD4 down-modulation of T cells is site-specifically mediated by CD64(+) cells. *Sci. Rep.* **5,** 18308 (2015).
29. König, R. Interactions between MHC molecules and co-receptors of the TCR. *Curr. Opin. Immunol.* **14,** 75–83 (2002).
30. Rudolph, M. G., Stanfield, R. L. & Wilson, I. A. How TCRs bind MHCs, peptides, and coreceptors. *Annu. Rev. Immunol.* **24,** 419–466 (2006).
31. Hennecke, J. & Wiley, D. C. T cell receptor-MHC interactions up close. *Cell* **104,** 1–4 (2001).
32. Koning, F., Maloy, W. L. & Coligan, J. E. The implications of subunit interactions for the structure of the T cell receptor-CD3 complex. *Eur. J. Immunol.* **20,** 299–305 (1990).
33. Clevers, H., Alarcon, B., Wileman, T. & Terhorst, C. The T cell receptor/CD3 complex: a dynamic protein ensemble. *Annu. Rev. Immunol.* **6,** 629–662 (1988).
34. Love, P. E. & Hayes, S. M. ITAM-mediated Signaling by the T-Cell Antigen Receptor. *Cold Spring Harb. Perspect. Biol.* **2,** (2010).
35. Krummel, M. F., Sjaastad, M. D., Wülfing, C. & Davis, M. M. Differential clustering of CD4 and CD3zeta during T cell recognition. *Science* **289,** 1349–1352 (2000).
36. Salmond, R. J., Filby, A., Qureshi, I., Caserta, S. & Zamoyska, R. T-cell receptor proximal signaling via the Src-family kinases, Lck and Fyn, influences T-cell activation, differentiation, and tolerance. *Immunol. Rev.* **228,** 9–22 (2009).

37. Shaw, A. S. *et al.* The lck tyrosine protein kinase interacts with the cytoplasmic tail of the CD4 glycoprotein through its unique amino-terminal domain. *Cell* **59,** 627–636 (1989).
38. Rudd, C. E., Trevillyan, J. M., Dasgupta, J. D., Wong, L. L. & Schlossman, S. F. The CD4 receptor is complexed in detergent lysates to a protein-tyrosine kinase (pp58) from human T lymphocytes. *Proc. Natl. Acad. Sci. U. S. A.* **85,** 5190–5194 (1988).
39. Veillette, A., Bookman, M. A., Horak, E. M. & Bolen, J. B. Pillars article: the CD4 and CD8 T cell surface antigens are associated with the internal membrane tyrosine-protein kinase p56lck. 1994. *J. Immunol. Baltim. Md 1950* **185,** 2650–2657 (2010).
40. Wang, H. *et al.* ZAP-70: an essential kinase in T-cell signaling. *Cold Spring Harb. Perspect. Biol.* **2,** a002279 (2010).
41. Baniyash, M., Garcia-Morales, P., Luong, E., Samelson, L. E. & Klausner, R. D. The T cell antigen receptor zeta chain is tyrosine phosphorylated upon activation. *J. Biol. Chem.* **263,** 18225–18230 (1988).
42. Klausner, R. D. *et al.* T cell receptor tyrosine phosphorylation. Variable coupling for different activating ligands. *J. Biol. Chem.* **262,** 12654–12659 (1987).
43. Samelson, L. E., Phillips, A. F., Luong, E. T. & Klausner, R. D. Association of the fyn protein-tyrosine kinase with the T-cell antigen receptor. *Proc. Natl. Acad. Sci. U. S. A.* **87,** 4358–4362 (1990).
44. Barclay, A. N., Brady, R. L., Davis, S. J. & Lange, G. CD4 and the immunoglobulin superfamily. *Philos. Trans. R. Soc. Lond. B. Biol. Sci.* **342,** 7–12 (1993).
45. Bowers, K., Pitcher, C. & Marsh, M. CD4: a co-receptor in the immune response and HIV infection. *Int. J. Biochem. Cell Biol.* **29,** 871–875 (1997).
46. Wang, J. *et al.* Atomic structure of a fragment of human CD4 containing two immunoglobulin-like domains. *Nature* **348,** 411–418 (1990).
47. Reinherz, E. L., Kung, P. C., Goldstein, G. & Schlossman, S. F. Separation of functional subsets of human T cells by a monoclonal antibody. *Proc. Natl. Acad. Sci. U. S. A.* **76,** 4061–4065 (1979).
48. Wood, G. S., Warner, N. L. & Warnke, R. A. Anti-Leu-3/T4 antibodies react with cells of monocyte/macrophage and Langerhans lineage. *J. Immunol. Baltim. Md 1950* **131,** 212–216 (1983).
49. Lucey, D. R., Dorsky, D. I., Nicholson-Weller, A. & Weller, P. F. Human eosinophils express CD4 protein and bind human immunodeficiency virus 1 gp120. *J. Exp. Med.* **169,** 327–332 (1989).
50. Maddon, P. J. *et al.* The isolation and nucleotide sequence of a cDNA encoding the T cell surface protein T4: a new member of the immunoglobulin gene family. *Cell* **42,** 93–104 (1985).
51. Clark, S. J., Jefferies, W. A., Barclay, A. N., Gagnon, J. & Williams, A. F. Peptide and nucleotide sequences of rat CD4 (W3/25) antigen: evidence for derivation from a structure with four immunoglobulin-related domains. *Proc. Natl. Acad. Sci. U. S. A.* **84,** 1649–1653 (1987).
52. UniProtKB - P01730 (CD4_HUMAN). (2016). Available at: http://www.uniprot.org/uniprot/P01730. (Accessed: 13th November 2016)
53. Harris, R. J., Chamow, S. M., Gregory, T. J. & Spellman, M. W. Characterization of a soluble form of human CD4. Peptide analyses confirm the expected amino acid sequence, identify glycosylation sites and

demonstrate the presence of three disulfide bonds. *Eur. J. Biochem. FEBS* **188,** 291–300 (1990).
54. Brady, R. L. *et al.* Crystal structure of domains 3 and 4 of rat CD4: relation to the NH2-terminal domains. *Science* **260,** 979–983 (1993).
55. Sweet, R. W., Truneh, A. & Hendrickson, W. A. CD4: its structure, role in immune function and AIDS pathogenesis, and potential as a pharmacological target. *Curr. Opin. Biotechnol.* **2,** 622–633 (1991).
56. Ryu, S. E. *et al.* Crystal structure of an HIV-binding recombinant fragment of human CD4. *Nature* **348,** 419–426 (1990).
57. Katz, B. A. & Kossiakoff, A. The crystallographically determined structures of atypical strained disulfides engineered into subtilisin. *J. Biol. Chem.* **261,** 15480–15485 (1986).
58. Huang, B., Yachou, A., Fleury, S., Hendrickson, W. A. & Sekaly, R. P. Analysis of the contact sites on the CD4 molecule with class II MHC molecule: co-ligand versus co-receptor function. *J. Immunol. Baltim. Md 1950* **158,** 216–225 (1997).
59. König, R., Shen, X. & Germain, R. N. Involvement of both major histocompatibility complex class II alpha and beta chains in CD4 function indicates a role for ordered oligomerization in T cell activation. *J. Exp. Med.* **182,** 779–787 (1995).
60. Sakihama, T., Smolyar, A. & Reinherz, E. L. Oligomerization of CD4 is required for stable binding to class II major histocompatibility complex proteins but not for interaction with human immunodeficiency virus gp120. *Proc. Natl. Acad. Sci. U. S. A.* **92,** 6444–6448 (1995).
61. Moldovan, M.-C., Sabbagh, L., Breton, G., Sékaly, R.-P. & Krummel, M. F. Triggering of T cell activation via CD4 dimers. *J. Immunol. Baltim. Md 1950* **176,** 5438–5445 (2006).
62. Wu, H., Kwong, P. D. & Hendrickson, W. A. Dimeric association and segmental variability in the structure of human CD4. *Nature* **387,** 527–530 (1997).
63. Ou, W. & Silver, J. Role of protein disulfide isomerase and other thiol-reactive proteins in HIV-1 envelope protein-mediated fusion. *Virology* **350,** 406–417 (2006).
64. Maekawa, A., Schmidt, B., Fazekas de St Groth, B., Sanejouand, Y.-H. & Hogg, P. J. Evidence for a domain-swapped CD4 dimer as the coreceptor for binding to class II MHC. *J. Immunol. Baltim. Md 1950* **176,** 6873–6878 (2006).
65. Leonard, W. J. *et al.* Molecular cloning and expression of cDNAs for the human interleukin-2 receptor. *Nature* **311,** 626–631 (1984).
66. Nikaido, T. *et al.* Molecular cloning of cDNA encoding human interleukin-2 receptor. *Nature* **311,** 631–635 (1984).
67. Taniguchi, T. *et al.* Structure and expression of a cloned cDNA for human interleukin-2. *Nature* **302,** 305–310 (1983).
68. Gillis, S., Baker, P. E., Ruscetti, F. W. & Smith, K. A. Long-term culture of human antigen-specific cytotoxic T-cell lines. *J. Exp. Med.* **148,** 1093–1098 (1978).
69. Létourneau, S., Krieg, C., Pantaleo, G. & Boyman, O. IL-2- and CD25-dependent immunoregulatory mechanisms in the homeostasis of T-cell subsets. *J. Allergy Clin. Immunol.* **123,** 758–762 (2009).

70. Germann, T. *et al.* Interleukin-12/T cell stimulating factor, a cytokine with multiple effects on T helper type 1 (Th1) but not on Th2 cells. *Eur. J. Immunol.* **23,** 1762–1770 (1993).
71. Hamza, T., Barnett, J. B. & Li, B. Interleukin 12 a key immunoregulatory cytokine in infection applications. *Int. J. Mol. Sci.* **11,** 789–806 (2010).
72. O'Garra, A. Cytokines induce the development of functionally heterogeneous T helper cell subsets. *Immunity* **8,** 275–283 (1998).
73. Zhu, J., Yamane, H. & Paul, W. E. Differentiation of effector CD4 T cell populations (*). *Annu. Rev. Immunol.* **28,** 445–489 (2010).
74. Xing, Z., Zganiacz, A. & Santosuosso, M. Role of IL-12 in macrophage activation during intracellular infection: IL-12 and mycobacteria synergistically release TNF-alpha and nitric oxide from macrophages via IFN-gamma induction. *J. Leukoc. Biol.* **68,** 897–902 (2000).
75. Szabo, S. J. *et al.* A novel transcription factor, T-bet, directs Th1 lineage commitment. *Cell* **100,** 655–669 (2000).
76. *Immunobiology: the immune system in health and disease ; [animated CD-ROM inside]*. (Garland Publ. [u.a.], 2001).
77. Lopes, N., Sergé, A., Ferrier, P. & Irla, M. Thymic Crosstalk Coordinates Medulla Organization and T-Cell Tolerance Induction. *Front. Immunol.* **6,** 365 (2015).
78. Dasgupta, A. & Saxena, R. Regulatory T cells: a review. *Natl. Med. J. India* **25,** 341–351 (2012).
79. Vila, J., Isaacs, J. D. & Anderson, A. E. Regulatory T cells and autoimmunity. *Curr. Opin. Hematol.* **16,** 274–279 (2009).
80. Gershon, R. K. & Kondo, K. Cell interactions in the induction of tolerance: the role of thymic lymphocytes. *Immunology* **18,** 723–737 (1970).
81. Sakaguchi, S., Sakaguchi, N., Asano, M., Itoh, M. & Toda, M. Immunologic self-tolerance maintained by activated T cells expressing IL-2 receptor alpha-chains (CD25). Breakdown of a single mechanism of self-tolerance causes various autoimmune diseases. *J. Immunol. Baltim. Md 1950* **155,** 1151–1164 (1995).
82. Hori, S., Nomura, T. & Sakaguchi, S. Control of regulatory T cell development by the transcription factor Foxp3. *Science* **299,** 1057–1061 (2003).
83. Sakaguchi, S., Yamaguchi, T., Nomura, T. & Ono, M. Regulatory T cells and immune tolerance. *Cell* **133,** 775–787 (2008).
84. Karim, M., Kingsley, C. I., Bushell, A. R., Sawitzki, B. S. & Wood, K. J. Alloantigen-induced CD25+CD4+ regulatory T cells can develop in vivo from CD25-CD4+ precursors in a thymus-independent process. *J. Immunol. Baltim. Md 1950* **172,** 923–928 (2004).
85. Thornton, A. M. *et al.* Expression of Helios, an Ikaros transcription factor family member, differentiates thymic-derived from peripherally induced Foxp3+ T regulatory cells. *J. Immunol. Baltim. Md 1950* **184,** 3433–3441 (2010).
86. Himmel, M. E., MacDonald, K. G., Garcia, R. V., Steiner, T. S. & Levings, M. K. Helios+ and Helios- cells coexist within the natural FOXP3+ T regulatory cell subset in humans. *J. Immunol. Baltim. Md 1950* **190,** 2001–2008 (2013).

87. Elkord, E., Abd Al Samid, M. & Chaudhary, B. Helios, and not FoxP3, is the marker of activated Tregs expressing GARP/LAP. *Oncotarget* **6,** 20026–20036 (2015).
88. Williams, L. M. & Rudensky, A. Y. Maintenance of the Foxp3-dependent developmental program in mature regulatory T cells requires continued expression of Foxp3. *Nat. Immunol.* **8,** 277–284 (2007).
89. Bennett, C. L. *et al.* The immune dysregulation, polyendocrinopathy, enteropathy, X-linked syndrome (IPEX) is caused by mutations of FOXP3. *Nat. Genet.* **27,** 20–21 (2001).
90. Wan, Y. Y. & Flavell, R. A. Regulatory T-cell functions are subverted and converted owing to attenuated Foxp3 expression. *Nature* **445,** 766–770 (2007).
91. Fontenot, J. D., Gavin, M. A. & Rudensky, A. Y. Foxp3 programs the development and function of CD4+CD25+ regulatory T cells. *Nat. Immunol.* **4,** 330–336 (2003).
92. Nie, H. *et al.* Phosphorylation of FOXP3 controls regulatory T cell function and is inhibited by TNF-α in rheumatoid arthritis. *Nat. Med.* **19,** 322–328 (2013).
93. Wang, J., Ioan-Facsinay, A., van der Voort, E. I. H., Huizinga, T. W. J. & Toes, R. E. M. Transient expression of FOXP3 in human activated nonregulatory CD4+ T cells. *Eur. J. Immunol.* **37,** 129–138 (2007).
94. Allan, S. E. *et al.* Activation-induced FOXP3 in human T effector cells does not suppress proliferation or cytokine production. *Int. Immunol.* **19,** 345–354 (2007).
95. Huynh, A. *et al.* Control of PI(3) kinase in Treg cells maintains homeostasis and lineage stability. *Nat. Immunol.* **16,** 188–196 (2015).
96. Shrestha, S. *et al.* Treg cells require the phosphatase PTEN to restrain TH1 and TFH cell responses. *Nat. Immunol.* **16,** 178–187 (2015).
97. Burchill, M. A., Yang, J., Vogtenhuber, C., Blazar, B. R. & Farrar, M. A. IL-2 receptor beta-dependent STAT5 activation is required for the development of Foxp3+ regulatory T cells. *J. Immunol. Baltim. Md 1950* **178,** 280–290 (2007).
98. Sauer, S. *et al.* T cell receptor signaling controls Foxp3 expression via PI3K, Akt, and mTOR. *Proc. Natl. Acad. Sci. U. S. A.* **105,** 7797–7802 (2008).
99. Walsh, P. T. *et al.* PTEN inhibits IL-2 receptor-mediated expansion of CD4+ CD25+ Tregs. *J. Clin. Invest.* **116,** 2521–2531 (2006).
100. Sakaguchi, S., Wing, K., Onishi, Y., Prieto-Martin, P. & Yamaguchi, T. Regulatory T cells: how do they suppress immune responses? *Int. Immunol.* **21,** 1105–1111 (2009).
101. Andersson, J. *et al.* CD4+ FoxP3+ regulatory T cells confer infectious tolerance in a TGF-beta-dependent manner. *J. Exp. Med.* **205,** 1975–1981 (2008).
102. Tran, D. Q. TGF-β: the sword, the wand, and the shield of FOXP3(+) regulatory T cells. *J. Mol. Cell Biol.* **4,** 29–37 (2012).
103. Rubtsov, Y. P. *et al.* Regulatory T cell-derived interleukin-10 limits inflammation at environmental interfaces. *Immunity* **28,** 546–558 (2008).
104. Collison, L. W. *et al.* The inhibitory cytokine IL-35 contributes to regulatory T-cell function. *Nature* **450,** 566–569 (2007).

105. Takahashi, T. *et al.* Immunologic self-tolerance maintained by CD25(+)CD4(+) regulatory T cells constitutively expressing cytotoxic T lymphocyte-associated antigen 4. *J. Exp. Med.* **192,** 303–310 (2000).
106. van der Merwe, P. A., Bodian, D. L., Daenke, S., Linsley, P. & Davis, S. J. CD80 (B7-1) binds both CD28 and CTLA-4 with a low affinity and very fast kinetics. *J. Exp. Med.* **185,** 393–403 (1997).
107. Parry, R. V. *et al.* CTLA-4 and PD-1 receptors inhibit T-cell activation by distinct mechanisms. *Mol. Cell. Biol.* **25,** 9543–9553 (2005).
108. Boasso, A., Herbeuval, J.-P., Hardy, A. W., Winkler, C. & Shearer, G. M. Regulation of indoleamine 2,3-dioxygenase and tryptophanyl-tRNA-synthetase by CTLA-4-Fc in human CD4+ T cells. *Blood* **105,** 1574–1581 (2005).
109. Mellor, A. L. & Munn, D. H. IDO expression by dendritic cells: tolerance and tryptophan catabolism. *Nat. Rev. Immunol.* **4,** 762–774 (2004).
110. Moffett, J. R. & Namboodiri, M. A. Tryptophan and the immune response. *Immunol. Cell Biol.* **81,** 247–265 (2003).
111. Munn, D. H. *et al.* Inhibition of T cell proliferation by macrophage tryptophan catabolism. *J. Exp. Med.* **189,** 1363–1372 (1999).
112. Yan, Z., Garg, S. K. & Banerjee, R. Regulatory T cells interfere with glutathione metabolism in dendritic cells and T cells. *J. Biol. Chem.* **285,** 41525–41532 (2010).
113. Yan, Z., Garg, S. K., Kipnis, J. & Banerjee, R. Extracellular redox modulation by regulatory T cells. *Nat. Chem. Biol.* **5,** 721–723 (2009).
114. Liang, B. *et al.* Regulatory T cells inhibit dendritic cells by lymphocyte activation gene-3 engagement of MHC class II. *J. Immunol. Baltim. Md 1950* **180,** 5916–5926 (2008).
115. Joller, N. *et al.* Treg Cells Expressing the Coinhibitory Molecule TIGIT Selectively Inhibit Proinflammatory Th1 and Th17 Cell Responses. *Immunity* **40,** 569–581 (2014).
116. Ohta, A. & Sitkovsky, M. Extracellular adenosine-mediated modulation of regulatory T cells. *Front. Immunol.* **5,** 304 (2014).
117. Antonioli, L., Pacher, P., Vizi, E. S. & Haskó, G. CD39 and CD73 in immunity and inflammation. *Trends Mol. Med.* **19,** 355–367 (2013).
118. Linden, J. & Cekic, C. Regulation of lymphocyte function by adenosine. *Arterioscler. Thromb. Vasc. Biol.* **32,** 2097–2103 (2012).
119. Haskó, G., Linden, J., Cronstein, B. & Pacher, P. Adenosine receptors: therapeutic aspects for inflammatory and immune diseases. *Nat. Rev. Drug Discov.* **7,** 759–770 (2008).
120. Deaglio, S. *et al.* Adenosine generation catalyzed by CD39 and CD73 expressed on regulatory T cells mediates immune suppression. *J. Exp. Med.* **204,** 1257–1265 (2007).
121. Klein, M. *et al.* Repression of cyclic adenosine monophosphate upregulation disarms and expands human regulatory T cells. *J. Immunol. Baltim. Md 1950* **188,** 1091–1097 (2012).
122. Bopp, T. *et al.* Cyclic adenosine monophosphate is a key component of regulatory T cell-mediated suppression. *J. Exp. Med.* **204,** 1303–1310 (2007).
123. Bodor, J., Fehervari, Z., Diamond, B. & Sakaguchi, S. Regulatory T cell-mediated suppression: potential role of ICER. *J. Leukoc. Biol.* **81,** 161–167 (2007).

124. Bodor, J. *et al.* Cyclic AMP underpins suppression by regulatory T cells. *Eur. J. Immunol.* **42,** 1375–1384 (2012).
125. Vaeth, M. *et al.* Regulatory T cells facilitate the nuclear accumulation of inducible cAMP early repressor (ICER) and suppress nuclear factor of activated T cell c1 (NFATc1). *Proc. Natl. Acad. Sci. U. S. A.* **108,** 2480–2485 (2011).
126. Grossman, W. J. *et al.* Human T regulatory cells can use the perforin pathway to cause autologous target cell death. *Immunity* **21,** 589–601 (2004).
127. Asano, M., Toda, M., Sakaguchi, N. & Sakaguchi, S. Autoimmune disease as a consequence of developmental abnormality of a T cell subpopulation. *J. Exp. Med.* **184,** 387–396 (1996).
128. Taguchi, O. & Takahashi, T. Administration of anti-interleukin-2 receptor alpha antibody in vivo induces localized autoimmune disease. *Eur. J. Immunol.* **26,** 1608–1612 (1996).
129. Dejaco, C., Duftner, C., Grubeck-Loebenstein, B. & Schirmer, M. Imbalance of regulatory T cells in human autoimmune diseases. *Immunology* **117,** 289–300 (2006).
130. Flores-Borja, F., Jury, E. C., Mauri, C. & Ehrenstein, M. R. Defects in CTLA-4 are associated with abnormal regulatory T cell function in rheumatoid arthritis. *Proc. Natl. Acad. Sci. U. S. A.* **105,** 19396–19401 (2008).
131. Cribbs, A. P. *et al.* Regulatory T cell function in rheumatoid arthritis is compromised by CTLA-4 promoter methylation resulting in a failure to activate the IDO pathway. *Arthritis Rheumatol. Hoboken NJ* **66,** 2344–54 (2014).
132. Ehrenstein, M. R. *et al.* Compromised Function of Regulatory T Cells in Rheumatoid Arthritis and Reversal by Anti-TNFα Therapy. *J. Exp. Med.* **200,** 277–285 (2004).
133. Li, Z. *et al.* PIM1 kinase phosphorylates the human transcription factor FOXP3 at serine 422 to negatively regulate its activity under inflammation. *J. Biol. Chem.* **289,** 26872–26881 (2014).
134. Li, S., Yu, Y., Yue, Y., Zhang, Z. & Su, K. Microbial Infection and Rheumatoid Arthritis. *J. Clin. Cell. Immunol.* **4,** (2013).
135. Pasare, C. & Medzhitov, R. Toll pathway-dependent blockade of CD4+CD25+ T cell-mediated suppression by dendritic cells. *Science* **299,** 1033–1036 (2003).
136. Cojocaru, M., Cojocaru, I. M., Silosi, I., Vrabie, C. D. & Tanasescu, R. Extra-articular Manifestations in Rheumatoid Arthritis. *Maedica* **5,** 286–291 (2010).
137. Hensvold, A. H. *et al.* Environmental and genetic factors in the development of anticitrullinated protein antibodies (ACPAs) and ACPA-positive rheumatoid arthritis: an epidemiological investigation in twins. *Ann. Rheum. Dis.* **74,** 375–380 (2015).
138. Mikuls, T. R. *et al.* Associations of disease activity and treatments with mortality in men with rheumatoid arthritis: results from the VARA registry. *Rheumatol. Oxf. Engl.* **50,** 101–109 (2011).
139. Sihvonen, S., Korpela, M., Laippala, P., Mustonen, J. & Pasternack, A. Death rates and causes of death in patients with rheumatoid arthritis: a population-based study. *Scand. J. Rheumatol.* **33,** 221–227 (2004).

140. 21149499, L., Silva, C., Stolt, P., Alfredsson, L. & Klareskog, L. A gene-environment interaction between smoking and shared epitope genes in HLA-DR provides a high risk of seropositive rheumatoid arthritis. *Arthritis Rheum.* **50,** 3085–3092 (2004).
141. Källberg, H. *et al.* Smoking is a major preventable risk factor for rheumatoid arthritis: estimations of risks after various exposures to cigarette smoke. *Ann. Rheum. Dis.* **70,** 508–511 (2011).
142. Stolt, P. *et al.* Quantification of the influence of cigarette smoking on rheumatoid arthritis: results from a population based case-control study, using incident cases. *Ann. Rheum. Dis.* **62,** 835–841 (2003).
143. Stahl, E. A. *et al.* Genome-wide association study meta-analysis identifies seven new rheumatoid arthritis risk loci. *Nat. Genet.* **42,** 508–514 (2010).
144. MacGregor, A. J. *et al.* Characterizing the quantitative genetic contribution to rheumatoid arthritis using data from twins. *Arthritis Rheum.* **43,** 30–37 (2000).
145. Raychaudhuri, S. *et al.* Five amino acids in three HLA proteins explain most of the association between MHC and seropositive rheumatoid arthritis. *Nat. Genet.* **44,** 291–296 (2012).
146. Rantapää-Dahlqvist, S. *et al.* Antibodies against cyclic citrullinated peptide and IgA rheumatoid factor predict the development of rheumatoid arthritis. *Arthritis Rheum.* **48,** 2741–2749 (2003).
147. Calin, A., Elswood, J. & Klouda, P. T. Destructive arthritis, rheumatoid factor, and HLA-DR4. Susceptibility versus severity, a case-control study. *Arthritis Rheum.* **32,** 1221–1225 (1989).
148. Gregersen, P. K., Silver, J. & Winchester, R. J. The shared epitope hypothesis. An approach to understanding the molecular genetics of susceptibility to rheumatoid arthritis. *Arthritis Rheum.* **30,** 1205–1213 (1987).
149. Pratt, A. G., Isaacs, J. D. & Mattey, D. L. Current concepts in the pathogenesis of early rheumatoid arthritis. *Best Pract. Res. Clin. Rheumatol.* **23,** 37–48 (2009).
150. Meyer, P. W. A. *et al.* Circulating cytokine profiles and their relationships with autoantibodies, acute phase reactants, and disease activity in patients with rheumatoid arthritis. *Mediators Inflamm.* **2010,** 158514 (2010).
151. Feldmann, M., Brennan, F. M. & Maini, R. N. Role of cytokines in rheumatoid arthritis. *Annu. Rev. Immunol.* **14,** 397–440 (1996).
152. Srirangan, S. & Choy, E. H. The role of interleukin 6 in the pathophysiology of rheumatoid arthritis. *Ther. Adv. Musculoskelet. Dis.* **2,** 247–256 (2010).
153. Park, J. Y. & Pillinger, M. H. Interleukin-6 in the pathogenesis of rheumatoid arthritis. *Bull. NYU Hosp. Jt. Dis.* **65 Suppl 1,** S4-10 (2007).
154. Churchman, S. M. & Ponchel, F. Interleukin-7 in rheumatoid arthritis. *Rheumatology* **47,** 753–759 (2008).
155. McInnes, I. B. *et al.* The role of interleukin-15 in T-cell migration and activation in rheumatoid arthritis. *Nat. Med.* **2,** 175–182 (1996).
156. Machado Diaz, A. C. *et al.* Proinflammatory Soluble Interleukin-15 Receptor Alpha Is Increased in Rheumatoid Arthritis. *Arthritis* **2012,** 1–7 (2012).
157. González-Alvaro, I. *et al.* Interleukin-15 and interferon-gamma participate in the cross-talk between natural killer and monocytic cells required for tumour necrosis factor production. *Arthritis Res. Ther.* **8,** R88 (2006).

158. Okamura, H., Kashiwamura, S., Tsutsui, H., Yoshimoto, T. & Nakanishi, K. Regulation of interferon-gamma production by IL-12 and IL-18. *Curr. Opin. Immunol.* **10,** 259–264 (1998).
159. Gracie, J. A. *et al.* A proinflammatory role for IL-18 in rheumatoid arthritis. *J. Clin. Invest.* **104,** 1393–1401 (1999).
160. Joosten, L. A. B. *et al.* IL-32, a proinflammatory cytokine in rheumatoid arthritis. *Proc. Natl. Acad. Sci. U. S. A.* **103,** 3298–3303 (2006).
161. Xu, W.-D., Zhang, M., Zhang, Y.-J. & Ye, D.-Q. IL-33 in rheumatoid arthritis: potential role in pathogenesis and therapy. *Hum. Immunol.* **74,** 1057–1060 (2013).
162. Geusens, P. The role of RANK ligand/osteoprotegerin in rheumatoid arthritis. *Ther. Adv. Musculoskelet. Dis.* **4,** 225–233 (2012).
163. Darrieutort-Laffite, C. *et al.* IL-1β and TNFα promote monocyte viability through the induction of GM-CSF expression by rheumatoid arthritis synovial fibroblasts. *Mediators Inflamm.* **2014,** 241840 (2014).
164. Haworth, C. *et al.* Expression of granulocyte-macrophage colony-stimulating factor in rheumatoid arthritis: regulation by tumor necrosis factor-alpha. *Eur. J. Immunol.* **21,** 2575–2579 (1991).
165. Seibl, R. *et al.* Expression and regulation of Toll-like receptor 2 in rheumatoid arthritis synovium. *Am. J. Pathol.* **162,** 1221–1227 (2003).
166. Sokolove, J. & Lepus, C. M. Role of inflammation in the pathogenesis of osteoarthritis: latest findings and interpretations. *Ther. Adv. Musculoskelet. Dis.* **5,** 77–94 (2013).
167. Lopez-Castejon, G. & Brough, D. Understanding the mechanism of IL-1β secretion. *Cytokine Growth Factor Rev.* **22,** 189–195 (2011).
168. Burrage, P. S., Mix, K. S. & Brinckerhoff, C. E. Matrix metalloproteinases: role in arthritis. *Front. Biosci. J. Virtual Libr.* **11,** 529–543 (2006).
169. Schneider, P. *et al.* BAFF, a novel ligand of the tumor necrosis factor family, stimulates B cell growth. *J. Exp. Med.* **189,** 1747–1756 (1999).
170. Seyler, T. M. *et al.* BLyS and APRIL in rheumatoid arthritis. *J. Clin. Invest.* **115,** 3083–3092 (2005).
171. Assi, L. K. *et al.* Tumor necrosis factor alpha activates release of B lymphocyte stimulator by neutrophils infiltrating the rheumatoid joint. *Arthritis Rheum.* **56,** 1776–1786 (2007).
172. Song, Y. W. & Kang, E. H. Autoantibodies in rheumatoid arthritis: rheumatoid factors and anticitrullinated protein antibodies. *QJM Mon. J. Assoc. Physicians* **103,** 139–146 (2010).
173. Mathsson, L., Lampa, J., Mullazehi, M. & Rönnelid, J. Immune complexes from rheumatoid arthritis synovial fluid induce FcgammaRIIa dependent and rheumatoid factor correlated production of tumour necrosis factor-alpha by peripheral blood mononuclear cells. *Arthritis Res. Ther.* **8,** R64 (2006).
174. Xiao, Y., Motomura, S. & Podack, E. R. APRIL (TNFSF13) regulates collagen-induced arthritis, IL-17 production and Th2 response. *Eur. J. Immunol.* **38,** 3450–3458 (2008).
175. Korn, T. *et al.* IL-21 initiates an alternative pathway to induce proinflammatory T(H)17 cells. *Nature* **448,** 484–487 (2007).
176. Peters, A., Lee, Y. & Kuchroo, V. K. The many faces of Th17 cells. *Curr. Opin. Immunol.* **23,** 702–706 (2011).

177. Kolls, J. K. & Lindén, A. Interleukin-17 family members and inflammation. *Immunity* **21,** 467–476 (2004).
178. Bedoya, S. K., Lam, B., Lau, K. & Larkin, J., 3rd. Th17 Cells in Immunity and Autoimmunity. *Clin. Dev. Immunol.* **2013,** 986789 (2013).
179. Kryczek, I. *et al.* Human TH17 cells are long-lived effector memory cells. *Sci. Transl. Med.* **3,** 104ra100 (2011).
180. Mai, J., Wang, H. & Yang, X.-F. Th 17 cells interplay with Foxp3+ Tregs in regulation of inflammation and autoimmunity. *Front. Biosci. Landmark Ed.* **15,** 986–1006 (2010).
181. Annunziato, F., Cosmi, L., Liotta, F., Maggi, E. & Romagnani, S. Main features of human T helper 17 cells. *Ann. N. Y. Acad. Sci.* **1284,** 66–70 (2013).
182. Basdeo, S. A. *et al.* Polyfunctional, Pathogenic CD161+ Th17 Lineage Cells Are Resistant to Regulatory T Cell-Mediated Suppression in the Context of Autoimmunity. *J. Immunol. Baltim. Md 1950* **195,** 528–540 (2015).
183. Ricciotti, E. & FitzGerald, G. A. Prostaglandins and inflammation. *Arterioscler. Thromb. Vasc. Biol.* **31,** 986–1000 (2011).
184. Aktories, K., Förstermann, U., Hofmann, F. B. & Starke, K. *Allgemeine und Spezielle Pharmakologie und Toxikologie*. (Elsevier (Urban & Fischer Verlag), 2006).
185. Coutinho, A. E. & Chapman, K. E. The anti-inflammatory and immunosuppressive effects of glucocorticoids, recent developments and mechanistic insights. *Mol. Cell. Endocrinol.* **335,** 2–13 (2011).
186. Brattsand, R. & Linden, M. Cytokine modulation by glucocorticoids: mechanisms and actions in cellular studies. *Aliment. Pharmacol. Ther.* **10 Suppl 2,** 81-90-92 (1996).
187. Perretti, M. & D'Acquisto, F. Annexin A1 and glucocorticoids as effectors of the resolution of inflammation. *Nat. Rev. Immunol.* **9,** 62–70 (2009).
188. Kumar, P. & Banik, S. Pharmacotherapy options in rheumatoid arthritis. *Clin. Med. Insights Arthritis Musculoskelet. Disord.* **6,** 35–43 (2013).
189. Cutolo, M., Sulli, A., Pizzorni, C., Seriolo, B. & Straub, R. H. Anti-inflammatory mechanisms of methotrexate in rheumatoid arthritis. *Ann. Rheum. Dis.* **60,** 729–735 (2001).
190. *Repetitorium allgemeine und spezielle Pharmakologie und Toxikologie: mit 135 Tabellen*. (Elsevier, Urban & Fischer, 2009).
191. Emery, P., Sebba, A. & Huizinga, T. W. J. Biologic and oral disease-modifying antirheumatic drug monotherapy in rheumatoid arthritis. *Ann. Rheum. Dis.* **72,** 1897–1904 (2013).
192. Egan, L. J. *et al.* Inhibition of interleukin-1-stimulated NF-kappaB RelA/p65 phosphorylation by mesalamine is accompanied by decreased transcriptional activity. *J. Biol. Chem.* **274,** 26448–26453 (1999).
193. Kaiser, G. C., Yan, F. & Polk, D. B. Mesalamine blocks tumor necrosis factor growth inhibition and nuclear factor kappaB activation in mouse colonocytes. *Gastroenterology* **116,** 602–609 (1999).
194. Scott, D. L. & Kingsley, G. H. Tumor necrosis factor inhibitors for rheumatoid arthritis. *N. Engl. J. Med.* **355,** 704–712 (2006).
195. Tanaka, T., Narazaki, M. & Kishimoto, T. Therapeutic targeting of the interleukin-6 receptor. *Annu. Rev. Pharmacol. Toxicol.* **52,** 199–219 (2012).

196. Moreland, L., Bate, G. & Kirkpatrick, P. Abatacept. *Nat. Rev. Drug Discov.* **5,** 185–186 (2006).
197. Kundu, S. *et al.* Oxidative stress as a potential biomarker for determining disease activity in patients with rheumatoid arthritis. *Free Radic. Res.* **46,** 1482–1489 (2012).
198. Hitchon, C. A. & El-Gabalawy, H. S. Oxidation in rheumatoid arthritis. *Arthritis Res. Ther.* **6,** 265–278 (2004).
199. Yi, M. C. & Khosla, C. Thiol-Disulfide Exchange Reactions in the Mammalian Extracellular Environment. *Annu. Rev. Chem. Biomol. Eng.* **7,** 197–222 (2016).
200. Hwang, C., Sinskey, A. J. & Lodish, H. F. Oxidized redox state of glutathione in the endoplasmic reticulum. *Science* **257,** 1496–1502 (1992).
201. Henrotin, Y. E., Bruckner, P. & Pujol, J.-P. L. The role of reactive oxygen species in homeostasis and degradation of cartilage. *Osteoarthr. Cartil. OARS Osteoarthr. Res. Soc.* **11,** 747–755 (2003).
202. Finkel, T. Signal transduction by reactive oxygen species. *J. Cell Biol.* **194,** 7–15 (2011).
203. Remans, P. H. J. *et al.* CTLA-4IG suppresses reactive oxygen species by preventing synovial adherent cell-induced inactivation of Rap1, a Ras family GTPASE mediator of oxidative stress in rheumatoid arthritis T cells. *Arthritis Rheum.* **54,** 3135–3143 (2006).
204. Remans, P. H. J. *et al.* Rap1 signaling is required for suppression of Ras-generated reactive oxygen species and protection against oxidative stress in T lymphocytes. *J. Immunol. Baltim. Md 1950* **173,** 920–931 (2004).
205. Gringhuis, S. I. *et al.* Displacement of linker for activation of T cells from the plasma membrane due to redox balance alterations results in hyporesponsiveness of synovial fluid T lymphocytes in rheumatoid arthritis. *J. Immunol. Baltim. Md 1950* **164,** 2170–2179 (2000).
206. Maurice, M. M. *et al.* Defective TCR-mediated signaling in synovial T cells in rheumatoid arthritis. *J. Immunol. Baltim. Md 1950* **159,** 2973–2978 (1997).
207. Gringhuis, S. I. *et al.* Effect of redox balance alterations on cellular localization of LAT and downstream T-cell receptor signaling pathways. *Mol. Cell. Biol.* **22,** 400–411 (2002).
208. Cemerski, S., van Meerwijk, J. P. M. & Romagnoli, P. Oxidative-stress-induced T lymphocyte hyporesponsiveness is caused by structural modification rather than proteasomal degradation of crucial TCR signaling molecules. *Eur. J. Immunol.* **33,** 2178–2185 (2003).
209. Altindag, O., Karakoc, M., Kocyigit, A., Celik, H. & Soran, N. Increased DNA damage and oxidative stress in patients with rheumatoid arthritis. *Clin. Biochem.* **40,** 167–171 (2007).
210. Jikimoto, T. *et al.* Thioredoxin as a biomarker for oxidative stress in patients with rheumatoid arthritis. *Mol. Immunol.* **38,** 765–772 (2002).
211. Hultqvist, M., Olsson, L. M., Gelderman, K. A. & Holmdahl, R. The protective role of ROS in autoimmune disease. *Trends Immunol.* **30,** 201–208 (2009).
212. Efimova, O., Szankasi, P. & Kelley, T. W. Ncf1 (p47phox) is essential for direct regulatory T cell mediated suppression of CD4+ effector T cells. *PloS One* **6,** e16013 (2011).

213. Mougiakakos, D., Johansson, C. C., Jitschin, R., Böttcher, M. & Kiessling, R. Increased thioredoxin-1 production in human naturally occurring regulatory T cells confers enhanced tolerance to oxidative stress. *Blood* **117,** 857–861 (2011).
214. Nordberg, J. & Arnér, E. S. Reactive oxygen species, antioxidants, and the mammalian thioredoxin system. *Free Radic. Biol. Med.* **31,** 1287–1312 (2001).
215. Schurmann, P. & Jacquot, J.-P. PLANT THIOREDOXIN SYSTEMS REVISITED. *Annu. Rev. Plant Physiol. Plant Mol. Biol.* **51,** 371–400 (2000).
216. Laurent, T. C., Moore, E. C. & Reichard, P. ENZYMATIC SYNTHESIS OF DEOXYRIBONUCLEOTIDES. IV. ISOLATION AND CHARACTERIZATION OF THIOREDOXIN, THE HYDROGEN DONOR FROM ESCHERICHIA COLI B. *J. Biol. Chem.* **239,** 3436–3444 (1964).
217. Martin, J. L. Thioredoxin--a fold for all reasons. *Struct. Lond. Engl. 1993* **3,** 245–250 (1995).
218. Lu, J. & Holmgren, A. The thioredoxin superfamily in oxidative protein folding. *Antioxid. Redox Signal.* **21,** 457–70 (2014).
219. Katti, S. K., LeMaster, D. M. & Eklund, H. Crystal structure of thioredoxin from Escherichia coli at 1.68 A resolution. *J. Mol. Biol.* **212,** 167–184 (1990).
220. Eklund, H., Gleason, F. K. & Holmgren, A. Structural and functional relations among thioredoxins of different species. *Proteins* **11,** 13–28 (1991).
221. Holmgren, A. Thioredoxin. *Annu. Rev. Biochem.* **54,** 237–271 (1985).
222. Weichsel, A., Kem, M. & Montfort, W. R. Crystal structure of human thioredoxin revealing an unraveled helix and exposed S-nitrosation site. *Protein Sci. Publ. Protein Soc.* **19,** 1801–1806 (2010).
223. Holmgren, A. Bovine thioredoxin system. Purification of thioredoxin reductase from calf liver and thymus and studies of its function in disulfide reduction. *J. Biol. Chem.* **252,** 4600–4606 (1977).
224. Casagrande, S. *et al.* Glutathionylation of human thioredoxin: a possible crosstalk between the glutathione and thioredoxin systems. *Proc. Natl. Acad. Sci. U. S. A.* **99,** 9745–9749 (2002).
225. Kondo, N., Nakamura, H., Masutani, H. & Yodoi, J. Redox regulation of human thioredoxin network. *Antioxid. Redox Signal.* **8,** 1881–1890 (2006).
226. Haendeler, J. *et al.* Redox regulatory and anti-apoptotic functions of thioredoxin depend on S-nitrosylation at cysteine 69. *Nat. Cell Biol.* **4,** 743–749 (2002).
227. Hashemy, S. I. & Holmgren, A. Regulation of the catalytic activity and structure of human thioredoxin 1 via oxidation and S-nitrosylation of cysteine residues. *J. Biol. Chem.* **283,** 21890–21898 (2008).
228. Kallis, G. B. & Holmgren, A. Differential reactivity of the functional sulfhydryl groups of cysteine-32 and cysteine-35 present in the reduced form of thioredoxin from Escherichia coli. *J. Biol. Chem.* **255,** 10261–10265 (1980).
229. Holmgren, A., Söderberg, B. O., Eklund, H. & Brändén, C. I. Three-dimensional structure of Escherichia coli thioredoxin-S2 to 2.8 A resolution. *Proc. Natl. Acad. Sci. U. S. A.* **72,** 2305–2309 (1975).

230. Lillig, C. H. & Holmgren, A. Thioredoxin and related molecules--from biology to health and disease. *Antioxid. Redox Signal.* **9,** 25–47 (2007).
231. Holmgren, A. Thioredoxin structure and mechanism: conformational changes on oxidation of the active-site sulfhydryls to a disulfide. *Struct. Lond. Engl. 1993* **3,** 239–243 (1995).
232. Szoszkiewicz, R. Single-molecule studies of disulfide bond reduction pathways used by human thioredoxin. *Biophys. Chem.* **173–174,** 31–38 (2013).
233. Vlamis-Gardikas, A. & Holmgren, A. Thioredoxin and glutaredoxin isoforms. *Methods Enzymol.* **347,** 286–296 (2002).
234. Spyrou, G., Enmark, E., Miranda-Vizuete, A. & Gustafsson, J. Cloning and expression of a novel mammalian thioredoxin. *J. Biol. Chem.* **272,** 2936–2941 (1997).
235. Rubartelli, A., Bajetto, A., Allavena, G., Wollman, E. & Sitia, R. Secretion of thioredoxin by normal and neoplastic cells through a leaderless secretory pathway. *J. Biol. Chem.* **267,** 24161–24164 (1992).
236. Kondo, N. *et al.* Redox-Sensing Release of Human Thioredoxin from T Lymphocytes with Negative Feedback Loops. *J. Immunol.* **172,** 442–448 (2004).
237. Kohárýová, M. & Kolárová, M. Oxidative stress and thioredoxin system. *Gen. Physiol. Biophys.* **27,** 71–84 (2008).
238. Chiurchiù, V. & Maccarrone, M. Chronic inflammatory disorders and their redox control: from molecular mechanisms to therapeutic opportunities. *Antioxid. Redox Signal.* **15,** 2605–2641 (2011).
239. Evans, M. D. & Cooke, M. S. Factors contributing to the outcome of oxidative damage to nucleic acids. *BioEssays News Rev. Mol. Cell. Dev. Biol.* **26,** 533–542 (2004).
240. Berlett, B. S. & Stadtman, E. R. Protein oxidation in aging, disease, and oxidative stress. *J. Biol. Chem.* **272,** 20313–20316 (1997).
241. Gough, D. R. & Cotter, T. G. Hydrogen peroxide: a Jekyll and Hyde signalling molecule. *Cell Death Dis.* **2,** e213 (2011).
242. Chae, H. Z. *et al.* Cloning and sequencing of thiol-specific antioxidant from mammalian brain: alkyl hydroperoxide reductase and thiol-specific antioxidant define a large family of antioxidant enzymes. *Proc. Natl. Acad. Sci. U. S. A.* **91,** 7017–7021 (1994).
243. Wood, Z. A., Schröder, E., Robin Harris, J. & Poole, L. B. Structure, mechanism and regulation of peroxiredoxins. *Trends Biochem. Sci.* **28,** 32–40 (2003).
244. Alphey, M. S., Bond, C. S., Tetaud, E., Fairlamb, A. H. & Hunter, W. N. The structure of reduced tryparedoxin peroxidase reveals a decamer and insight into reactivity of 2Cys-peroxiredoxins. *J. Mol. Biol.* **300,** 903–916 (2000).
245. Ellis, H. R. & Poole, L. B. Roles for the two cysteine residues of AhpC in catalysis of peroxide reduction by alkyl hydroperoxide reductase from Salmonella typhimurium. *Biochemistry (Mosc.)* **36,** 13349–13356 (1997).
246. Kang, S. W., Baines, I. C. & Rhee, S. G. Characterization of a mammalian peroxiredoxin that contains one conserved cysteine. *J. Biol. Chem.* **273,** 6303–6311 (1998).

247. Hall, A., Nelson, K., Poole, L. B. & Karplus, P. A. Structure-based insights into the catalytic power and conformational dexterity of peroxiredoxins. *Antioxid. Redox Signal.* **15,** 795–815 (2011).
248. Ueno, M. *et al.* Thioredoxin-dependent redox regulation of p53-mediated p21 activation. *J. Biol. Chem.* **274,** 35809–35815 (1999).
249. Pedrajas, J. R. *et al.* Glutathione Is the Resolving Thiol for Thioredoxin Peroxidase Activity of 1-Cys Peroxiredoxin Without Being Consumed During the Catalytic Cycle. *Antioxid. Redox Signal.* **24,** 115–128 (2016).
250. Noguera-Mazon, V. *et al.* Glutathionylation induces the dissociation of 1-Cys D-peroxiredoxin non-covalent homodimer. *J. Biol. Chem.* **281,** 31736–31742 (2006).
251. Hattori, K., Naguro, I., Runchel, C. & Ichijo, H. The roles of ASK family proteins in stress responses and diseases. *Cell Commun. Signal. CCS* **7,** 9 (2009).
252. Ichijo, H. *et al.* Induction of apoptosis by ASK1, a mammalian MAPKKK that activates SAPK/JNK and p38 signaling pathways. *Science* **275,** 90–94 (1997).
253. Kylarova, S. *et al.* Cysteine residues mediate high-affinity binding of thioredoxin to ASK1. *FEBS J.* **283,** 3821–3838 (2016).
254. Saitoh, M. *et al.* Mammalian thioredoxin is a direct inhibitor of apoptosis signal-regulating kinase (ASK) 1. *EMBO J.* **17,** 2596–2606 (1998).
255. Liu, Y. & Min, W. Thioredoxin promotes ASK1 ubiquitination and degradation to inhibit ASK1-mediated apoptosis in a redox activity-independent manner. *Circ. Res.* **90,** 1259–1266 (2002).
256. Patwari, P., Higgins, L. J., Chutkow, W. A., Yoshioka, J. & Lee, R. T. The interaction of thioredoxin with Txnip. Evidence for formation of a mixed disulfide by disulfide exchange. *J. Biol. Chem.* **281,** 21884–21891 (2006).
257. Junn, E. *et al.* Vitamin D3 up-regulated protein 1 mediates oxidative stress via suppressing the thioredoxin function. *J. Immunol. Baltim. Md 1950* **164,** 6287–6295 (2000).
258. Spindel, O. N., World, C. & Berk, B. C. Thioredoxin interacting protein: redox dependent and independent regulatory mechanisms. *Antioxid. Redox Signal.* **16,** 587–596 (2012).
259. Watanabe, R., Nakamura, H., Masutani, H. & Yodoi, J. Anti-oxidative, anti-cancer and anti-inflammatory actions by thioredoxin 1 and thioredoxin-binding protein-2. *Pharmacol. Ther.* **127,** 261–270 (2010).
260. Zhou, R., Tardivel, A., Thorens, B., Choi, I. & Tschopp, J. Thioredoxin-interacting protein links oxidative stress to inflammasome activation. *Nat. Immunol.* **11,** 136–140 (2010).
261. Davis, B. K. & Ting, J. P.-Y. NLRP3 has a sweet tooth. *Nat. Immunol.* **11,** 105–106 (2010).
262. Beech, D. J. & Sukumar, P. Channel regulation by extracellular redox protein. *Channels Austin Tex* **1,** 400–403 (2007).
263. Xu, S.-Z. *et al.* TRPC channel activation by extracellular thioredoxin. *Nature* **451,** 69–72 (2008).
264. Rosen, A. *et al.* A CD4+ T cell line-secreted factor, growth promoting for normal and leukemic B cells, identified as thioredoxin. *Int. Immunol.* **7,** 625–633 (1995).

265. Bertini, R. *et al.* Thioredoxin, a redox enzyme released in infection and inflammation, is a unique chemoattractant for neutrophils, monocytes, and T cells. *J. Exp. Med.* **189,** 1783–1789 (1999).
266. Schenk, H., Vogt, M., Dröge, W. & Schulze-Osthoff, K. Thioredoxin as a potent costimulus of cytokine expression. *J. Immunol. Baltim. Md 1950* **156,** 765–771 (1996).
267. Hirota, K. *et al.* AP-1 transcriptional activity is regulated by a direct association between thioredoxin and Ref-1. *Proc. Natl. Acad. Sci. U. S. A.* **94,** 3633–3638 (1997).
268. Karlenius, T. C. & Tonissen, K. F. Thioredoxin and Cancer: A Role for Thioredoxin in all States of Tumor Oxygenation. *Cancers* **2,** 209–232 (2010).
269. Welsh, S. J., Bellamy, W. T., Briehl, M. M. & Powis, G. The redox protein thioredoxin-1 (Trx-1) increases hypoxia-inducible factor 1alpha protein expression: Trx-1 overexpression results in increased vascular endothelial growth factor production and enhanced tumor angiogenesis. *Cancer Res.* **62,** 5089–5095 (2002).
270. Abate, C., Patel, L., Rauscher, F. J. & Curran, T. Redox regulation of fos and jun DNA-binding activity in vitro. *Science* **249,** 1157–1161 (1990).
271. Meyer, M., Schreck, R. & Baeuerle, P. A. H2O2 and antioxidants have opposite effects on activation of NF-kappa B and AP-1 in intact cells: AP-1 as secondary antioxidant-responsive factor. *EMBO J.* **12,** 2005–2015 (1993).
272. Lee, S.-R. *et al.* Reversible inactivation of the tumor suppressor PTEN by H2O2. *J. Biol. Chem.* **277,** 20336–20342 (2002).
273. Meuillet, E. J., Mahadevan, D., Berggren, M., Coon, A. & Powis, G. Thioredoxin-1 binds to the C2 domain of PTEN inhibiting PTEN's lipid phosphatase activity and membrane binding: a mechanism for the functional loss of PTEN's tumor suppressor activity. *Arch. Biochem. Biophys.* **429,** 123–133 (2004).
274. Ghosh, G., van Duyne, G., Ghosh, S. & Sigler, P. B. Structure of NF-kappa B p50 homodimer bound to a kappa B site. *Nature* **373,** 303–310 (1995).
275. Hayashi, T., Ueno, Y. & Okamoto, T. Oxidoreductive regulation of nuclear factor kappa B. Involvement of a cellular reducing catalyst thioredoxin. *J. Biol. Chem.* **268,** 11380–11388 (1993).
276. Matthews, J. R., Wakasugi, N., Virelizier, J. L., Yodoi, J. & Hay, R. T. Thioredoxin regulates the DNA binding activity of NF-kappa B by reduction of a disulphide bond involving cysteine 62. *Nucleic Acids Res.* **20,** 3821–3830 (1992).
277. Hirota, K. *et al.* Distinct roles of thioredoxin in the cytoplasm and in the nucleus. A two-step mechanism of redox regulation of transcription factor NF-kappaB. *J. Biol. Chem.* **274,** 27891–27897 (1999).
278. Hirota, K. *et al.* Nucleoredoxin, glutaredoxin, and thioredoxin differentially regulate NF-kappaB, AP-1, and CREB activation in HEK293 cells. *Biochem. Biophys. Res. Commun.* **274,** 177–182 (2000).
279. Pekkari, K. & Holmgren, A. Truncated thioredoxin: physiological functions and mechanism. *Antioxid. Redox Signal.* **6,** 53–61 (2004).
280. Dessein, A. J. *et al.* Modulation of eosinophil cytotoxicity by blood mononuclear cells from healthy subjects and patients with chronic schistosomiasis mansoni. *Cell. Immunol.* **85,** 100–113 (1984).

281. Balcewicz-Sablinska, M. K., Wollman, E. E., Gorti, R. & Silberstein, D. S. Human eosinophil cytotoxicity-enhancing factor. II. Multiple forms synthesized by U937 cells and their relationship to thioredoxin/adult T cell leukemia-derived factor. *J. Immunol. Baltim. Md 1950* **147,** 2170–2174 (1991).
282. Silberstein, D. S., Ali, M. H., Baker, S. L. & David, J. R. Human eosinophil cytotoxicity-enhancing factor. Purification, physical characteristics, and partial amino acid sequence of an active polypeptide. *J. Immunol. Baltim. Md 1950* **143,** 979–983 (1989).
283. Silberstein, D. S., McDonough, S., Minkoff, M. S. & Balcewicz-Sablinska, M. K. Human eosinophil cytotoxicity-enhancing factor. Eosinophil-stimulating and dithiol reductase activities of biosynthetic (recombinant) species with COOH-terminal deletions. *J. Biol. Chem.* **268,** 9138–9142 (1993).
284. Pekkari, K., Gurunath, R., Arner, E. S. & Holmgren, A. Truncated thioredoxin is a mitogenic cytokine for resting human peripheral blood mononuclear cells and is present in human plasma. *J. Biol. Chem.* **275,** 37474–37480 (2000).
285. Pekkari, K., Goodarzi, M. T., Scheynius, A., Holmgren, A. & Avila-Cariño, J. Truncated thioredoxin (Trx80) induces differentiation of human CD14+ monocytes into a novel cell type (TAMs) via activation of the MAP kinases p38, ERK, and JNK. *Blood* **105,** 1598–1605 (2005).
286. Pekkari, K. *et al.* Truncated thioredoxin (Trx80) induces production of interleukin-12 and enhances CD14 expression in human monocytes. *Blood* **97,** 3184–3190 (2001).
287. Mustacich, D. & Powis, G. Thioredoxin reductase. *Biochem. J.* **346,** 1–8 (2000).
288. Zhong, L., Arnér, E. S., Ljung, J., Aslund, F. & Holmgren, A. Rat and calf thioredoxin reductase are homologous to glutathione reductase with a carboxyl-terminal elongation containing a conserved catalytically active penultimate selenocysteine residue. *J. Biol. Chem.* **273,** 8581–8591 (1998).
289. Williams, C. H. *et al.* Thioredoxin reductase. *Eur. J. Biochem.* **267,** 6110–6117 (2000).
290. Arnér, E. S. J. Focus on mammalian thioredoxin reductases--important selenoproteins with versatile functions. *Biochim. Biophys. Acta* **1790,** 495–526 (2009).
291. Zhong, L., Arnér, E. S. & Holmgren, A. Structure and mechanism of mammalian thioredoxin reductase: the active site is a redox-active selenolthiol/selenenylsulfide formed from the conserved cysteine-selenocysteine sequence. *Proc. Natl. Acad. Sci. U. S. A.* **97,** 5854–5859 (2000).
292. Arscott, L. D., Gromer, S., Schirmer, R. H., Becker, K. & Williams, C. H. The mechanism of thioredoxin reductase from human placenta is similar to the mechanisms of lipoamide dehydrogenase and glutathione reductase and is distinct from the mechanism of thioredoxin reductase from Escherichia coli. *Proc. Natl. Acad. Sci. U. S. A.* **94,** 3621–3626 (1997).
293. Gasdaska, P. Y., Gasdaska, J. R., Cochran, S. & Powis, G. Cloning and sequencing of a human thioredoxin reductase. *FEBS Lett.* **373,** 5–9 (1995).

294. Russel, M. & Model, P. Sequence of thioredoxin reductase from Escherichia coli. Relationship to other flavoprotein disulfide oxidoreductases. *J. Biol. Chem.* **263,** 9015–9019 (1988).
295. Moore, E. C., Reichard, P. & Thelander, L. ENZYMATIC SYNTHESIS OF DEOXYRIBONUCLEOTIDES.V. PURIFICATION AND PROPERTIES OF THIOREDOXIN REDUCTASE FROM ESCHERICHIA COLI B. *J. Biol. Chem.* **239,** 3445–3452 (1964).
296. Kumar, S., Björnstedt, M. & Holmgren, A. Selenite is a substrate for calf thymus thioredoxin reductase and thioredoxin and elicits a large non-stoichiometric oxidation of NADPH in the presence of oxygen. *Eur. J. Biochem. FEBS* **207,** 435–439 (1992).
297. Söderberg, A., Sahaf, B. & Rosén, A. Thioredoxin reductase, a redox-active selenoprotein, is secreted by normal and neoplastic cells: presence in human plasma. *Cancer Res.* **60,** 2281–2289 (2000).
298. Biterova, E. I., Turanov, A. A., Gladyshev, V. N. & Barycki, J. J. Crystal structures of oxidized and reduced mitochondrial thioredoxin reductase provide molecular details of the reaction mechanism. *Proc. Natl. Acad. Sci. U. S. A.* **102,** 15018–15023 (2005).
299. Gromer, S. *et al.* A hypothesis on the catalytic mechanism of the selenoenzyme thioredoxin reductase. *Biochem. J.* **332 (Pt 2),** 591–592 (1998).
300. Arnér, E. S. & Holmgren, A. Measurement of thioredoxin and thioredoxin reductase. *Curr. Protoc. Toxicol. Editor. Board Mahin Maines Ed.--Chief Al* **Chapter 7,** Unit 7.4. (2001).
301. Moriarty-Craige, S. E. & Jones, D. P. Extracellular thiols and thiol/disulfide redox in metabolism. *Annu. Rev. Nutr.* **24,** 481–509 (2004).
302. Kemp, M., Go, Y.-M. & Jones, D. P. Nonequilibrium thermodynamics of thiol/disulfide redox systems: a perspective on redox systems biology. *Free Radic. Biol. Med.* **44,** 921–937 (2008).
303. Go, Y.-M. & Jones, D. P. Thiol/disulfide redox states in signaling and sensing. *Crit. Rev. Biochem. Mol. Biol.* **48,** 173–181 (2013).
304. Ishii, T., Sugita, Y. & Bannai, S. Regulation of glutathione levels in mouse spleen lymphocytes by transport of cysteine. *J. Cell. Physiol.* **133,** 330–336 (1987).
305. Suthanthiran, M., Anderson, M. E., Sharma, V. K. & Meister, A. Glutathione regulates activation-dependent DNA synthesis in highly purified normal human T lymphocytes stimulated via the CD2 and CD3 antigens. *Proc. Natl. Acad. Sci. U. S. A.* **87,** 3343–3347 (1990).
306. Garg, S. K., Yan, Z., Vitvitsky, V. & Banerjee, R. Differential dependence on cysteine from transsulfuration versus transport during T cell activation. *Antioxid. Redox Signal.* **15,** 39–47 (2011).
307. Bridges, R. J., Natale, N. R. & Patel, S. A. System xc^- cystine/glutamate antiporter: an update on molecular pharmacology and roles within the CNS. *Br. J. Pharmacol.* **165,** 20–34 (2012).
308. Yan, Z. & Banerjee, R. Redox remodeling as an immunoregulatory strategy. *Biochemistry (Mosc.)* **49,** 1059–1066 (2010).
309. Angelini, G. *et al.* Antigen-presenting dendritic cells provide the reducing extracellular microenvironment required for T lymphocyte activation. *Proc. Natl. Acad. Sci. U. S. A.* **99,** 1491–1496 (2002).

310. Di Trapani, G., Perkins, A. & Clarke, F. Production and secretion of thioredoxin from transformed human trophoblast cells. *Mol. Hum. Reprod.* **4,** 369–375 (1998).
311. Oderup, C., Cederbom, L., Makowska, A., Cilio, C. M. & Ivars, F. Cytotoxic T lymphocyte antigen-4-dependent down-modulation of costimulatory molecules on dendritic cells in CD4+ CD25+ regulatory T-cell-mediated suppression. *Immunology* **118,** 240–249 (2006).
312. Wendling, D. *et al.* A randomized, double blind, placebo controlled multicenter trial of murine anti-CD4 monoclonal antibody therapy in rheumatoid arthritis. *J. Rheumatol.* **25,** 1457–1461 (1998).
313. Canva-Delcambre, V. *et al.* Treatment of severe Crohn's disease with anti-CD4 monoclonal antibody. *Aliment. Pharmacol. Ther.* **10,** 721–727 (1996).
314. Racadot, E. *et al.* Treatment of multiple sclerosis with anti-CD4 monoclonal antibody. A preliminary report on B-F5 in 21 patients. *J. Autoimmun.* **6,** 771–786 (1993).
315. Wijdenes, J. Patent WO 2004083247 A1: Humanized anti-CD4 antibody with immunosuppressive properties. (2004).
316. Uherek, C. *et al.* The Novel Regulatory T Cell (Treg) Agonistic Monoclonal Antibody (mAb) Tregalizumab (BT-061): Further Characterization of Mechanism of Action, Epitope Binding, and Clinical Effects in Patients with Rheumatoid Arthritis. *IBC Life Sciences* [abstract] (2011).
317. Helling, B. Analysis of the mode of action of the monoclonal antibody tregalizumab (BT-061). Dissertation. (Johann Wolfgang Goethe - Universität, 2015).
318. Ng, C. M., Stefanich, E., Anand, B. S., Fielder, P. J. & Vaickus, L. Pharmacokinetics/pharmacodynamics of nondepleting anti-CD4 monoclonal antibody (TRX1) in healthy human volunteers. *Pharm. Res.* **23,** 95–103 (2006).
319. Takai, T. Fc receptors and their role in immune regulation and autoimmunity. *J. Clin. Immunol.* **25,** 1–18 (2005).
320. Helling, B. *et al.* The Therapeutic Antibody Tregalizumab (BT-061) Induces Activation of Regulatory T Cells by Engaging a Unique CD4 Mediated Signaling That Strongly Differs From Signaling Events Induced by Standard Anti-CD4 Antibodies. *Arthritis Rheum.* **64,** 988 [2343 abstract] (2012).
321. Schulze-Koops, H. *et al.* Selective activation of regulatory T cells (Tregs) by BT-061: clinical data from a completed phase IIa trial in rheumatoid arthritis (RA) and design of a multi-centre, double-blind, randomised, placebo-controlled, phase IIb dose-finding trial. *Z. Für Rheumatol.* **70,** 86 [RA.35 abstract] (2011).
322. Helling, B. *et al.* A specific CD4 epitope bound by tregalizumab mediates activation of regulatory T cells by a unique signaling pathway. *Immunol. Cell Biol.* (2014). doi:10.1038/icb.2014.102
323. Czeloth, N. *et al.* Selective activation of naturally occurring regulatory T cells (Tregs) by the monoclonal antibody BT-061 as a novel therapeutic opportunity: preclinical and early clinical results. *Ann. Rheum. Dis.* **69 (Suppl.3),** 99 [OP0138 abstract] (2010).
324. Khalil, N. TGF-beta: from latent to active. *Microbes Infect.* **1,** 1255–1263 (1999).

325. Humblet-Baron, S. & Baron, F. Boosting regulatory T-cell function with the humanized CD4-specific humanized monoclonal antibody Tregalizumab (BT-061). *Immunol. Cell Biol.* **93,** 321–322 (2015).
326. Müller-Eberhard, H. J. Molecular organization and function of the complement system. *Annu. Rev. Biochem.* **57,** 321–347 (1988).
327. Kubach, J. *et al.* The Effect of a Pro-inflammatory Milieu on Tregalizumab (BT-061)-Induced Regulatory T-cell Activity. *Arthritis Rheum.* **66,** S767–S768 (2014).
328. Song, R. *et al.* Epitope mapping of ibalizumab, a humanized anti-CD4 monoclonal antibody with anti-HIV-1 activity in infected patients. *J. Virol.* **84,** 6935–6942 (2010).
329. Healey, D. *et al.* Novel anti-CD4 monoclonal antibodies separate human immunodeficiency virus infection and fusion of CD4+ cells from virus binding. *J. Exp. Med.* **172,** 1233–1242 (1990).
330. Hong, Y. L. *et al.* New reporter cell lines to study macrophage-tropic HIV envelope protein-mediated cell-cell fusion. *AIDS Res. Hum. Retroviruses* **15,** 1667–1672 (1999).
331. Baecher-Allan, C. & Hafler, D. A. Human regulatory T cells and their role in autoimmune disease. *Immunol. Rev.* **212,** 203–216 (2006).
332. Leipe, J., Skapenko, A., Lipsky, P. E. & Schulze-Koops, H. Regulatory T cells in rheumatoid arthritis. *Arthritis Res. Ther.* **7,** 93 (2005).
333. Haas, J. *et al.* Reduced suppressive effect of CD4+CD25high regulatory T cells on the T cell immune response against myelin oligodendrocyte glycoprotein in patients with multiple sclerosis. *Eur. J. Immunol.* **35,** 3343–3352 (2005).
334. Cerutti, N., Killick, M., Jugnarain, V., Papathanasopoulos, M. & Capovilla, A. Disulfide reduction in CD4 domain 1 or 2 is essential for interaction with HIV glycoprotein 120 (gp120), which impairs thioredoxin-driven CD4 dimerization. *J. Biol. Chem.* **289,** 10455–10465 (2014).
335. Krieger, E. & Vriend, G. YASARA View - molecular graphics for all devices - from smartphones to workstations. *Bioinforma. Oxf. Engl.* **30,** 2981–2982 (2014).
336. Mongardon, N. *et al.* Plasma thioredoxin levels during post-cardiac arrest syndrome: relationship with severity and outcome. *Crit. Care* **17,** R18 (2013).
337. Miwa, K. *et al.* Increased oxidative stress with elevated serum thioredoxin level in patients with coronary spastic angina. *Clin. Cardiol.* **26,** 177–181 (2003).
338. Otaki, Y. *et al.* Association of plasma thioredoxin-1 with renal tubular damage and cardiac prognosis in patients with chronic heart failure. *J. Cardiol.* **64,** 353–359 (2014).
339. Iwata, Y. *et al.* Elevated levels of thioredoxin 1 in the lungs and sera of idiopathic pulmonary fibrosis, non-specific interstitial pneumonia and cryptogenic organizing pneumonia. *Intern. Med. Tokyo Jpn.* **49,** 2393–2400 (2010).
340. Callister, M. E. *et al.* Extracellular thioredoxin levels are increased in patients with acute lung injury. *Thorax* **61,** 521–527 (2006).
341. Yamada, Y. *et al.* Elevated serum levels of thioredoxin in patients with acute exacerbation of asthma. *Immunol. Lett.* **86,** 199–205 (2003).

342. Sumida, Y. *et al.* Serum thioredoxin levels as a predictor of steatohepatitis in patients with nonalcoholic fatty liver disease. *J. Hepatol.* **38,** 32–38 (2003).
343. Miyazaki, K. *et al.* Elevated serum level of thioredoxin in patients with hepatocellular carcinoma. *Biotherapy Dordr. Neth.* **11,** 277–288 (1998).
344. Kozlowski, A. & Harris, J. M. Improvements in protein PEGylation: pegylated interferons for treatment of hepatitis C. *J. Control. Release Off. J. Control. Release Soc.* **72,** 217–224 (2001).
345. MacColl, R., Csatorday, K., Berns, D. S. & Traeger, E. Chromophore interactions in allophycocyanin. *Biochemistry (Mosc.)* **19,** 2817–2820 (1980).
346. Schwertassek, U. *et al.* Selective redox regulation of cytokine receptor signaling by extracellular thioredoxin-1. *EMBO J.* **26,** 3086–3097 (2007).
347. Gromer, S., Urig, S. & Becker, K. The thioredoxin system--from science to clinic. *Med. Res. Rev.* **24,** 40–89 (2004).
348. Morikawa, S., Tatsumi, E., Baba, M., Harada, T. & Yasuhira, K. Two E-rosette-forming lymphoid cell lines. *Int. J. Cancer J. Int. Cancer* **21,** 166–170 (1978).
349. Lu, J., Ellsworth, J. L., Hamacher, N., Oak, S. W. & Sun, P. D. Crystal Structure of Fcγ Receptor I and Its Implication in High Affinity γ-Immunoglobulin Binding. *J. Biol. Chem.* **286,** 40608–40613 (2011).
350. Nilsson, K., Bennich, H., Johansson, S. G. & Pontén, J. Established immunoglobulin producing myeloma (IgE) and lymphoblastoid (IgG) cell lines from an IgE myeloma patient. *Clin. Exp. Immunol.* **7,** 477–489 (1970).
351. Abraham, R. T. & Weiss, A. Jurkat T cells and development of the T-cell receptor signalling paradigm. *Nat. Rev. Immunol.* **4,** 301–308 (2004).
352. Datta, S. *et al.* Correlation of oxidant status with oxidative tissue damage in patients with rheumatoid arthritis. *Clin. Rheumatol.* **33,** 1557–1564 (2014).
353. Maiese, K. New Insights for Oxidative Stress and Diabetes Mellitus. *Oxid. Med. Cell. Longev.* **2015,** 875961 (2015).
354. Schweizer, U., Bräuer, A. U., Köhrle, J., Nitsch, R. & Savaskan, N. E. Selenium and brain function: a poorly recognized liaison. *Brain Res. Brain Res. Rev.* **45,** 164–178 (2004).
355. Uttara, B., Singh, A. V., Zamboni, P. & Mahajan, R. T. Oxidative stress and neurodegenerative diseases: a review of upstream and downstream antioxidant therapeutic options. *Curr. Neuropharmacol.* **7,** 65–74 (2009).
356. Alexander, R. W. Theodore Cooper Memorial Lecture. Hypertension and the pathogenesis of atherosclerosis. Oxidative stress and the mediation of arterial inflammatory response: a new perspective. *Hypertension* **25,** 155–161 (1995).
357. Siti, H. N., Kamisah, Y. & Kamsiah, J. The role of oxidative stress, antioxidants and vascular inflammation in cardiovascular disease (a review). *Vascul. Pharmacol.* **71,** 40–56 (2015).
358. Taniguchi, Y., Taniguchi-Ueda, Y., Mori, K. & Yodoi, J. A novel promoter sequence is involved in the oxidative stress-induced expression of the adult T-cell leukemia-derived factor (ADF)/human thioredoxin (Trx) gene. *Nucleic Acids Res.* **24,** 2746–2752 (1996).
359. Nakamura, H. *et al.* Adult T cell leukemia-derived factor/human thioredoxin protects endothelial F-2 cell injury caused by activated neutrophils or hydrogen peroxide. *Immunol. Lett.* **42,** 75–80 (1994).

360. Szabó-Taylor, K. É. *et al.* Lymphocytes from rheumatoid arthritis patients have elevated levels of intracellular peroxiredoxin 2, and a greater frequency of cells with exofacial peroxiredoxin 2, compared with healthy human lymphocytes. *Int. J. Biochem. Cell Biol.* **44,** 1223–1231 (2012).
361. Cleland, W. W. DITHIOTHREITOL, A NEW PROTECTIVE REAGENT FOR SH GROUPS. *Biochemistry (Mosc.)* **3,** 480–482 (1964).
362. Schmidt, B., Ho, L. & Hogg, P. J. Allosteric disulfide bonds. *Biochemistry (Mosc.)* **45,** 7429–7433 (2006).
363. Bourgeois, R., Mercier, J., Paquette-Brooks, I. & Cohen, E. A. Association between disruption of CD4 receptor dimerization and increased human immunodeficiency virus type 1 entry. *Retrovirology* **3,** 31 (2006).
364. Thome, M. & Acuto, O. Molecular mechanism of T-cell activation: role of protein tyrosine kinases in antigen receptor-mediated signal transduction. *Res. Immunol.* **146,** 291–307 (1995).
365. Hanke, J. H. *et al.* Discovery of a novel, potent, and Src family-selective tyrosine kinase inhibitor. Study of Lck- and FynT-dependent T cell activation. *J. Biol. Chem.* **271,** 695–701 (1996).
366. Vahl, J. C. *et al.* Continuous T cell receptor signals maintain a functional regulatory T cell pool. *Immunity* **41,** 722–736 (2014).
367. Möttönen, M. *et al.* CD4+ CD25+ T cells with the phenotypic and functional characteristics of regulatory T cells are enriched in the synovial fluid of patients with rheumatoid arthritis. *Clin. Exp. Immunol.* **140,** 360–367 (2005).
368. Azimi, I., Wong, J. W. H. & Hogg, P. J. Control of mature protein function by allosteric disulfide bonds. *Antioxid. Redox Signal.* **14,** 113–126 (2011).

10 Erklärung

Hiermit erkläre ich, dass ich die vorliegende Doktorarbeit "*High thioredoxin-1 levels in rheumatoid arthritis patients diminish binding and signalling of the monoclonal antibody Tregalizumab"* selbständig verfasst habe und keine anderen als die angegebenen Quellen und Hilfsmittel benutzt habe. Die Arbeit wurde unter Beachtung der Grundsätze der guten wissenschaftlichen Praxis durchgeführt.

Die vorliegende Arbeit wurde im Zeitraum vom Februar 2012 bis April 2015 bei der Biotest AG in Dreieich unter der Anleitung von Frau PD Dr. Schirrmacher angefertigt.

Die Betreuung seitens der Johann Wolfgang Goethe-Universität Frankfurt übernahm Herr Prof. Dr. Theodor Dingermann.

Ich erkläre, dass diese Dissertation weder in gleicher noch in ähnlicher Form in einem anderen Prüfungsverfahren vorgelegt wurde. Außer den mit dem Zulassungsgesuch urkundlich vorgelegten Graden habe ich früher keine weiteren akademischen Grade erworben oder zu erwerben versucht.

Teile dieser Arbeit wurden bereits bzw. werden noch veröffentlicht:

Heim, K, Dälken B, Faust, S, Rharbaoui F, Engling A, Wallmeier H *et al*. High thioredoxin-1 levels in rheumatoid arthritis patients diminish binding and signalling of the monoclonal antibody Tregalizumab. *Clinical & Translational Immunology* (2016) 5, e00; doi:10.1038/cti.2016.69;

(Paper received 1 April 2016; revised 21 September 2016; accepted 13 October 2016 by Clinical & Translational Immunology).

Frankfurt, den _____

_____

Katharina Heim